Aus dem

Lehrstuhl für Neuroanatomie, Anatomische Anstalt

Institut der Universität München

Vorstand: Prof. Dr. med. Christoph Schmitz

C. elegans as a Model for Blast-Related Mild Traumatic Brain Injury

Dissertation

zum Erwerb des Doktorgrades der Humanbiologie

an der Medizinischen Fakultät der

Ludwig-Maximilians-Universität zu München

vorgelegt von

Nicholas Angstman

aus

Burlington, Vermont, USA

Jahr

2025

Mit Genehmigung der Medizinischen Fakultät
der Universität München

Berichterstatter:	Prof. Dr. Christoph Schmitz
Mitberichterstatter:	PD Dr. Philipp Karschnia
	Prof. Dr. Nikolaus Plesnila
Dekan:	Prof. Dr. med. Thomas Gudermann
Tag der mündlichen Prüfung:	14.10.2025

Affidavit

Affidavit

Angstman, Nicholas Baker
_____
Surname, first name

_____
Street

_____
Zip code, town, country

I hereby declare, that the submitted thesis entitled:

***C. elegans* as a Model for Blast-Related Mild Traumatic Brain Injury**

is my own work. I have only used the sources indicated and have not made unauthorized use of services of a third party. Where the work of others has been quoted or reproduced, the source is always given.

I further declare that the dissertation presented here has not been submitted in the same or similar form to any other institution for the purpose of obtaining an academic degree.

Raubling, den 17.10.2025 Nicholas Angstman

_____ _____

place, date Signature doctoral candidate

Table of contents

List of abbreviations

Abbreviation	Full Form
br-mTBI	Blast-related Mild Traumatic Brain Injury
C. elegans	*Caenorhabditis elegans*
E. coli	*Escherichia coli*
mTBI	Mild Traumatic Brain Injury
NGM	Nematode Growth Medium
PVA	Polyvinyl Alcohol
rESWT	Radial Extracorporeal Shock Wave Therapy
S-medium	Standard medium for *C. elegans*
TBI	Traumatic Brain Injury

List of publications

- **Angstman NB**, Kiessling MC, Frank HG, Schmitz C. High interindividual variability in dose-dependent reduction in speed of movement after exposing C. elegans to shock waves. Front Behav Neurosci. 2015;9:12. doi: 10.3389/fnbeh.2015.00012.
- **Angstman NB**, Frank HG, Schmitz C. Advanced behavioral analyses show that the presence of food causes subtle changes in *C. elegans* movement. Front Behav Neurosci 2016;10:60. doi: 10.3389/fnbeh.2016.00060.
- **Angstman NB**, Frank HG, Schmitz C. Hypothermia ameliorates blast-related lifespan reduction of C. elegans. Sci Rep 2018;8(1):10549. doi: 10.1038/s41598-018-28910-z.
- Császár NB, **Angstman NB**, Milz S, Sprecher CM, Kobel P, Farhat M, Furia JP, Schmitz C. Radial shock wave devices generate cavitation. PLoS One 2015;10(10):e0140541. doi: 10.1371/journal.pone.0140541.
- Weichmann F, Hett R, Schepers A, Ito-Kureha T, Flatley A, Slama K, Hastert FD, Angstman NB, Cardoso MC, König J, Hüttelmaier S, Dieterich C, Canzar S, Helm M, Heissmeyer V, Feederle R, Meister G. Validation strategies for antibodies targeting modified ribonucleotides. RNA 2020;26(10):1489-1506. doi: 10.1261/rna.076026.120.
- Wang T, Du L, Shan L, Dong H, Feng J, Kiessling MC, Angstman NB, Schmitz C, Jia F. A prospective case-control study of radial extracorporeal shock wave therapy for spastic plantar flexor muscles in very young children with cerebral palsy. Medicine 2016;95(19):e3649. doi: 10.1097/MD.0000000000003649.
- Korr H, Angstman NB, Born TB, Bosse K, Brauns B, Demmler M, Fueller K, Kántor O, Kever BM, Rahimyar N, Salimi S, Silny J, Schmitz C. No evidence of persisting unrepaired nuclear DNA single strand breaks in distinct types of cells in the brain, kidney, and liver of adult mice after continuous eight-week 50 Hz magnetic field exposure with flux density of 0.1 mT or 1.0 mT. PLoS One 2014;9(10):e109774. doi: 10.1371/journal.pone.0109774.
- Müller-Starck J, Büttner A, Kiessling MC, Angstman NB, Császár NB, Haeussner E, Hochstrasser T, Sternecker K, Hof PR, Milz S, Frank HG, Schmitz C. No changes in cerebellar microvessel length density in sudden infant death syndrome: implications for pathogenetic mechanisms. J Neuropathol Exp Neurol 2014;73(4):312-23. doi: 10.1097/NEN.0000000000000055.

Your contribution to the publications

Contribution to paper I

Publication:

Angstman NB, Kiessling MC, Frank HG, Schmitz C. High interindividual variability in dose-dependent reduction in speed of movement after exposing C. elegans to shock waves. Front Behav Neurosci. 2015 Feb 6;9:12. doi: 10.3389/fnbeh.2015.00012.

Contribution:

I conceived and designed the experiments, performed the experiments, analyzed the data and wrote the original draft of the manuscript.

Contribution to paper II

Publication:

Angstman NB, Frank HG, Schmitz C. Advanced behavioral analyses show that the presence of food causes subtle changes in *C. elegans* movement. Front Behav Neurosci 2016;10:60. doi: 10.3389/fnbeh.2016.00060.

Contribution:

I conceived and designed the experiments, performed the experiments, analyzed the data and wrote the original draft of the manuscript.

Contribution to paper III (Appendix)

Angstman NB, Frank HG, Schmitz C. Hypothermia ameliorates blast-related lifespan reduction of C. elegans. Sci Rep 2018;8(1):10549. doi: 10.1038/s41598-018-28910-z.

Contribution:

I conceived and designed the experiments, performed the experiments, analyzed the data and wrote the original draft of the manuscript.

Contribution to paper IV (Appendix)

Publication:

Császár NB, Angstman NB, Milz S, Sprecher CM, Kobel P, Farhat M, Furia JP, Schmitz C. Radial shock wave devices generate cavitation. PLoS One 2015;10(10):e0140541. doi: 10.1371/journal.pone.0140541.

Together with N.B.C., C.M.S., P.K. and M.F. I was involved in conceiving and designing the experiments, performing the experiments, analyzing the data and editing the manuscript.

1. Introduction

1.1 General Purpose

Blast-related mild traumatic brain injury (br-mTBI) presents a significant challenge due to its complex mechanisms and difficulty in diagnosis (Rosenfeld et al., 2013). Current *in vivo* and *in vitro* research models often fall short in capturing the multifaceted nature of br-mTBI (Marklund & Hillered, 2011; Panzer et al., 2014), leading to a need for innovative models to bridge the gap. *Caenorhabditis elegans* (*C. elegans*), a microscopic nematode, offers a unique platform for such research due to its ease of genetic manipulation, high-throughput capabilities, and well-documented neural and behavioral systems (Driscoll & Gerstbrein, 2003).

We have hypothesized that utilizing *C. elegans* in conjunction with a therapeutic shock wave device as a model for br-mTBI will reveal both short- and long-term dose-dependent effects of shock wave exposure. Cavitation effects, previously noted in other br-mTBI models, are expected to be present in our *C. elegans* model as well. More detailed behavioral analyses in *C. elegans* are hypothesized to uncover insights into the effects of shock wave exposure that might be missed by standard behavioral methods. Furthermore, cavitation is hypothesized to be a primary damaging mechanism in shock wave exposure within the *C. elegans* br-mTBI model. Potential long-term effects of shock wave exposure in *C. elegans* likely indicate distinct short- and long-term death-causing mechanisms. Potential treatment options, such as hypothermia treatment, may mitigate the long-term effects of shock wave exposure in the *C. elegans* model of br-mTBI. Overall, our newly established model for br-mTBI research is hypothesized to effectively investigate damage-causing mechanisms and potential treatment options.

1.2 Blast-related Mild Traumatic Brain Injury

All injuries, including death, resulting from exposure to explosion can be classified as blast injuries. Such injuries are classified based on the damage causing mechanism. Primary blast injuries result from exposure to shock wave components. Injuries resulting from projectiles propelled by the blast, such as shrapnel, are classified as secondary injuries. Tertiary blast injuries can occur when, for example, victims are propelled by the blast wave into stationary objects. Lastly, quaternary injuries represent injuries that do not fall into the first three categories, for example, crushing injuries due to structures damaged by the explosion (Cernak & Noble-Haeusslein, 2010).

Although all blast injuries are potentially immediately life-threatening, secondary, tertiary and quaternary injuries generally are easier to identify, while primary blast injuries often lack signs of external injury, leading to difficulty in the diagnosis of primary blast injuries (Rosenfeld et al., 2013). Damage is caused by components of the blast wave itself, which consist of a high positive pressure consequent to the first part of the blast wave followed by negative pressure in the tensile (second) part of the blast wave (Nakagawa et al., 2011; Goeller et al., 2012; Rosenfeld et al., 2013). Due to the change in pressure, cavitation, the form and collapse of bubbles, could occur as a potential damage causing component (Gross, 1958; Marsh and Bentil, 2021). It has been previously shown that blast and shock waves can result in cavitation (Pishchalnikov et al., 2003; Moore et al., 2008), and likewise it has been shown that cavitation can cause tissue damage (Zimberlin et al., 2007; Kang et al., 2018). While primary blast effects can lead to a wide range of symptoms across the body, such as pulmonary and auditory symptoms, primary blast injuries are also associated with traumatic brain injuries, which can cause cognitive, sensory and motor impairments (Cernak & Noble-Haeusslein, 2010; Rosenfeld et al., 2013).

Due in large part to the complexity of the brain, such symptoms are more difficult to diagnose, yet could potentially result in serious long-term impairment.

Traumatic brain injury (TBI), in general, is a significant health concern that is typically categorized into mild, moderate, and severe cases (Carney et al., 2017). A study by Faul et al. (2010) estimated that in the United States alone, approximately 1.7 million cases of TBI occur each year. In 2020, more than 214,000 TBI-related hospitalizations and 69,000 deaths were recorded in the U.S., with males and older adults particularly affected (Centers for Disease Control and Prevention, 2024). Among these cases, approximately 75% are classified as mild TBI (mTBI), commonly referred to as concussion, with nearly 15-22% of military personnel returning from combat zones experiencing blast-related TBIs, which are often associated with exposure to explosive events (Kong et al., 2022). Likewise, research also indicated a high prevalence of military personnel returning from Iraq having experienced br-mTBI, often complicated by co-occurring post-traumatic stress disorder (PTSD), adding complexity to diagnosis and treatment (Hoge et al., 2008).

The problem of TBI extends beyond its prevalence, as it poses various challenges in diagnosis, measurement of exposure, and understanding disease mechanisms (Menon et al., 2010). TBI can manifest in a range of clinical conditions and associated diseases, making it difficult to diagnose accurately. Furthermore, measuring exposure to TBI and quantifying its severity present additional complexities. Mechanisms of TBI damage are multifaceted, with numerous factors contributing to its pathogenesis. Delineation of damage causing mechanisms, i.e. primary, secondary, tertiary and quaternary, can also prove difficult, especially when investigating injuries caused in the field (Cernak & Noble-Haeusslein, 2010; Rosenfeld et al., 2013). While several mechanisms have been demonstrated to cause TBI, there are also hypothesized mechanisms, especially in br-mTBI, that warrant further investigation, such as the roles of high positive pressure and cavitation within the brain tissue. While blast overpressure waves have been demonstrated to be a damaging mechanism, cavitation has also been suggested as a potential contributor to the damaging effects of TBI (Ling et al., 2009). Cavitation has been shown to induce cell permeability, damage the blood-brain barrier, and otherwise damage cellular structures (Adhikari et al., 2016).

Although the mechanisms of TBI are not well understood, several treatment approaches have been explored, such as hyperventilation, seizure prophylaxis, hyperosmolar therapy, and hypothermia therapy (Galgano et al., 2017). By intentionally inducing hypothermia in TBI patients, hypothermia therapy is hypothesized to reduce oxidative injury, leading to mitigated secondary brain injury and improved outcomes. However, while hypothermia therapy has shown promise in some studies, its efficacy and optimal implementation require further investigation and clinical validation (Sandestig et al., 2014). Therefore, additional research is necessary to further evaluate hypothermia therapy as a possible treatment of TBI. In general, there is a need to refine and expand the range of treatments for TBI.

1.3 Models for br-mTBI Research

While the mechanisms of and possible treatments for TBI, and more specifically br-mTBI, have previously been studied, much remains unknown. Various approaches have been used, and generally, studies can be broken into two groups - *in vivo* and *in vitro*, each offering different advantages as well as limitations. Likewise, varying approaches have been used to simulate blast waves and identify which components of these may serve as potential damaging physical mechanisms.

Animal models play a crucial role in the study of br-mTBI. These models aim to replicate blast conditions and evaluate the resulting physiological, molecular and behavioral changes observed in the

brain. By exposing rodents, such as mice or rats, or other animals, such as cats, sheep, pigs and dogs, to controlled blast waves, researchers can assess the impact of blast forces on brain tissue, neuronal function, inflammation and neurobehavioral outcomes (Estrada-Rojo et al., 2018; Harris et al., 2019). Animal models provide several benefits, including the ability to study complex systemic interactions and evaluate the long-term effects of blast exposure (Elder, 2015), as well as allowing for the investigation of therapeutic interventions and the assessment of their efficacy in mitigating blast-induced brain injuries (Bauman et al., 2009). However, animal models have notable limitations, such as ethical considerations and differences within animal and human physiology (Cernak, 2010). The limitation of sample size in animal models can make it difficult to attain statistically significant results, especially considering potential variability in blast exposure models. Furthermore, although animal models offer high similarity to human physiology, differences in species between animal models and humans may not fully capture the complexity of human brain injuries (Marklund & Hillered, 2011).

In vitro models, including tissue and cell culture, offer complementary approaches to study br-mTBI (Morrison et al., 2011; Effgen et al., 2014). These models enable researchers to investigate the cellular and molecular responses to blast forces in a controlled laboratory setting. By exposing cultured cells or tissue constructs to simulated blast conditions, researchers can examine specific cellular processes, molecular signaling pathways and drug effects (Tümer et al., 2018). *In vitro* models provide advantages such as precise control over experimental variables, the ability to study human-derived cells, and high-throughput screening capabilities (Effgen et al., 2016). They also offer an opportunity to explore mechanistic insights at the cellular and molecular levels. However, *in vitro* models may not fully capture the complexity of the intact organism and the systemic interactions that occur *in vivo* (Panzer et al., 2014). These models also face challenges in replicating the dynamic and multicellular nature of the brain tissue and the influence of the surrounding microenvironment (LaPlaca et al., 2007).

To expose *in vivo* and *in vitro* models to shock waves, various strategies have been used. Explosions in shock tubes, blast tubes, as well as open air explosions have been used to replicate blast waves (Bauman et al., 2009, Cernak & Noble-Haeusslein, 2010). These methods, though attempting to replicate realistic blast exposure conditions, are generally difficult to control, exhibiting high variability (Arun et al., 2011). Therapeutic radial extracorporeal shock wave therapy (rESWT) devices also generate shock waves with similar characteristics to primary blast waves (Wu et al., 2017). These medical instruments are generally used for various therapeutic purposes such as, but not limited to, fragmenting kidney stones (Rassweiler et al., 2011) and treating conditions such as tendinopathies, non-unions, and musculoskeletal injuries (Wang, 2012; Schmitz et al., 2015; Speed, 2014). According to Jokinen et al. (2023), shock waves generated by rESWT devices are characterized by a sequence of high positive pressure followed by negative pressure, which can induce cavitation, traits that are shared with primary blast waves. For this reason, rESWT research has previously been relevant to primary blast wave research (Nakagawa et al., 2011).

Created because of the negative pressure following exposure to blast waves and rESWT, cavitation may be of particular interest as a damaging mechanism. To isolate this mechanism, it has previously been shown that the generation of cavitation by shock waves can be significantly reduced by transmitting the shock waves through polyvinyl alcohol (PVA) instead of using frog Ringer's solution as a control (Schelling et al., 1994). PVA, known for its high viscosity and minimal cavitation activity (Hayakawa et al., 1989), possesses an acoustic impedance like that of water (Delius & Gambihler, 1991). As a result, PVA only slightly dampens shock waves compared to water (Robinson & Kossoff, 1978). Thus, by removing cavitation, inferences can be made about the role of cavitation as a damaging mechanism of primary blast waves.

While animal models offer a holistic approach in investigating blast-related mTBI, considering systemic interactions and long-term effects, these may not fully represent human brain injuries and face limitations in sample size due to ethical concerns. *In vitro* models provide a focused exploration of cellular and molecular responses, offering control and high-throughput capabilities, but also lack the complexity offered by *in vivo* models. While combining insights from both approaches can provide a more comprehensive understanding of blast-related mTBI, there is a need for models that mitigate the drawbacks of *in vivo* and *in vitro* models. Such models could further help to facilitate the development of effective diagnostic tools, therapies and preventive strategies.

1.4 *Caenorhabditis* elegans

Caenorhabditis elegans, a microscopic nematode, serves as a powerful model organism for scientific research due to its compact size, short lifespan, and fully sequenced genome (Brenner, 1974; Chen et al., 2005). Unlike traditional *in vivo* models, its amenability to genetic manipulation and large-scale culturing facilitates high-throughput experimentation with reduced ethical constraints (Driscoll & Gerstbrein, 2003). This allows researchers to explore systemic effects and behavioral intricacies, aided by a wide array of genetic knockouts (Poulin et al., 2004). Despite its relatively simple anatomy, *C. elegans* exhibits a diverse range of complex behaviors, particularly in locomotion, regulated by intricate neural circuits (Collin et al., 2014). Advanced tracking software enables research into behavioral dynamics, enabling measurement of subtle changes often overlooked in traditional analyses (Contreras et al., 2014). Leveraging these capabilities, *C. elegans* models could bridge the gap between *in vivo* and *in vitro* models, offering a unique platform for investigating phenomena such as br-mTBI and potential treatments.

The locomotion of *C. elegans* is an important aspect of its behavior and is controlled by a complex interplay of sensory inputs, motor outputs, and neuromuscular modulation (Lewis et al., 1980). *C. elegans* can move in different ways, including forward and backward crawling, turning and swimming (Martin et al., 2002). In many previous assays, video analysis of *C. elegans* on Nematode Growth Medium (NGM) agar plates has been used, although some studies have measured swimming worms, and behavioral arenas have been used (Contreras et al., 2014). While many previous software tools have been limited, mainly in the number of worms concurrently tracked and the simplification to a single center point, improved tracking software has opened possibilities in tracking *C. elegans* movement (Charan et al., 2011). By tracking an outline of worms, as well as increasing the number of worms tracked per video, deeper behavioral analyses are now possible, and typical behavioral readouts such as omega bending and reversal have been identified (Pierce-Shimomura et al., 1999). Using such analyses, it is possible to observe subtle behavioral changes that may otherwise be overlooked in more simplified analyses.

Combining the ability to measure complex behavioral change on a system level in a high-throughput manner, *C. elegans* models have the potential to fill the gap between *in vivo* and *in vitro* models of blast-related mTBI. As an established model organism for studying the relationship between neural circuits and behavior, a *C. elegans* model of br-mTBI may provide a suitable setting for investigating damaging mechanisms as well as potential treatment options.

2. Publications

2.1 High interindividual variability in dose-dependent reduction in speed of movement after exposing *C. elegans* to shock waves

(Angstman et al., Front Behav Neurosci 2015;9:12)

To evaluate *C. elegans* as a potential model for br-mTBI, we exposed *C. elegans* to shock waves generated by a clinically used radial extracorporeal shock wave device (Swiss DolorClast; Electro Medical Systems, Nyon, Switzerland). Behavioral endpoints of speed of locomotion and percent of worms paralyzed were measured to investigate response to varied levels of shock wave exposure, as well as effects of exposure medium, recovery period and growth medium.

Through dose-dependent, statistically significantly ($p < 0.05$) reduced speed of locomotion and increased prevalence of paralysis, *C. elegans* exhibited a clear behavioral response to shock wave exposure. The interindividual variability observed in *C. elegans*, despite the same genetics and consistent, controlled conditions, demonstrated the critical need for large sample sizes when investigating shock wave effects.

Following exposure to shock waves, *C. elegans* were allowed a latent period to recover between 0 and 180 minutes prior to behavioral assay. This led to a significant, time-dependent recovery of locomotive function, exhibited by improved speed of locomotion and decreased fraction of worms paralyzed, demonstrating the temporary and reversible properties of the damaging effects of shock wave exposure.

To investigate the possible effects of cavitation as a damaging mechanism, we compared *C. elegans* exposed to shock waves in a standard medium to those exposed in PVA, a medium that is known to reduce cavitation greatly (Schelling et al., 1994). Following assay in PVA, *C. elegans* were measured to have significantly greater speed of locomotion and a significantly decreased proportion were rendered immobile. This implicates cavitation as a significant mechanism that leads to diminished *C. elegans* locomotion following shock wave exposure.

We further compared differing growth media (in liquid cultures vs. on agar plates) to determine whether any differing effects in behavioral response occur following shock wave exposure. *C. elegans* grown on agar plates exhibited similar behavioral responses to shock waves, namely dose-dependent reduced speed of locomotion. Although differences were found between the locomotion of *C. elegans* grown in liquid cultures and those grown on agar plates, the same general trend held true, including high interindividual variability.

In summary, we introduced a *C. elegans* model of br-mTBI, in which dose-dependent effects, including loss- and recovery-of-function, can be observed. We also implicated cavitation as a damage causing mechanism, and ruled out growth media as a possible confounding factor. The high interindividual variability measured in this study demonstrated the lack of a predictable outcome based on known input, which in turn makes sufficient sample size critical for the study of br-mTBI and necessitates the treatment of patients on a case-by-case basis.

2.2 Advanced behavioral analyses show that the presence of food causes subtle changes in *C. elegans* movement

(Angstman et al., Front Behav Neurosci 2016;10:60)

In our previous publication, we used a *C. elegans* tracking software, WormLab® (MBF Bioscience, Williston, VT, USA), to gather data on *C. elegans*' locomotion. In that case, we only used analyses based on *C. elegans* centroid data, i.e. one X, Y point representing each worm. Throughout the literature, many analyses of and methods for analysis of *C. elegans*' behavior are also limited to measuring the movement of a single point (centroid) (Husson et al., 2013). Although simple endpoints, such as speed of locomotion, can be measured using such analysis, the potential readouts of such assays are limited. In contrast, current technology, including WormLab®, allows for further tracking ability of *C. elegans*. In this study, we implemented advanced behavioral analyses, using extended *C. elegans* tracking capabilities, to investigate the possibility of increased sensitivity in detecting subtle behavioral change. Here, we looked at the movement of four strains of *C. elegans* with and without the presence of food.

Using seven different behavioral readouts, we found statistically significant ($p < 0.05$) differences in movement across the four strains of *C. elegans* on plates with *Escherichia coli (E. coli)* vs. plates without *E. coli* in 25/28 analyses. Within each grouping, there was large interindividual variation observed, further indicating that sufficient sample size is critical.

To assay *C. elegans*, we took advantage of the ability of WormLab® to track multiple worms within one field of view, rather than assaying single worms. Here, 15-30 worms were assayed per NGM-agar plates, and this nesting set up led us to investigate the effect of nesting on significant differences. Using nested ANOVA with each analysis as a dependent variable, lawn type as fixed factor and plate number as random factor, we found a statistically significant difference in 13/28 analyses. Due to this finding, it can be inferred that large sample size is even more relevant.

In order to investigate the correlation between the various advanced analyses and speed of locomotion, for each analysis, we used the runs test to determine whether the data showed significant deviation from linearity. Then, using either linear regression or non-parametric correlation, we analyzed the correlation between the various advanced behavioral endpoints and speed of locomotion. Between the worms on plates with no lawn and worms on plates with an *E. coli* lawn, we found 12/24 and 20/24 cases, respectively, of significant correlation between speed of locomotion and advanced behavioral analyses. Only reversal percentage was found to significantly correlate to average speed of locomotion in all investigated cases, indicating that the various analyses represent more than basic movement, but rather represent different behavioral traits of *C. elegans*.

In summary, these findings indicated that more advanced behavioral analyses of *C. elegans* can lead to more detailed inferences, and the current study showed this in combination with behavior with and without the presence of food. For further fields of study, including, but not limited to toxicology, drug discovery and RNAi screening, these analyses could be of particular importance, potentially adding depth to analyses by measuring subtle behavioral change that may otherwise not be reflected via single X,Y coordinates and speed of locomotion.

2.3 Hypothermia ameliorates blast-related lifespan reduction of *C. elegans*

(Angstman et al., Sci Rep 2018;8(1):10549)

For br-mTBI, there is a missing link between damaging effect and resulting long-term disease. Confounding the problem is a lack of effective models to investigate such effects. Mammalian models offer a closer analog to the human nervous system, but also come with the limitation of sample size. As we have seen previously, even in relatively simple organisms such as *C. elegans*, a high interindividual variability following blast-like treatment was observed (Angstman et al., 2015). In that publication, we established *C. elegans* as an alternative to mammalian models of br-mTBI, though in that case we only investigated a recovery time frame of up to 3 hours. In this experiment, we investigated the long-term effects of shock wave exposure by shock wave effect on lifespan of *C. elegans*. Furthermore, we explored the role of cavitation in causing lifespan affecting damage, as well as the potential effectiveness of hypothermia as a therapy solution.

Following application of shock waves to *C. elegans* as previously described (Angstman et al., 2015), we measured the lifespan of N2 *C. elegans* both raised in liquid cultures and on NGM-agar plates. Decreased lifespan of N2 (wild type) *C. elegans* exposed to 500 shock waves, when compared to those exposed to 100 shock waves, indicated a dose-dependent long term negative effect of shock wave exposure. We had previously observed a reduced immediate effect of shock wave on N2 *C. elegans* exposed to shock wave in PVA (Császár et al., 2015; c.f. Section 1.2.4), which was again confirmed in this study. Investigating long term effects following exposure to shock wave in PVA, we observed lifespan significantly greater than in N2 *C. elegans* exposed to shock wave in S-medium, but still a significantly decreased lifespan compared to N2 *C. elegans* exposed to no shock wave. This decrease can likely be attributed to a slight toxicological effect of PVA, as the addition of a short washing step removed any significant effect on life span.

Using strains of *C. elegans* known to have increased (*daf-2*) and decreased (*daf-16*) lifespans, we observed relatively similar effects as in N2 *C. elegans*. Introducing hypothermia via maintenance at 11°C following shock wave exposure, we investigated any potential short- or long-term effects on lifespan of *C. elegans*. In this case, we still observed statistically significantly ($p < 0.05$) decreased lifespan following shock wave exposure, and a similar short-term effect regardless of temperature. However, by comparing the survival percentage of *C. elegans* exposed to shock waves at the 50% survival point for control *C. elegans* not exposed to shock waves, we observed a greater percentage of survival for *C. elegans* undergoing hypothermia treatment.

In summary, we posited that there are separate short- and long-term death-causing mechanisms following shock wave exposure, and that hypothermia could result in attenuation of long-term effects caused by shock wave exposure.

2.4 Radial shock wave devices generate cavitation

(Csaszar, Angstman, et al., PLoS One 2015;10(10):e0140541)

Shock wave devices and vibrating massage devices share certain aspects of their energy signatures. To determine whether these similar energy signatures produce similar biological effects, we used our established *C. elegans* model to test the effects caused by a rESWT device (Swiss DolorClast; Electro Medical Systems) and a vibrating massage device (Vibracare; G5/General Physiotherapy, Earth City, MO, USA). Additionally, we investigated the role of cavitation by applying treatment using two different media – standard medium for *C. elegans* (S-medium) and PVA, which is known to reduce the formation of cavitation bubbles (Schelling et al., 1994).

To quantify the biological effects on *C. elegans*, we analyzed the speed of locomotion and percentage of worms rendered paralyzed following shock wave application, using our previously described model (Angstman et. al, 2015), in each media. As previously published, a significant decrease in locomotive ability, both in speed of locomotion and increased incidence of paralysis, was found in *C. elegans* that were exposed to shock waves within standard S-medium. For the vibrating massage device, no significant difference in locomotion was found. There was no significant difference found between *C. elegans* exposed in PVA to no device, shock waves and the massage device, indicating that cavitation plays a role in the shock wave effect on *C. elegans* found in S-medium application. Further tests within this study such as high-speed imaging and mechanical damage on the surface of x-ray film indicated that the shock wave device, but not the vibrating massage device, generated cavitation. These tests, however, did not involve *C. elegans*, and therefore are beyond the scope of the present dissertation.

In conclusion, this publication indicated the role of cavitation as a damaging mechanism in shock wave therapy. Furthermore, it was inferred that cavitation is a likely damage causing mechanism in our *C. elegans* model.

3. Summary

We established a new model for blast-related, mild traumatic brain injury (br-mTBI) research and demonstrated the ability to investigate damage causing mechanisms as well as potential treatment options. Within our initial publication, we established the first protocol for using *C. elegans* in conjunction with a therapeutic shock wave device as a model for br-mTBI, in which we observed both short- and long-term dose-dependent effects of shock wave exposure on *C. elegans*. Cavitation effects, which have previously been observed in other models of br-mTBI research, were also observed in our model. Our results showed high interindividual variability, which lends credence to the high-throughput output of our *C. elegans* model. In our second publication, we demonstrated that further behavioral analyses can be used to gather deeper information, leading to observations that, under standard *C. elegans* behavioral analyses, may have been overlooked. Next, we took a deeper look into the role of cavitation as a damaging mechanism of shock waves, establishing cavitation as a main damaging factor in shock wave exposure. Finally, we demonstrated the ability to observe long term effects of shock wave exposure in *C. elegans*, indicating the presence of separate short- and long-term death-causing mechanisms following shock wave exposure, as well as exploring a potential treatment method, hypothermia, that could result in attenuation of long-term effects caused by shock wave exposure.

With the groundwork laid for a *C. elegans* model, further potential research could lead to revelations in br-mTBI. Although the model has limitations, such as limited analogy to human physiology and less maneuverability than *in vitro* models, the model mitigates the main drawbacks of *in vivo* and *in vitro* models, filling a previous research gap. The abilities to perform high-throughput investigations and circumvent ethical issues offer potential advantages compared to *in vivo* models, while the ability to work within a complex system with behavioral output is advantageous compared to *in vitro* models. While the *C. elegans* model for br-mTBI should not be expected to fully replace such models, it serves as a useful complement that could provide initial support in determining damage causing mechanisms or potential treatment avenues warranting further investigation in, for example, animal models with more stringent ethical constraints.

4. Zusammenfassung

Wir haben ein neues Modell für die Erforschung von durch Explosionen bedingte, leichte Schädel-Hirn-Verletzungen (blast-related, mild traumatic brain injury; br-mTBI) etabliert und gezeigt, dass wir in der Lage sind, die schadensverursachenden Mechanismen sowie Behandlungsmöglichkeiten zu untersuchen. In unserer ersten Veröffentlichung erstellten wir das erste Protokoll für die Verwendung von *C. elegans* zusammen mit einem therapeutischen Stoßwellengerät als Modell für br-mTBI, in dem wir sowohl kurz- als auch langfristige dosisabhängige Effekte der Stoßwellenexposition auf *C. elegans* beobachteten. Kavitationseffekte, die zuvor in anderen Modellen der br-mTBI-Forschung beobachtet worden waren, wurden auch in unserem Modell beobachtet. Unsere Ergebnisse wiesen eine hohe interindividuelle Variabilität auf, was die hohe Durchsatzleistung unseres *C.-elegans*-Modells bestätigt. In unserer zweiten Publikation haben wir gezeigt, dass weitere Verhaltensanalysen genutzt werden können, um tiefere Informationen zu sammeln, die zu Beobachtungen führen, die im Rahmen von Standard-Verhaltensanalysen von *C. elegans* möglicherweise übersehen worden wären. Als Nächstes untersuchten wir die Rolle der Kavitation als schädigender Mechanismus von Stoßwellen und stellten fest, dass Kavitation ein Hauptschadensfaktor bei Stoßwellenexposition ist. Schließlich haben wir gezeigt, dass wir in der Lage sind, Langzeiteffekte der Stoßwellenexposition in *C. elegans* zu beobachten, was auf das Vorhandensein separater kurz- und langfristiger tödlicher Mechanismen nach der Stoßwellenexposition hindeutet, und wir haben eine potenzielle Behandlungsmethode, die Hypothermie, untersucht, die zu einer Abschwächung der durch die Stoßwellenexposition verursachten Langzeiteffekte führen könnte.

Da die Grundlagen für ein *C. elegans*-Modell geschaffen wurden, könnte die weitere Forschung zu neuen Erkenntnissen im Bereich br-mTBI führen. Obwohl das Modell Einschränkungen aufweist, wie zum Beispiel eine begrenzte Analogie zur menschlichen Physiologie und eine geringere Manövrierfähigkeit als bei In-vitro-Modellen, mildert das Modell die wichtigsten Nachteile von *In-vivo*- und *In-vitro*-Modellen und schließt eine bisherige Forschungslücke. Die Möglichkeit, Hochdurchsatzuntersuchungen durchzuführen und ethische Fragen zu umgehen, bietet potenzielle Vorteile gegenüber *In-vivo*-Modellen, während die Fähigkeit, in einem komplexen System mit Verhaltensresultaten zu arbeiten, im Vergleich zu In-vitro-Modellen von Vorteil ist. Obwohl das *C. elegans*-Modell für br-mTBI solche Modelle nicht vollständig ersetzen sollte, dient es als nützliche Ergänzung, die eine erste Hilfestellung bei der Bestimmung von schadensverursachenden Mechanismen oder Behandlungsmöglichkeiten bieten könnte, die in Tiermodellen mit strengeren ethischen Auflagen weiter untersucht werden müssten.

5. Paper I

frontiers in
BEHAVIORAL NEUROSCIENCE

ORIGINAL RESEARCH ARTICLE
published: 06 February 2015
doi: 10.3389/fnbeh.2015.00012

High interindividual variability in dose-dependent reduction in speed of movement after exposing *C. elegans* to shock waves

Nicholas B. Angstman, Maren C. Kiessling, Hans-Georg Frank and Christoph Schmitz*

Department of Neuroanatomy, Ludwig-Maximilians University of Munich, Munich, Germany

Edited by:
Katharina A. Braun, Otto-von-Guericke University, Germany

Reviewed by:
Richard Nass, Indiana University School of Medicine, USA
Dominique A. Glauser, University of Fribourg, Switzerland

****Correspondence:***
Christoph Schmitz, Department of Neuroanatomy, Ludwig-Maximilians University of Munich, Pettenkoferstr. 11, D-80336 Munich, Germany
e-mail: christoph_schmitz@med.uni-muenchen.de

In blast-related mild traumatic brain injury (br-mTBI) little is known about the connections between initial trauma and expression of individual clinical symptoms. Partly due to limitations of current *in vitro* and *in vivo* models of br-mTBI, reliable prediction of individual short- and long-term symptoms based on known blast input has not yet been possible. Here we demonstrate a dose-dependent effect of shock wave exposure on *C. elegans* using shock waves that share physical characteristics with those hypothesized to induce br-mTBI in humans. Increased exposure to shock waves resulted in decreased mean speed of movement while increasing the proportion of worms rendered paralyzed. Recovery of these two behavioral symptoms was observed during increasing post-traumatic waiting periods. Although effects were observed on a population-wide basis, large interindividual variability was present between organisms exposed to the same highly controlled conditions. Reduction of cavitation by exposing worms to shock waves in polyvinyl alcohol resulted in reduced effect, implicating primary blast effects as damaging components in shock wave induced trauma. Growing worms on NGM agar plates led to the same general results in initial shock wave effect in a standard medium, namely dose-dependence and high interindividual variability, as raising worms in liquid cultures. Taken together, these data indicate that reliable prediction of individual clinical symptoms based on known blast input as well as drawing conclusions on blast input from individual clinical symptoms is not feasible in br-mTBI.

Keywords: *C. elegans*, mild traumatic brain injury, blast trauma, shock wave, locomotion, paralysis, tracking

INTRODUCTION

The increasing prevalence of blast-related mild traumatic brain injury (br-mTBI) has become a considerable health and economic issue (Hoge et al., 2008). Although exact figures are unknown due to difficulties in identifying cases of mTBI, it has been speculated that as many as one in six troops in the Iraq and Afghanistan military conflicts may be affected (Associated Press, 2007). Due to the variety of ways that the brain can be injured through blast exposure, damaging mechanisms can be defined by the injurious aspect of blast exposure. Damage caused by components of the blast wave itself, namely high positive pressure consequent to the first part of the blast wave as well as cavitation consequent to the tensile (second) part of the blast wave, is referred to as a primary blast effect (Nakagawa et al., 2011; Goeller et al., 2012; Rosenfeld et al., 2013). Secondary (penetrating objects), tertiary (bodily impact with other objects), and quaternary (e.g. crushing injuries from falling objects) blast effects are also defined (DePalma et al., 2005; Scott et al., 2006). While injuries resulting from secondary, tertiary, and quaternary blast effects may be more straightforward in terms of diagnosis and prognosis, injuries resulting from primary blast effects are more difficult. Specifically, accurate assessment of blast wave exposure is nearly impossible, as symptoms are generally not externally expressed. Furthermore, there are a wide range of clinical symptoms (such as headaches, loss of vision, fatigue, confusion, and memory loss) observed in br-mTBI that occur over both short- and the long-term scales (Heltemes et al., 2012). Much research has been done with the goal of furthering knowledge of the various aspects of the clinical picture and the neuropathology of br-mTBI (Cernak and Noble-Haeusslein, 2010; Morrison et al., 2011). There is still, however, little understanding of the mechanisms connecting initial trauma and expression of clinical br-mTBI symptoms, a limiting factor in the efficacy of br-mTBI protection and treatment.

High positive pressure followed by negative pressure that generates cavitation, as observed in blast waves, is also associated with therapeutic (extracorporeal) shock waves used in medicine for cracking kidney stones (Rassweiler et al., 2011) and treating tendinopathies, non-unions, and other injuries of the musculoskeletal system (Wang, 2012; Schmitz et al., 2013; Speed, 2014). It has also been demonstrated that the production of cavitation by shock waves can be highly reduced through propagation of shock waves through polyvinyl alcohol (PVA) rather than a control of frog Ringer's solution (Schelling et al., 1994). Specifically, PVA has high viscosity and very low cavitation activity (Hayakawa, 1991), and nearly the same acoustic impedance as water (Delius and Gambihler, 1992). Accordingly, PVA attenuates shock waves

only very slightly more than water (Robinson and Kossoff, 1978). Hence, the exposure of *C. elegans* to shock waves in PVA enables the testing of the hypothesis that cavitation is an injurious component of primary blast waves.

Current *in vivo* models of br-mTBI generally investigate pathology in higher organisms (e.g., mice, rats, pigs) exposed to mock blasts, but generally are limited in sample size (Morrison et al., 2011). Typical *in vitro* methods of investigating br-mTBI use neuron cell cultures to investigate cellular and molecular cascades that are typically observed in mTBI, but the reproduction of such cascades is not done using known br-mTBI inducing causes (Morrison et al., 2011). *Caenorhabditis elegans* worms are widely used as a model organism alternative to vertebrate animals. Offering advantages including, but not limited to easy maintenance and handling, forward, and reverse genetic manipulability (Jorgensen and Mango, 2002), and a fully known nervous system connectome of 302 neurons (White et al., 1986), *C. elegans* worms are ideal for large population analysis of behavior. The simplicity of the *C. elegans* nervous system has the potential to link change in behavior to observed cellular change at a much more accessible level than in higher organisms. The possibility to investigate br-mTBI at a simple, high-throughput level makes *C. elegans* a useful model organism in the attempt to connect the bridge between cause and effect in br-mTBI.

In the present study we have developed a novel high-throughput method for br-mTBI research by exposing *C. elegans* worms to therapeutic shock waves in a manner that utilizes only primary blast effects to model mTBI. This novel method, by combining high throughput methods and analysis of *C. elegans* behavior, provides new, promising opportunities to study primary blast effects and their role in causing br-mTBI. We also demonstrate that cavitation contributes significantly to the damaging effect of shock waves on *C. elegans.* Here we tested the hypothesis that direct relationships exist between individual alterations of behavior of *C. elegans* and known blast input, which allows conclusions to be drawn on blast input from individual alterations of behavior.

MATERIALS AND METHODS

NEMATODES

Wild type (N2, Bristol) *Caenorhabditis elegans (C. elegans)* and OP50 *Escherichia coli* were obtained from the Caenorhabditis Genetics Center (Minneapolis, MN). Liquid cultures of *C. elegans* fed with *E. coli* were maintained in 500 ml baffled flasks with 250 ml S-Medium (Sulston and Brenner, 1974) with 0.1% Tween 20. Cultures were kept at 24°C in an incubated shaker (NB-205V, N-Biotek, South Korea).

Cultures with many gravid hermaphrodites were selected, poured into a 500 ml separatory funnel (Nalgene, Rochester, NY), and allowed to settle for 15 min. The first 35 ml from the funnel, containing settled worms, were collected in a 50 ml tube. Eggs were then separated from stock liquid cultures using sodium hypochlorite treatment. Synchronized worms were obtained by allowing liquid cultures of eggs to hatch overnight and arrest at the L1 stage. Starved L1 larvae were fed using concentrated OP50 bacteria and allowed to grow at 24°C in S-medium with 0.1% Tween 20 to reach the young adult stage. After 46 h, young adult worms were extracted from culture using a separatory funnel, cleaned using the sucrose floatation method (Portman, 2006), and transferred to S-Medium.

In order to determine the influence of raising worms in liquid cultures on the results of shock wave exposure, we also raised worms on NGM agar plates. To this end, starved L1 larvae were pipetted from liquid cultures on to four NGM agar plates seeded with OP50 *E. coli* at the same time as the addition of *E. coli* to the synchronous liquid culture. Plates were then placed alongside the liquid culture in the incubated shaker at 24°C. In order to prepare for assaying, worms were washed off of plates with S-Medium with all following steps performed exactly the same as with the worms raised in liquid cultures.

APPLICATION OF SHOCK WAVES

Synchronized, young adult worms of approximately 900–1000 μm in length were diluted to approximately 2 worms/μl S-Medium. In order to avoid contamination of adjacent probes, 10 μl of the worm stock were pipetted into non-adjacent U-bottom, 330 μl volume wells of a 96-well plate (VWR, Radnor, PA). Wells were then filled to 300 μl with S-Medium, or in the case of the cavitation assay, approximately 31,000 g/mol PVA (Mowiol 4-88, Karl Roth, Karlsruhe, Germany).

The handpiece of a therapeutic (extracorporeal) shock wave device (Swiss DolorClast; Electro Medical Systems, S.A., Nyon, Switzerland; **Figure 1A**) was set vertically in a drill stand (Wolfcraft, Kempenich, Germany). The Swiss DolorClast generates therapeutic shock waves ballistically, i.e., by accelerating a projectile to strike an applicator, which transforms the kinetic energy of the projectile into a radially expanding pressure wave (Gerdesmeyer et al., 2008; Császár and Schmitz, 2013; Schmitz et al., 2013). The interior (6 mm internal diameter by 2 mm thick) rubber O-rings of the 6-mm applicator of the handpiece of the Swiss Dolorclast were replaced with identically sized 6 × 2 fluorinated rubber O-rings (Vi 975,G/FKM 75, C. Otto Gehrckens, Pinneberg, Germany) to better resist deterioration. A 5.5 × 2 fluorinated rubber O-ring (Vi 670/FKM 80, C. Otto Gehrckens) was placed externally around the applicator to provide a tight connection with the well plate, guarding against loss of sample. For dose-response analysis, the recovery assay, and the cavitation assay, the air pressure of the device was set to a constant 2 bar (yielding an energy flux density of the shock waves of 0.016 mJ/mm^2 at a distance of 5 mm to the applicator). The application frequency was set to 5 Hz in all studies.

The shock wave applicator was slowly lowered into the center of a well and fixed in place once the downward pressure from the handpiece prevented lateral movement of the 96-well plate (**Figure 1B**). Proper placement of the device was confirmed by the direct connection of the applicator tip to the liquid medium, absent of air bubbles. Upon confirmation that the outer O-ring laid flush on top of the edge of the appropriate well, each sample of worms was exposed to a certain number of shock waves ranging from 0 to 500 impulses. The shock waves (**Figures 1C,D**) produced a mixing effect on the liquid sample, ensuring that all worms in the well were exposed to shock waves (**Figures 1E–G** and **Video S1**). Following application, the handpiece was slowly raised from the 96-well plate and the applicator was cleaned

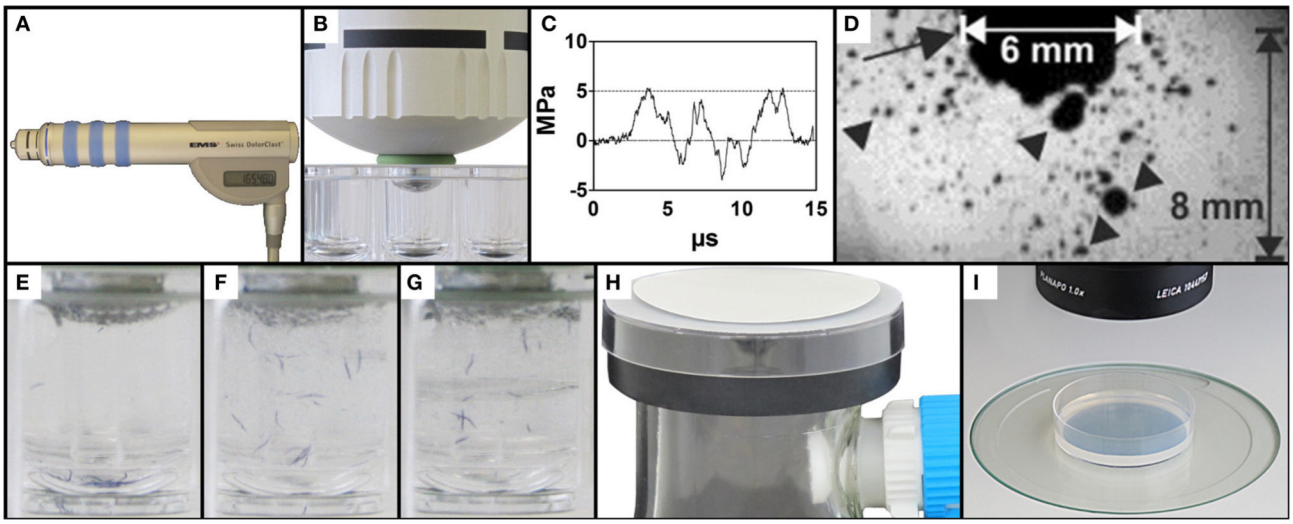

FIGURE 1 | Exposure of *C. elegans* to therapeutic shock waves. (A) Handpiece of the Swiss DolorClast therapeutic shock wave device used in the present study. **(B)** Placement of the shock wave device 6-mm applicator tip and specialized O-ring in a single well of a 96-well plate. **(C)** Pressure as a function of time of the shock waves applied in the present study. Measurements were taken at 5 mm distance to the applicator with a fiber optic probe laser hydrophone (FOPH, 2000; RP Acoustics, Leutenbach, Germany) coupled to an oscilloscope (LeCroy 9361; LeCroy, Chestnut Ridge; NY). **(D)** Cavitation bubbles (arrowheads) produced by the shock waves applied in the present study. The arrow points to the 6-mm applicator of the shock wave device. The size of the cavitation field generated by the shock wave device as operated in the present study guaranteed that each worm was always exposed to cavitation when subjected to a shock wave, regardless of the position of the worm within the well. The image was taken with a high-speed CCD camera (Photron Ultima APX; Photron, Tokyo, Japan) with a framing rate of 300,000 frames per second and an exposure time of 1/2700,000 s. (**E**–**G**) Mixing property of shock wave application as shown by position of blue stained worms following 0, 10, and 50 shock waves, respectively, ensuring random, uniform exposure of *C. elegans* worms to shock waves. (**H**) Rapid-transfer method using membrane filters and vacuum suction to transfer *C. elegans* worms from liquid media to agar-plates in a matter of seconds. (**I**) Position of a worm-containing agar-plate under a dissecting microscope prepared for video capture.

before further usage to prevent sample contamination. Worms were allowed to recover from shock wave application in the well for between 0 and 180 min. For dose-response analysis, 15 groups of worms were exposed to different shock wave doses (between 0 and 500 shock waves) and no recovery time was allowed. Males were systematically removed through manual video observation from the data set, occurring twice in the dose response analysis and not at all in the other assays. Data from 2285 worms were included in the dose-response experiment. A total of 30 different groups of worms were assayed in the recovery assay (six different numbers of shock waves applied times five different recovery periods), with data from a total of 3322 worms included in the experiment. In the cavitation assay, 727 worms were included in the experiment.

RAPID TRANSFER OF WORMS FROM LIQUID TO AGAR PLATES

In order to rapidly transfer *C. elegans* worms from the (three-dimensional) liquid medium to (quasi-two-dimensional) agar plates, a modified membrane filter-vacuum filtration system was created (**Figure 1H**; **Video S2**). A 250 ml side-arm flask was attached to a vacuum pump (BVC-21, Vacuubrand, Wertheim, Germany) and fitted with a rubber safety cuff (E350.1, Carl Roth) with grease on both sides to improve the vacuum seal. The top of a 6 cm plastic petri dish with an approximately 1 cm diameter hole in the middle was placed on top of the safety cup. Thin mesh was sealed over the hole to help prevent bubbling of the above membrane during vacuum filtration. A polyethersulfone Millipore Express PLUS Membrane (47 mm diameter, 0.22 µm pore size, Millipore, Billerica, MA) was placed on top of the assembly shiny side up.

To prevent worms from sticking to pipette tips, 30 µl of S-Medium with 10% Tween 20 were added to each well. The contents were then removed from wells using a pipette. Over 5–10 s under vacuum suction, the contents were dispensed drop by drop on to the membrane. Drops were dispensed so that the liquid did not spread beyond the 1 cm hole in the plastic petri dish. Once the liquid passed through the membrane, the vacuum pump was turned off and the membrane was removed with forceps. The membrane was then flipped over and laid flat on a 6 cm NGM agar plate seeded with OP50 *E. coli*. The transfer process was completed upon removal of the membrane from the agar plate. **Video S2** shows the entire procedure.

LOCOMOTION DATA COLLECTION

After the transfer of worms, NGM agar plates were placed under a dissecting microscope (MZ75, Leica, Wetzlar, Germany; equipped with a 1.0× PlanApo objective) with an LCD light source set to a color temperature of 2800 K (KL 1500, Schott, Mainz, Germany) (**Figure 1I**). Using a 5.0 megapixel, mono digital camera (Grasshopper 2, Point Grey Research, Richmond, BC, Canada) and the video capture function of the software, WormLab (Version 2.0.1, MBF Bioscience, Williston, VT), plates were aligned so that all worms were within the field of view of the camera. One minute long videos were then captured at

15 frames per second (FPS) with a resolution of 1280 × 960 pixels.

Using a horizontal mm ruler and the measure function of WormLab, videos were determined to have a scale of 8.37 μm/pixel. Accordingly, the field-of-view of the camera was 10.7 by 8.0 mm. Using the settings defined in **Table S1**, videos were tracked from frame 1 to 900 (covering a one-minute period with 15 FPS) using WormLab (**Video S3**). Worm mid-point (x, y) position data was exported following the completion of tracking.

DATA PROCESSING AND ANALYSIS

Transformation of raw mid-point position (x, y) data was performed using Microsoft Excel 2010 (Microsoft, Redmond, WA). Worm tracks were only included in the final data set when position values were present for greater than 75 of the first 150 frames. This eliminated the possibility of double counting worms while also allowing a reasonable time window (6 s) to demonstrate movement.

From each worm track that met the inclusion parameters, average speed was calculated from up to 1 min tracked. One speed value, without regard to direction, was calculated for each second as the difference in distance over fifteen frames. Single-second speed values of greater than 500 μm/second were regarded as single frame tracking errors and thrown out of the data set (less than 0.1% of data points). The average of these values was then used to represent the worm's average speed. When reporting average speed of population groups, all qualifying worms were represented equally regardless of number of frames tracked.

In order to determine whether worms were moving or not, each included worm's distance from first frame tracked was calculated for each following frame tracked. Worms that, at any point during tracking, reached a distance of greater than 100 μm from the first frame tracked were considered to be moving. Likewise, those that did not reach 100 μm from the first frame tracked were counted as paralyzed. As with speed, each qualifying worm was counted equally in the reporting of the relative number of worms rendered paralyzed, regardless of number of frames tracked.

STATISTICAL AND DOSE-RESPONSE ANALYSIS

Speed of movement in the dose-response assay was analyzed using the Kruskal–Wallis test with Dunns post test using GraphPad Prism version 5.04 for Windows (GraphPad Software, San Diego, CA). Distribution of speed within individual treatment groups for the dose-response assay was assessed using the Kolmogrov-Smirnov normality test using GraphPad Prism. The recovery, cavitation, and NGM agar plates vs. liquid cultures assays were assessed using univariate ANOVA using IBM SPSS Statistics (version 22, IBM Corp., Armonk, NY). Shock wave exposure and waiting period were fixed factors in the recovery assay, while shock wave exposure and medium of exposure were fixed factors in the cavitation assay. Shock wave exposure and medium of growth were fixed factors in the NGM agar plates vs. liquid cultures assay. Speed of movement was used as dependent variables in all three assays. *Post-hoc* tests for pairwise comparisons were performed with Bonferroni multiple comparison tests.

For each dose group, distribution of averaged speed data of single worms was analyzed using the software, R (R Development Core Team, 2008) by calculation of medians, quartiles, means, and outliers using the Tukey method (Tukey, 1977). The average speed data of single worms were also used to determine the dose-response relationship based on the speed data of all worms in the various dose groups with R using the package, "drc" (Ritz and Streibig, 2005) with the LL.4 function (maximal and minimal values of y not fixed). The fractions of moving and affected worms were calculated for each dose group using Microsoft Excel, and used as the input for binomial dose-response analysis. Binomial dose-response analysis was performed in R using the package, "drc" (Ritz and Streibig, 2005) with the LL.2 function (binomial dose-response analysis with maximal y value of 1 and minimal y value of 0).

A p-value of 0.05 was used as the criterion for statistical significance.

RESULTS

DOSE-DEPENDENT BEHAVIORAL RESPONSE OF *C. ELEGANS* TO SHOCK WAVE EXPOSURE

Using two behavioral endpoints, we were able to demonstrate, for the first time, a dose-dependent effect of shock wave exposure on *C. elegans*. Increased exposure to shock waves resulted in statistically significantly ($p < 0.05$) decreased mean speed of movement while simultaneously increasing the proportion of worms rendered paralyzed (**Figure 2A**; **Videos S4**, **S5**; see also **Figures 4A–C**). Both parameters exhibited sigmoidal dose-response relationship (**Figures 2B,C**), and the half-maximal effective doses (ED_{50}) at EFD = 0.016 mJ/mm^2 (measured at a distance of 5 mm to the applicator) and shock wave frequency of 5 Hz were calculated to be 44.6 and 112.9 shock waves for speed of movement and the proportion of worms rendered paralyzed, respectively (**Figures 2B,C**).

Dose dependence of the shock wave effect was observed on a population-wide basis. Within each dose level there were large interindividual differences in speed of movement observed. Across 15 dose groups, a total of 97 worms were labeled as outliers using Tukey's method for outlier detection (**Figure 2A**) (Tukey, 1977). Further investigation of the distribution of worm speed of movement within dose groups showed that all groups of worms exposed to more than five shock waves exhibited statistically significant ($p < 0.05$) right handed skew (Kolmogorov–Smirnov test; **Figures 2D–F**). Accordingly, high interindividual variability within shock wave exposure groups was observed in *C. elegans* even though the subjects were genetically identical and exposed to shock waves under consistent, controlled conditions.

C. ELEGANS RECOVER LOCOMOTIVE ABILITY

Worm speed of movement over increasing waiting periods after shock wave exposure approached control values, indicating a recovery of function (**Figure 3A**). Univariate analysis of variance (with shock wave exposure and waiting period as fixed factors, and speed of movement as dependent variable) showed that both the amount of shock waves and the waiting period had statistically significant ($p < 0.001$) influence on the speed of movement, as well as the combined shock wave/waiting period effect. Specifically, with increasing waiting period after shock wave exposure, worms showed, on average, higher speed

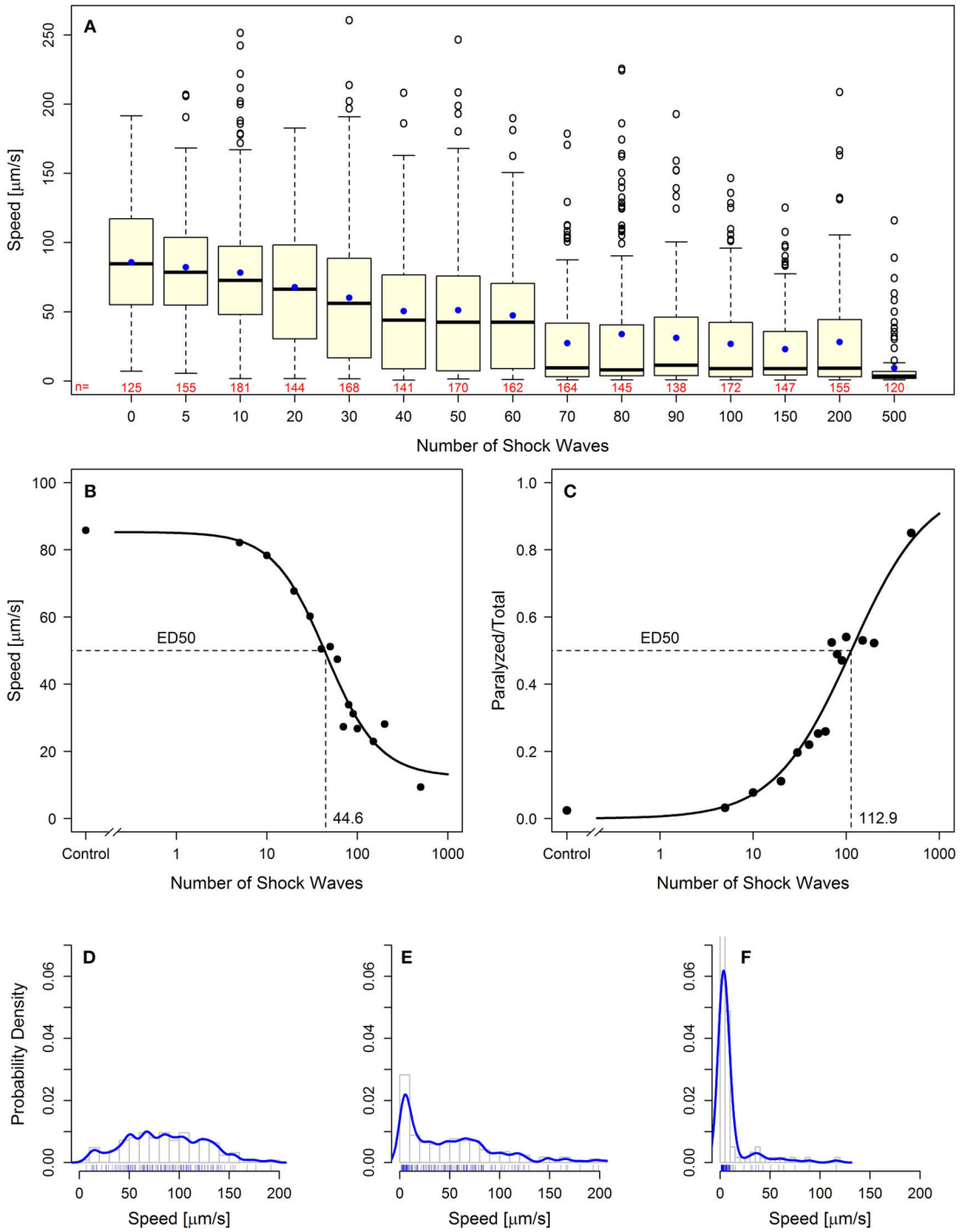

FIGURE 2 | Behavioral loss-of-function of *C. elegans* worms following shock wave exposure. (A) Increased exposure to shock waves resulted in decreased mean speed of movement in all groups of worms exposed to at least 30 shock waves ($p < 0.05$). Represented as individual points, 97 positive-lying outliers were found within shock wave exposed groups of worms. Horizontal lines within the boxes represent median speeds, dots within the boxes average speeds, and box and whiskers were plotted using the Tukey method. The numbers below the boxes indicate the numbers of worms per group. **(B)** Worms exhibited dose-dependent response to shock wave application ($ED_{50} = 44.6$ shock waves) using the parameter "speed of movement" (calculated using the average speed of each individual worm). The dots represent average speed of the worms in each exposure groups. **(C)** Worms exhibited dose-dependent response to shock wave application ($ED_{50} = 112.9$ shock waves) using the parameter "relative number of worms paralyzed." The dots represent the fraction of worms paralyzed in each exposure group. **(E)** Control worms showed a normal distribution of speed of movement. (**E**,**F**) Groups of worms exposed to more than five shock waves exhibited significant right-hand skew ($p < 0.05$). Probability density curves are shown for 50 **(E)** and 500 **(F)** shock waves, respectively.

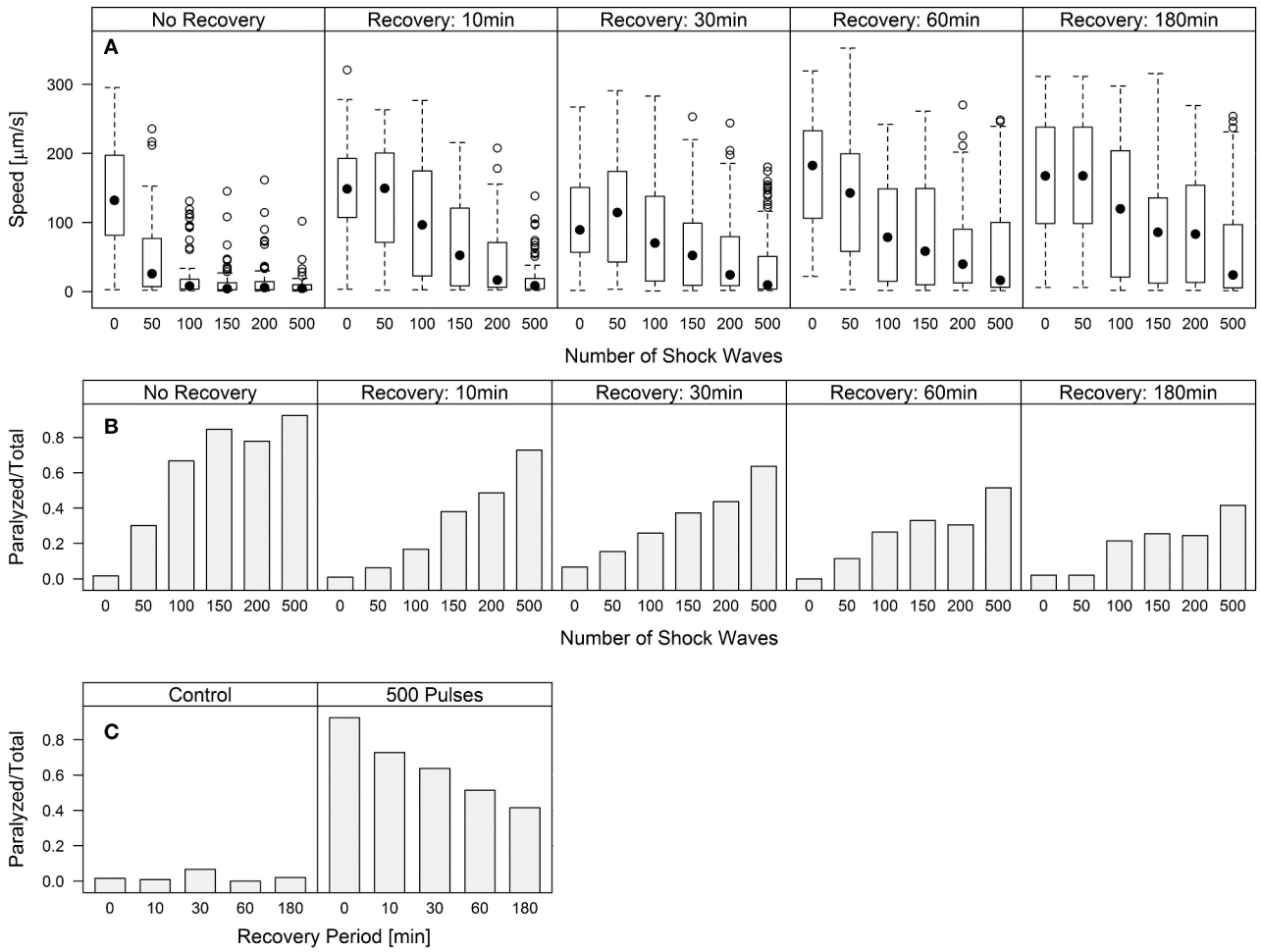

FIGURE 3 | *C. elegans* regain behavioral function following the application of shock waves. (A) Increased shock wave exposure reduced average worm speed ($p < 0.001$), while increased recovery period of up to 180 min resulted in increased speed ($p < 0.001$) **(B)** Fraction of worms paralyzed decreased over a 180 min recovery period. Regaining of function was observed in all groups after only 10 min, while control worms exhibited no noticeable difference between groups. **(C)** Worms exposed to 500 shock waves demonstrated gradually increasing recovery over four time points up to 180 min.

of movement (**Figure 3A**). The proportion of worms rendered paralyzed showed the same statistically significant ($p < 0.001$) effects, with decreasing amounts of worms rendered paralyzed over a 180 min waiting period after shock wave exposure (**Figure 3B**). This was best exemplified by worms that were exposed to 500 shock waves. These worms showed marked improvement at each time point over the course of 3 h (**Figure 3C**, **Video S6**).

POLYVINYL ALCOHOL REDUCES SHOCK WAVE EFFECT ON *C. ELEGANS*

Worms exposed to shock waves in PVA showed increased speed of locomotion and decreased proportion of worms rendered paralyzed than controls in S-Medium (**Figures 4D–I**, **5A**). Univariate analysis of variance (with shock wave exposure and medium of exposure as fixed factors, and speed of movement as dependent variable) showed that the amount of shock waves exposed, as well as the medium of exposure, had a statistically significant effect on speed of movement ($p < 0.001$). Furthermore, the combined shock wave and medium of exposure effect was statistically significant ($p = 0.011$). Post-hoc Bonferroni tests showed statistically significant differences between worms exposed to shock waves in PVA and worms exposed to shock waves in S-Medium after application of 100 ($p < 0.001$) and 500 shock waves ($p < 0.01$) but not after zero shock waves ($p > 0.05$). This indicates that, regardless of in which media, shock waves had a dose-dependent effect on worms. Control worms not exposed to shock waves indicated no ill-effects from PVA, as speed of locomotion was not found to be lower and proportion of worms rendered paralyzed was not higher. Worms exposed to 100 and 500 shock waves in PVA demonstrated higher speed of movement and lower proportion of worms rendered paralyzed than their respective S-Medium controls. Note that the high inter-individual variability reported in the main experiment (**Figure 2**) was not specifically favored by one medium in which worms were exposed to shock waves over another (S-Medium or polyvinyl alcohol).

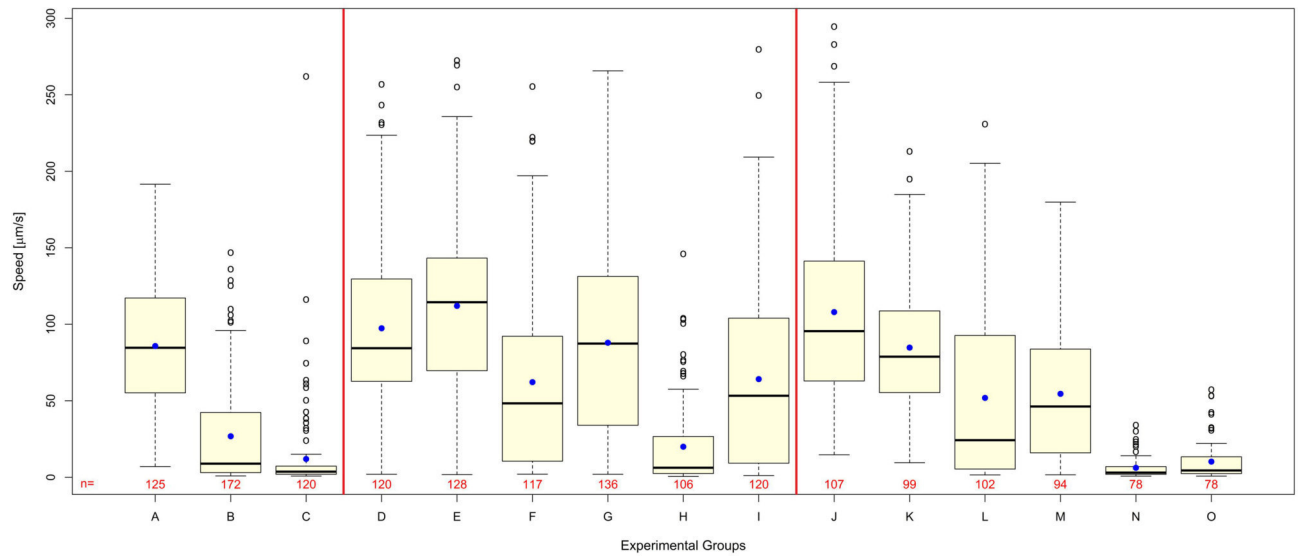

FIGURE 4 | Polyvinyl alcohol reduces shock wave effect on *C. elegans*, whereas shock wave exposed *C. elegans* grown on NGM agar plates exhibit similar behavioral change to shock wave exposed *C. elegans* raised in liquid cultures. (A–C) Worms exposed to 0 **(A)**, 100 **(B)**, or 500 **(C)** shock waves in the main experiment of this study (these data are the same as those shown in **Figure 2A** and are displayed again here as a comparison only). **(D–I)** Worms exposed to 0 **(D)**, 100 **(F)**, or 500 **(H)** shock waves in S-Medium, compared to worms exposed to 0 **(E)**, 100 **(G),** or 500 **(I)** shock waves in polyvinyl alcohol, a medium with low cavitation activity. Note that worms exposed to shock waves in polyvinyl alcohol demonstrated higher average worm speed than controls in S-medium ($p < 0.001$) immediately following application of shock wave. **(J–O)** Worms raised in liquid cultures and exposed to 0 **(J)**, 100 **(L)**, or 500 **(N)** shock waves in S-Medium, compared to worms grown on NGM agar plates and exposed to 0 **(K)**, 100 **(M)**, or 500 **(O)** shock waves. Note that shock wave exposure resulted in decreased speed of locomotion in both worms grown on NGM agar plates and worms raised in liquid cultures ($p < 0.001$). Medium of growth was not found to significantly affect speed of locomotion ($p = 0.154$), but the combined effect of medium of growth and shock wave exposure was found to be significant ($p = 0.004$). Horizontal lines within the boxes represent median speeds, dots within the boxes average speeds, and box and whiskers were plotted using the Tukey method. Positive-lying outlies are represented as individual points. It is of note that the high inter-individual variability reported in the main experiment (**Figure 2**) was neither specifically favored by one nature of medium in which worms were exposed to shock waves over another (S-Medium or polyvinyl alcohol) nor one culture media over another (S-medium vs. NGM agar plates). The numbers below the boxes indicate the numbers of worms per group.

C. ELEGANS GROWN ON NGM AGAR PLATES EXHIBIT SIMILAR BEHAVIORAL RESPONSE TO SHOCK WAVE

Worms grown on NGM agar plates showed response to shock wave similar to that of worms raised in liquid cultures (**Figures 4J–O**, **5B**). Namely, univariate analysis of variance (with shock wave exposure and medium of growth as fixed factors, and speed of movement as dependent variable) showed a statistically significant decrease in speed of locomotion ($p < 0.001$) caused by exposure to shock wave. The speed of locomotion was not found to be significantly different between worms grown on NGM agar plates and worms raised in liquid cultures ($p = 0.154$), while the combined effect of shock wave and medium of growth was significant ($p = 0.004$). *Post-hoc* Bonferroni tests showed statistically significant differences between worms grown on NGM agar plates and worms raised in liquid cultures after application of zero ($p < 0.001$) but not after 100 shock waves ($p > 0.05$) or 500 shock waves ($p > 0.05$). Note that the high inter-individual variability reported in the main experiment (**Figure 2**) was not specifically favored by one nature of culture media over another (S-medium vs. NGM agar plates).

DISCUSSION

The results of the present study can be summarized as follows: *C. elegans* worms exposed to shock waves generated with a therapeutic shock wave device demonstrate, within a population group, (i) dose-dependent reduction in mean speed of movement and (ii) dose-dependent increase in percentage of worms rendered paralyzed. Both effects were reversible and represented a species-specific behavioral outcome that is comparable to that of higher organisms. Importantly, individual speed of movement showed high interindividual variability within shock wave exposure groups despite the fact that all exposed subjects were genetically identical and exposed to shock waves under consistent, highly controlled conditions. Accordingly, our null hypothesis was rejected. Furthermore, cavitation appears to be a significant injurious component of the shock waves used in the present study.

With regard to the validity of our novel C. *elegans*/shock wave model of br-mTBI, we aimed to produce symptoms in *C. elegans* that were measurable, like in humans, using a behavioral readout. In humans, mTBI is characterized by a wide range of short- and long-term neurologic symptoms such as headaches, loss of vision, fatigue, confusion, memory loss, and temporary loss of consciousness, among others (Heltemes et al., 2012). Using the behavioral endpoint of locomotion that is well-established in the literature (Rajini et al., 2008), we showed that *C. elegans* display reversible effects of paralysis following shock wave exposure. While much simpler than the complex behavioral outcomes observed in humans and mammalian models, the effects observed

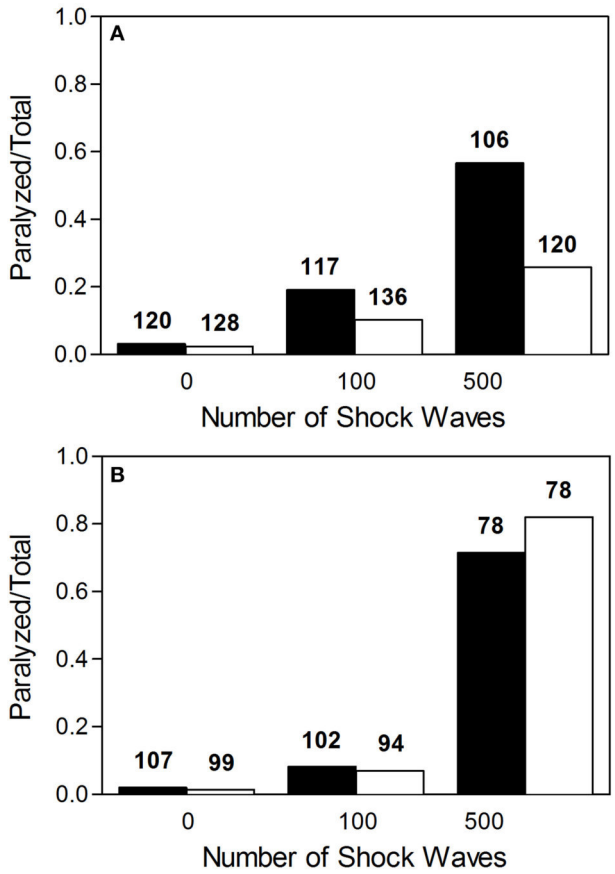

FIGURE 5 | Proportion of worms rendered paralyzed after exposure to shock waves. (A) Fraction of worms paralyzed increased with added shock wave exposure, while the instance of paralysis was lower in worms exposed in polyvinyl alcohol (open bars) than in worms exposed in S-medium (closed bars). **(B)** Fraction of worms paralyzed increased with added shock wave exposure in both worms grown on NGM agar plates (open bars) and worms raised in liquid cultures (closed bars). The numbers above the boxes indicate the numbers of worms per group.

in *C. elegans* have—to some extent—similar characteristics as those observed in humans and mammalian models in that they contain a loss-of-function and a recovery. Moreover, the cause is analogous to hypothesized causes of br-mTBI. Specifically, the shock waves produced by the therapeutic shock wave generator used in the present study (i) have a duration on the order of microseconds, (ii) are characterized by a high positive pressure peak (approximately 5 MPa at a distance of 5 mm to the applicator in the present study) with (iii) an extremely short rising period (on the order of less than 1 μs), (iv) a high positive energy flux density (approximately 0.016 mJ/mm^2 at a distance of 5 mm to the applicator in the present study), and (v) a final tensile period that causes cavitation (**Figures 1C,D**). These characteristics are shared with those of blast overpressure waves (also known as shock waves), a possible inducer of mTBI (Chavko et al., 2007; Elder and Cristian, 2009). Particularly, cavitation has been hypothesized to be a substantial factor in the causation of br-mTBI (Goeller et al., 2012). Thus, we have created a model in which behavioral effects with similar characteristics to those observed in humans and mammalian models of br-mTBI (loss-of-function, recovery) were observed in *C. elegans*. Furthermore, such effects were observed after exposure to shock waves that have similar physical characteristics to shock waves that are hypothesized to induce br-mTBI in humans.

Cernak and Noble-Haeusslein (2010) have proposed the following criteria for blast-related neurotrauma models: (i) the injurious component of the blast should be clearly identified and reproduced in a controlled, reproducible, and quantifiable manner; (ii) the inflicted injury should be reproducible, quantifiable, and mimic components of human blast-induced neurotrauma; (iii) the injury outcome established based on morphological, physiological, biochemical, and/or behavioral parameters should be related to the chosen injurious component of the blast; and (iv) the mechanical properties (intensity, complexity of blast signature, and/or its duration) of the injurious factor should predict the outcome severity. Our novel *C. elegans*/shock wave model of br-mTBI fully meets the first and third of these criteria. As our data showed that the inflicted injury was quantifiable but only reproducible on a statistical basis within a population group, the second and fourth of these criteria match our results on a population basis only. In accordance with this, predicting alterations in speed of movement of a single worm was neither possible based on the number of applied shock waves nor the recovery time. Nor was it possible to determine the number of applied shock waves and the recovery time based on the speed of movement of a single worm. These observations may have far-reaching implications for br-mTBI research, diagnosis, and therapy in humans. It thus becomes greatly important to determine what factors, outside of a known primary blast input and genetic heterogeneity (both are controlled in this model of br-mTBI), result in the considerable prognostic variability seen in human patients with br-mTBI (Heltemes et al., 2012).

In humans, rapid diagnosis of TBI severity is recommended in order for proper initial treatment and expectancy of forthcoming effects (Department of Defense and Department of Veterans Affairs, 2013). In order to do so, initial evaluation of mTBI severity is typically performed using behavioral endpoints. Specifically, the U.S. Department of Defense and Department of Veteran Affairs (Washington, DC, USA) has recommended assessing mTBI severity by combining the scores of three tests to classify mTBI as mild, moderate, or severe (Department of Defense and Department of Veterans Affairs, 2013). The model bases classification on duration of amnesia, reactions to stimuli (verbal, motor, and eye-opening), and duration of loss of consciousness. Thus, behavior is considered an extremely important parameter in determining mTBI severity in humans. The results of the present study indicate that mTBI severity can indeed best be predicted by clinical analysis and not—on an individual basis—by knowledge of the severity of the initial traumatizing impact. Although genetic variation has been proposed as a possible factor in mTBI pathology (Jordan, 2007; Waters et al., 2013), the discovery made in the present study furthers the importance of determining what factors beyond genetic difference contribute to the pathogenesis of br-mTBI in humans. Furthermore, it shows that efforts to base treatment regimens on the magnitude of

exposure may be less fruitful than one might expect due to the lack of predictability of outcome. The findings in the present study are in line with clinical experience that br-mTBI remains best evaluated clinically on a patient-by-patient basis rather than based on known stimulus.

Both *in vitro* and *in vivo* methods have been developed to model mTBI; some were specifically developed to model br-mTBI. *In vitro* models of mTBI generally attempt to reproduce and investigate the cascades of molecular and cellular events that follow mTBI-induction (reviewed in Morrison et al., 2011); *in vivo* models, usually exposing mammals to blast or blunt trauma, mainly focus on the investigation of mTBI-related neuropathology (reviewed in Cernak and Noble-Haeusslein, 2010).

Mechanical stress applied to an *in vitro* isolation of neurons, although not produced using known mTBI inducers, allows for the observation and analysis of specific pathways that lead to observed mTBI effects. By limiting conditions and pathways, *in vitro* methods can be useful for the understanding of very specific mechanisms. However, these methods, while reproducible and potentially high-throughput, are incomplete models of mTBI. Molecular and cellular changes can be observed, but these changes are not directly linked to behavior. Our novel *C. elegans*/shock wave model of br-mTBI shares the same advantages of *in vitro* methods in terms of being high-throughput and reproducible, but also provides a dynamic model using an *in vivo* system with behavioral readout. Combined with the fact that *C. elegans* has a fully known nervous system, *C. elegans* can be used to investigate individual neurons and other cellular/tissue effects, while linking such changes on an individual basis to behavioral output (de Bono and Maricq, 2005). Furthermore, the ability of *C. elegans* to live in a liquid environment allows for easy, reliable, and reproducible application of both positive and negative pressure of shock waves. Thus, the novel *C. elegans*/shock wave model developed in the present study offers superior possibilities than established *in vitro* methods for br-mTBI research. It is of note that both worms grown on NGM agar plates and worms raised in liquid cultures showed the same general dose-dependent response to exposure of shock waves (**Figures 4J–O**, **5B**). However, worms were not identical at baseline. Rather, worms raised in liquid cultures showed on average a higher speed of movement on agar plates than worms grown on NGM agar plates. The reason for this phenomenon is unknown and has to our knowledge not reported in the literature before. It was also this difference at baseline that caused the combined effect of shock wave and medium of growth to be statistically significant.

Mammalian models of br-mTBI have been established in multiple species. Mice and rats represent more than 90% of the corresponding literature, although other animals have also been used. In these models, mTBI-like conditions similar to those observed in humans have been successfully reproduced using various inducers. One of the most recent of these models was introduced by Goldstein et al. (2012). These authors developed a blast neurotrauma mouse model and found that head immobilization of the mice prevented blast-induced effects present following exposure without head immobilization. Thus, head movement as a result of blast wind was implicated as a damage-causing factor in the learning and memory deficits observed in specimen without head immobilization. Furthermore, pathology similar to that observed in br-mTBI victims was found in such mice. The findings by Goldstein et al. (2012) and others have furthered the understanding of mTBI neuropathology and have also led to the finding of biomarkers (Papa et al., 2012) and even possible pharmacological treatments that may reduce observed mTBI effects (Golding and Vink, 1994; Buki et al., 1999; Ohta et al., 2013). Although these findings represent progress, there remains a large void in the understanding of mTBI. The filling of such a knowledge gap may be slowed due to the difficulty of using mammalian models in a high-throughput manner. In mammalian models, subjects must be handled individually. Combined with the need that, in order to reliably determine ED_{50} doses, hundreds or even thousands of individuals must be investigated (as in the present study), mammalian models are simply inefficient. Even attempting to approach such a sample size is rendered impossible by concerns surrounding animal testing. To this end, our novel *C. elegans*/shock wave model of br-mTBI provides a viable alternative to conventional animal testing that reduces the need to subject mammals to pain, distress, and suffering. It should be noted that various methods have been proposed as alternatives to conventional animal testing, with the aim of replacing animals, reducing the numbers used, or refining the techniques to alleviate or minimize potential pain, distress and/or suffering (the so-called "3Rs" concept). Specifically, the U.S. National Toxicology Program, the U.S. Environmental Protection Agency, and other national and international agencies are committing significant resources toward the development of alternative species to be used as replacements for mammalian models in toxicological studies with particular emphasis on *C. elegans* (Boyd et al., 2010).

Our finding of outliers as an important endpoint of experimental br-mTBI research also required the analysis of thousands of *C. elegans* worms. Human outliers are known to exist (Heltemes et al., 2012) but–to our knowledge–have never been systematically addressed in br-mTBI research because of low sample sizes. On top of procedural and ethical issues, the increased sample-size ability of our novel *C. elegans*/shock wave model of br-mTBI provides the opportunity for in-depth investigation of subjects that display an unexpectedly positive or negative outlook. With sample sizes on the order of thousands combined with the presence of positive and negative outliers, this model provides a unique opportunity to reliably find an adequate sample of outliers. Side-by-side comparison of these outliers to worms that exhibit roughly the median effect could provide useful novel insight into the pathogenesis of br-mTBI.

The reduction in damaging effect on *C. elegans* in PVA indicates that cavitation is an important damage-causing component underlying the decrease of *C. elegans* locomotive ability. Cavitation has previously been shown to have an effect on nervous tissue, as Schelling et al. (1994) demonstrated reduced excitability in frog sciatic nerves following shock wave exposure in PVA as compared to control. Furthermore, cavitation is hypothesized to play an important role in the causation of br-mTBI (Goeller et al., 2012). This finding in *C. elegans* offers the potential to specifically investigate the effect of cavitation in an *in vivo* system. It is important to realize that the aforementioned recent

br-mTBI model of Goldstein et al. (2012) does not offer this potential because it is technically nearly impossible to expose mice to shock waves in liquid media such as PVA that reduce cavitation. Hence, comparing molecular and cellular consequences of exposing *C. elegans* to shock waves (present study) with molecular and cellular consequences of exposing mice to blast events as done by Goldstein et al. (2012) may be completely misleading due to the fact that in the latter model, primarily tertiary effects (in this case head movement caused by blast wind) are to blame for observed phenomena. In the present study, however, primary blast effects (blast overpressure and cavitation) are implicated as the main damage causing factors.

In summary, exposing *C. elegans* worms to shock waves generated by a therapeutic shock wave device shares (i) similar physical characteristics of the applied shock waves to shock waves that are hypothesized to induce br-mTBI in humans, and (ii) species-specific behavioral characteristics similar to those observed in humans and mammalian models of br-mTBI, with known ED_{50} doses for two behavioral endpoints (average speed of movement; relative number of worms rendered paralyzed). Based on the observation of large interindividual variability (i.e. lack of predictable outcome based on known input), we hypothesize that br-mTBI treatment methodology based on measured blast input is an unreliable solution. This finding supports the clinical experience that br-mTBI patients are best treated on a patient-by-patient basis.

AUTHOR CONTRIBUTIONS

Nicholas B. Angstman, Hans-Georg Frank and Christoph Schmitz conceived and designed the experiments, Nicholas B. Angstman performed experiments, and Nicholas B. Angstman, Maren C. Kiessling, Hans-Georg Frank and Christoph Schmitz analyzed data and wrote the manuscript.

FUNDING

This work was supported by a grant from the Friedrich-Baur Foundation at the Ludwig-Maximilians University of Munich (to Maren C. Kiessling and Christoph Schmitz).

ACKNOWLEDGMENTS

The authors wish to thank Pia Unterberger (Department of Neuroanatomy, Ludwig-Maximilians University of Munich) for expert technical assistance, Pierre-Alain Bionda and Florian Colombo (Electro Medical Systems) for providing the laser hydrophone measurements (**Figure 1C**), and Drs. Philippe Kobel and Mohamed Farhat (Laboratory for Hydraulic Machines, École Polytechnique Fédérale de Lausanne, Switzerland) for the image showing cavitation bubbles (**Figure 1D**).

SUPPLEMENTARY MATERIAL

The Supplementary Material for this article can be found online at: http://www.frontiersin.org/journal/10.3389/fnbeh.2015.00012/abstract

Video S1 | Uniform exposure of *C. elegans* to therapeutic shock waves. Blue dyed worms demonstrate the mixing property of the therapeutic shock wave device.

Video S2 | Novel method for rapid transfer of *C. elegans* from liquid media to agar plates. Transfer of worms took place in under 30 s—from time of well-extraction to placement of worms on ready-for-analysis agar plates.

Video S3 | Tracking of *C. elegans* movement using the WormLab software. Video demonstrates tracking of control worms. Each worm assigned a number, green dot indicating mid-point of the worm.

Video S4 | Control sample of *C. elegans*. Worms exposed to zero shock waves.

Video S5 | *C. elegans* exposed to shock waves. Worms not allowed recovery period following exposure to 500 shock waves.

Video S6 | *C. elegans* following post-shock wave recovery period. Worms exposed to 500 shock waves and allowed to recover for 180 min before analysis.

Table S1 | Tracking Settings used in WormLab software.

REFERENCES

Associated Press. (2007). *Carson Study: 1 in 6 Shows TBI Symptoms. Fort Carson, Colorado*. Available online at: www.armytimes.com/article/20070411/NEWS/704110335/Carson-study-1-6-shows-TBI-symptoms (Assessed October 16, 2014).

Boyd, W. A., Smith, M. V., Kissling, G. E., and Freedman, J. H. (2010). Medium- and high-throughput screening of neurotoxicants using *C. elegans*. *Neurotoxicol. Teratol.* 32, 68–73. doi: 10.1016/j.ntt.2008.12.004

Buki, A., Okonkwo, D. O., and Povlishock, J. T. (1999). Postinjury cyclosporin A administration limits axonal damage and disconnection in traumatic brain injury. *J. Neurotrauma* 16, 511–21.

Cernak, I., and Noble-Haeusslein, L. J. (2010). Traumatic brain injury: an overview of pathobiology with emphasis on military populations. *J. Cereb. Blood Flow Metab.* 30, 255–266. doi: 10.1089/neu.1999.16.511

Chavko, M., Koller, W. A., Prusaczyk, W. K., and McCarron, R. M. (2007). Measurement of blast wave by a miniature fiber optic pressure transducer in the rat brain. *J. Neurosci. Methods* 159, 277–281. doi: 10.1016/j.jneumeth.2006.07.018

Császár, N. B. M., and Schmitz, C. (2013). Extracorporeal shock wave therapy in musculoskeletal disorders. *J. Orthop. Surg. Res.* 8:22. doi: 10.1186/1749-799X-8-22

de Bono, M., and Maricq, A. V. (2005). Neuronal substrates of complex behaviors in *C. elegans*. *Annu. Rev. Neurosci.* 28, 451–501. doi: 10.1146/annurev.neuro.27.070203.144259

Delius, M., and Gambihler, S. (1992). "Effect of shock waves on gallstones and materials," *in Lithotripsy and Related Techniques for Gallstone Treatment*, eds G. Paumgartner, T. Sauerbruch, M. Sackmann, and H. Burhenne (St. Louis; Baltimore; Boston; Chicago; London: Mosby Year Book), 27–33.

DePalma, R. G., Burris, D. G., Champion, H. R., and Hodgson, M. J. (2005). Blast injuries. *N. Engl. J. Med.* 352, 1335–1342. doi: 10.1056/NEJMra042083

Department of Defense and Department of Veterans Affairs. (2013). *DoD/VA Code Final Proposal - 508 compliant*. http://www.cdc.gov/nchs/data/icd9/Sep08TBI.pdf (Accessed July 9, 2014)

Elder, G. A., and Cristian, A. (2009). Blast-related mild traumatic brain injury: mechanisms of injury and impact on clinical care. *Mt. Sinai J. Med.* 76, 111–118. doi: 10.1002/msj.20098

Gerdesmeyer, L., Frey, C., Vester, J., Maier, M., Weil, L. Jr., Weil, L. Sr., et al. (2008). Radial extracorporeal shock wave therapy is safe and effective in the treatment of chronic recalcitrant plantar fasciitis: results of a confirmatory randomized placebo-controlled multicenter study. *Am. J. Sports Med.* 36, 2100–2109. doi: 10.1177/0363546508324176

Goeller, J., Wardlaw, A., Treichler, D., O'Bruba, J., and Weiss, G. (2012). Investigation of cavitation as a possible damage mechanism in blast-induced traumatic brain injury. *J. Neurotrauma* 29, 1970–1981. doi: 10.1089/neu.2011.2224

Golding, E. M., and Vink, R. (1994). Inhibition of phospholipase C with neomycin improves metabolic and neurologic outcome following traumatic brain injury. *Brain Res.* 668, 46–53. doi: 10.1016/0006-8993(94)90509-6

Goldstein, L. E., Fisher, A. M., Tagge, C. A., Zhang, X.-L., Velisek, L., Sullivan, J. A., et al. (2012). Chronic traumatic encephalopathy in blast-exposed military veterans and a blast neurotrauma mouse model. *Sci. Transl. Med.* 4:134ra60. doi: 10.1126/scitranslmed.3003716

Hayakawa, K. (1991). Acoustic characteristics of PVA gel. 1991 IEEE Ultrasonics Symposium. *N.Y. Inst. Electr. Electron. Eng*. 1989, 969–972.

Heltemes, K. J., Holbrook, T. L., Macgregor, A. J., and Galarneau, M. R. (2012). Blast-related mild traumatic brain injury is associated with a decline in self-rated health amongst US military personnel. *Injury* 43, 1990–1995. doi: 10.1016/j.injury.2011.07.021

Hoge, C. W., McGurk, D., Thomas, J. L., Cox, A. L., Engel, C. C., and Castro, C. A. (2008). Mild traumatic brain injury in U.S. Soldiers returning from Iraq. *N. Engl. J. Med.* 358, 453–463. doi: 10.1056/NEJMoa072972

Jordan, B. D. (2007). Genetic influences on outcome following traumatic brain injury. *Neurochem. Res.* 32, 905–915. doi: 10.1007/s11064-006-9251-3

Jorgensen, E. M., and Mango, S. E. (2002). The art and design of genetic screens: caenorhabditis elegans. *Nat. Rev. Genet.* 3, 356–369. doi: 10.1038/nrg794

Morrison, B. III, Elkin, B. S., Dolle, J.-P., and Yarmush, M. L. (2011). In vitro models of traumatic brain injury. *Annu. Rev. Biomed. Eng.* 13, 91–126. doi: 10.1146/annurev-bioeng-071910-124706

Nakagawa, A., Manley, G. T., Gean, A. D., Ohtani, K., Armonda, R., Tsukamoto, A., et al. (2011). Mechanisms of primary blast-induced traumatic brain injury: insights from shock-wave research. *J. Neurotrauma* 28, 1101–1119. doi: 10.1089/neu.2010.1442

Ohta, M., Higashi, Y., Yawata, T., Kitahara, M., Nobumoto, A., Ishida, R., et al. (2013). Attenuation of axonal injury and oxidative stress by edaravone protects against cognitive impairments after traumatic brain injury. *Brain Res.* 1490, 184–192. doi: 10.1016/j.brainres.2012.09.011

Papa, L., Lewis, L. M., Silvestri, S., Falk, J. L., Giordano, P., Brophy, G. M., et al. (2012). Serum levels of ubiquitin C-terminal hydrolase distinguish mild traumatic brain injury from trauma controls and are elevated in mild and moderate traumatic brain injury patients with intracranial lesions and neurosurgical intervention. *J. Trauma Acute Care Surg.* 72, 1335–1344. doi: 10.1097/TA.0b013e3182491e3d

Portman, D. S. (2006). *Profiling C. Elegans Gene Expression with DNA Microarrays*. Rochester, NY: WormBook.

Rajini, P. S., Melstrom, P., and Williams, P. L. (2008). A comparative study on the relationship between various toxicological endpoints in Caenorhabditis elegans exposed to organophosphorus insecticides. *J. Toxicol. Environ. Health Part A* 71, 1043–1050. doi: 10.1080/15287390801989002

Rassweiler, J. J., Knoll, T., Kohrmann, K.-U., McAteer, J. A., Lingeman, J. E., Cleveland, R. O., et al. (2011). Shock wave technology and application: an update. *Eur. Urol.* 59, 784–796. doi: 10.1016/j.eururo.2011.02.033

R Development Core Team. (2008). *R: A Language and Environment for Statistical Computing*. Vienna, Austria.

Ritz, C., and Streibig, J. C. (2005). Bioassay analysis using R. *J. Stat. Softw.* 12, 1–22. Available online at: www.jstatsoft.org/v12/i05/paper

Robinson, D. E., and Kossoff, G. (1978). "Pulse echo visualisation," in *Ultrasound: Its Applications in Medicine and Biology*, ed F. J. Fry (Amsterdam: Elsevier), 593–596. doi: 10.1016/B978-0-444-41641-4.50008-X

Rosenfeld, J. V., McFarlane, A. C., Bragge, P., Armonda, R. A., Grimes, J. B., and Ling, G. S. (2013). Blast-related traumatic brain injury. *Lancet Neurol.* 12, 882–893. doi: 10.1016/S1474-4422(13)70161-3

Schelling, G., Delius, M., Gschwender, M., Grafe, P., and Gambihler, S. (1994). Extracorporeal shock waves stimulate frog sciatic nerves indirectly via a cavitation-mediated mechanism. *Biophys. J.* 66, 133–140. doi: 10.1016/S0006-3495(94)80758-1

Schmitz, C., Császár, N. B., Rompe, J.-D., Chaves, H., and Furia, J. P. (2013). Treatment of chronic plantar fasciopathy with extracorporeal shock waves (review). *J. Orthop. Surg. Res.* 8:31. doi: 10.1186/1749-799X-8-31

Scott, S. G., Belanger, H. G., Vanderploeg, R. D., Massengale, J., and Scholten, J. (2006). Mechanism-of-injury approach to evaluating patients with blast-related polytrauma. *J. Am. Osteopath. Assoc.* 106, 265–270.

Speed, C. (2014). A systematic review of shockwave therapies in soft tissue conditions: focusing on the evidence. *Br. J. Sports Med*. 48, 1538–1542. doi: 10.1136/bjsports-2012-091961

Sulston, J. E., and Brenner, S. (1974). The DNA of Caenorhabditis elegans. *Genetics* 77, 95–104.

Tukey, J. W. (1977). *Exploratory Data Analysis*. Reading, MA: Addison-Wesley Pub. Co.

Wang, C.-J. (2012). Extracorporeal shockwave therapy in musculoskeletal disorders. *J. Orthop. Surg. Res.* 7:11. doi: 10.1186/1749-799X-7-11

Waters, R. J., Murray, G. D., Teasdale, G. M., Stewart, J., Day, I., Lee, R. J., et al. (2013). Cytokine gene polymorphisms and outcome after traumatic brain injury. *J. Neurotrauma* 30, 1710–1716. doi: 10.1089/neu.2012.2792

White, J. G., Southgate, E., Thomson, J. N., and Brenner, S. (1986). The structure of the nervous system of the nematode Caenorhabditis elegans. *Philos. Trans. R. Soc. Lond. B. Biol. Sci.* 314, 1–340. doi: 10.1098/rstb.1986.0056

Conflict of Interest Statement: Christoph Schmitz serves as paid consultant for Electro Medical Systems (Nyon, Switzerland), the manufacturer of the Swiss DolorClast that was used in the present study to generate shock waves, as well as paid consultant for MBF Bioscience (Williston, VT, USA), the manufacturer of the WormLab software that was used in the present study to analyze data. However, Christoph Schmitz has not received financial support directly or indirectly related to this manuscript. The authors declare that the research was conducted in the absence of any commercial or financial relationships that could be construed as a potential conflict of interest.

*Received: 09 July 2014; accepted: 13 January 2015; published online: 06 February 2015. Citation: Angstman NB, Kiessling MC, Frank H-G and Schmitz C (2015) High interindividual variability in dose-dependent reduction in speed of movement after exposing C. elegans to shock waves. Front. Behav. Neurosci. **9**:12. doi: 10.3389/fnbeh.2015.00012*

This article was submitted to the journal Frontiers in Behavioral Neuroscience.

6. Paper II

frontiers in Behavioral Neuroscience

ORIGINAL RESEARCH
published: 31 March 2016
doi: 10.3389/fnbeh.2016.00060

Advanced Behavioral Analyses Show that the Presence of Food Causes Subtle Changes in *C. elegans* Movement

Nicholas B. Angstman, Hans-Georg Frank and Christoph Schmitz *

Department of Neuroanatomy, Ludwig-Maximilians University of Munich, Munich, Germany

As a widely used and studied model organism, *Caenorhabditis elegans* worms offer the ability to investigate implications of behavioral change. Although, investigation of *C. elegans* behavioral traits has been shown, analysis is often narrowed down to measurements based off a single point, and thus cannot pick up on subtle behavioral and morphological changes. In the present study videos were captured of four different *C. elegans* strains grown in liquid cultures and transferred to NGM-agar plates with an *E. coli* lawn or with no lawn. Using an advanced software, WormLab, the full skeleton and outline of worms were tracked to determine whether the presence of food affects behavioral traits. In all seven investigated parameters, statistically significant differences were found in worm behavior between those moving on NGM-agar plates with an *E. coli* lawn and NGM-agar plates with no lawn. Furthermore, multiple test groups showed differences in interaction between variables as the parameters that significantly correlated statistically with speed of locomotion varied. In the present study, we demonstrate the validity of a model to analyze *C. elegans* behavior beyond simple speed of locomotion. The need to account for a nested design while performing statistical analyses in similar studies is also demonstrated. With extended analyses, *C. elegans* behavioral change can be investigated with greater sensitivity, which could have wide utility in fields such as, but not limited to, toxicology, drug discovery, and RNAi screening.

Keywords: *C. elegans*, *E. coli*, food, locomotion, tracking

OPEN ACCESS

Edited by:
Nuno Sousa,
University of Minho, Portugal

Reviewed by:
Andreia Teixeira-Castro,
University of Minho, Portugal
Andre Brown,
Imperial College London, UK

***Correspondence:**
Christoph Schmitz
christoph_schmitz@med.uni-muenchen.de

Received: *29 June 2015*
Accepted: *14 March 2016*
Published: *31 March 2016*

Citation:
Angstman NB, Frank H-G and Schmitz C (2016) Advanced Behavioral Analyses Show that the Presence of Food Causes Subtle Changes in C. elegans Movement. Front. Behav. Neurosci. 10:60. doi: 10.3389/fnbeh.2016.00060

INTRODUCTION

As a highly-used model organism, *Caenorhabditis elegans* (*C. elegans*) worms offer a wide range of possibilities for scientific research. With advantages including, but not limited to, easy maintenance and handling, forward and reverse genetic manipulability (Jorgensen and Mango, 2002), and a fully mapped nervous system connectome of 302 neurons (White et al., 1986), *C. elegans* offer an alternative to larger rodent model organisms. Furthermore, *C. elegans* can be cultured in both liquid media and on agar plates (Sulston and Brenner, 1974; Angstman et al., 2015) and fed with concentrated *Escherichia coli* (*E. coli*).

Behavioral analysis of *C. elegans* is generally performed on NGM-agar plates in a quasi 2D model under a dissecting microscope using video capturing software, although assays measuring behavior in liquid have been demonstrated (Hardaway et al., 2014; Restif et al., 2014), as have

assays in behavioral arenas (Albrecht and Bargmann, 2011). As NGM-agar plate behavior assays remain the status quo, various tracking software is available to generate a readout on such behavior (summarized in Husson et al., 2012). Features of such software range from single worm tracking to multi-worm tracking, and from single point (centroid) tracking to full worm outline tracking (**Table 1**). Although, readouts using methods are often limited to speed of locomotion, more complicated behavioral phenotypes such as omega bending and reversals have been defined and detected (Huang et al., 2006). Some authors have attempted to identify as many as 702 features of worm movement by splitting certain features into sub-features (for example breaking up tail motion direction into forward, paused, and negative tail motion direction; Yemini et al., 2013).

As *C. elegans* are often raised on NGM-agar plates with an *E. coli* lawn, behavioral assays can be performed in the presence of food or on bare NGM-agar plates. The presence of food has previously been shown to decrease *C. elegans* speed of locomotion (Ramot et al., 2008). Thus, the effect of an *E. coli* lawn in a behavioral assay is of relevance to, at the very least, investigations of feeding related genes (see, e.g., de Bono and Bargmann, 1998).

In the present study we demonstrate that statistically significant behavioral differences beyond speed of locomotion can be observed when investigating four different strains of *C. elegans* on either NGM-agar plates with an *E. coli* lawn or with no lawn. Furthermore, we show that such a change in environment also affects the relationship of speed with other behavioral traits—that is behavioral change can be observed even in the lack of an observed change in speed of locomotion. Specifically we tested the hypothesis that various behavioral traits can be measured to show the effect of the presence of *E. coli* in the moving properties of *C. elegans*.

MATERIALS AND METHODS

Nematodes

Wild type (N2, Bristol), DA508 *npr-1(n1353),* DA609 *npr-1(ad609)*, and CX4148 *npr-1(ky13) C. elegans*, as well as OP50 *E. coli* were obtained from the Caenorhabditis Genetics Center (Minneapolis, MN, USA), which is funded by NIH Office of Research Infrastructure Programs (P40 OD010440). Mutant *npr-1* strains of *C. elegans* were selected based on previous findings that such strains are hyperactive on plates containing food as compared to wild type worms (de Bono and Bargmann, 1998). From a stock liquid culture, synchronous young adult worms were produced via sodium hypochlorite treatment and sucrose cleaning as described in detail in Angstman et al. (2015). Worms were raised in liquid cultures at 24°C in an incubated shaker (NB 205V, N Biotek, Bucheon, South Korea).

Assay

From a tube of worms in S-Medium, 10 μl containing 15–30 worms were pipetted on to a modified membrane filter-vacuum filtration system (Angstman et al., 2015). Following removal of liquid, membrane filters were flipped and placed on to a 6 cm NGM-agar plate (see Supplemental Video 2 in Angstman et al., 2015). Plates contained either an *E. coli* lawn (created by spreading over the agar surface and allowing to grow overnight) or no lawn (control).

Plates were immediately placed under a dissecting microscope (MZ75; Leica, Wetzlar, Germany; equipped with 1.0X PlanApo objective) with an LCD light source with a color temperature of 2800 K (KL 1500; Schott, Mainz, Germany). Using the video capture function of the software, WormLab (Version 3.0.0, MBF Bioscience, Williston, VT, USA), 60 s long videos with a resolution of 1280 × 960 pixels were taken at 15 frames/s using a mono digital camera (Grasshopper 2, Point Grey Research, Richmond, BC, Canada). Using a horizontal mm ruler and the measure function of WormLab, videos were determined to have a scale of 8.37 μm/pixel, which enabled precise and accurate investigation of the parameters described in the next section. Accordingly, the field-of-view of the camera was 10.7 by 8.0 mm and, thus, 3% of the base area of the agar plates (**Figure 1** and **Supplementary Videos S1**, **S2**).

At the beginning of each video plates were adjusted so that all worms were within the field-of-view of the camera. All worms that were tracked for >75 of the first 150 frames were included in the final analysis, with track lengths of up to 900 frames possible. Tracks that started after the first 150 frames were excluded from

TABLE 1 | Summary of *C. elegans* tracking software features.

Tracker	Nemo[a]	The parallel worm Tracker[b]	OptoTracker[c]	Multimodal illumination and tracking system[d]	CoLBeRT[e]	The multi worm tracker[f]	Optomechanical system for virtual environments[g]	Worm Tracker 2.0[h]	WormLab[i]
Single/ Multiple worms	Single	Multiple	Multiple	Single	Single	Multiple	Single	Single	Multiple
Tracking capability	Skeleton and outline	Mid-point	Mid-point	Skeleton and outline	Skeleton and outline	Skeleton and outline	Bright spot	Skeleton and outline	Skeleton and outline

[a] *Tsibidis and Tavernarakis, 2007*; [b] *Ramot et al., 2008*; [c] *Ramot et al., 2008*; [d] *Stirman et al., 2011*; [e] *Leifer et al., 2011*; [f] *Swierczek et al., 2011*; [g] *Faumont et al., 2011*; [h] *Geng et al., 2004*; [i] *Roussel et al., 2014*.

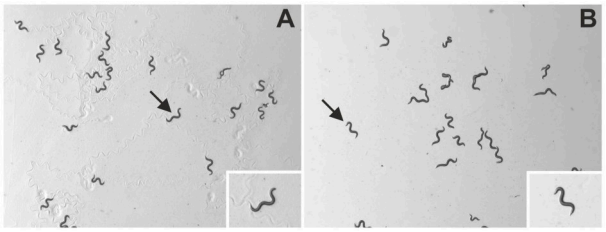

FIGURE 1 | Representative images of *C. elegans* as analyzed in the present study. The panels show unprocessed frames of videos of wild type (N2) *C. elegans* on NGM-agar plates with an *E. coli* lawn **(A)** or with no lawn **(B)**. The insets show individual worms (indicated by arrows) at higher magnification. The slightly uneven illumination of the panels stems from the fact that in the experimental setup of the present study, the field-of-view was placed offset from the middle of the agar plates. However, this had no impact on unequivocal identification and tracking of the worms on the plates (evaluation data not shown).

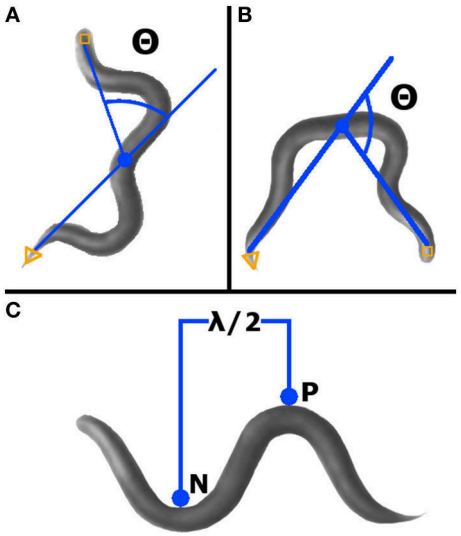

FIGURE 2 | WormLab advanced analyses. (A) Bending angle (Θ) was measured as the supplement of the angle between the head, mid-point, and tail. Worms with head, mid-point, and tail in line have an angle of zero. **(B)** Omega bending is indicated when the angle (Θ) created between the head, mid-point, and tail is <90° (i.e., the bending angle is >90°). **(C)** Wavelength was measured as two times the distance between the positive (P) and negative (N) stationary points.

the analysis because they could have represented worms that initially moved out of but then came back into the field-of-view of the camera. These parameters avoided the possibility of double counting individual worms.

Captured videos were tracked with WormLab using settings outlined in **Supplementary Table 1**. Results from each video including Position–Midpoint (x, y), Bending Angle-Mid-Point, Wavelength, Omega Bend, and Reversal were exported and processed using Microsoft Excel 2010 (Microsoft, Redmond, WA, USA).

Investigated Parameters

Speed of Locomotion

Speed of worms was calculated from Position to Midpoint (x, y) data as in our earlier study (Angstman et al., 2015). Direction was not taken into account. Using coordinates, speed was calculated for each second as the distance traveled over 15 frames. Single point values of >500 μm/s were considered outliers and removed from the data set. Each qualifying worm was represented with one value for average speed determined by the arithmetic mean of the values calculated each second.

Bending Angle

The bending angle is defined as the angle between the midpoint-head and midpoint-tail segments, with a straight worm set as zero degrees (**Figure 2A**). For a given worm, a bending angle was measured for each frame tracked. In the final readout of average bending angle for a given worm, the absolute value of the angle measured in each frame was averaged. Standard deviation of all absolute value bending angles was calculated for each qualifying worm.

Omega Bending

As defined by WormLab, omega bending occurs when the bending angle exceeds 90 degrees and continues until the bending angle goes below 90° (**Figure 2B**). Omega bending was counted only when a minimum duration of 10 frames was reached. For each worm meeting qualifying requirements, omega bending was expressed as a percentage of frames tracked.

Wavelength

This parameter is defined as the two times the measurement between the positive and the negative inflection points (**Figure 2C**). Wavelength was calculated for each worm in each frame tracked, except when at zero or only one inflection point was found. For qualifying worms, average wavelength was expressed as the average of all calculated wavelengths (i.e., from each frame tracked).

Reversal Frequency

This parameter was calculated based on smoothed speed provided by WormLab, a smoothed moving average speed taken over a 20 frame span (based on Cleveland and Devlin, 1988). In order to remove bias from possible incorrect head/tail recognition, smoothed speed was inversed if over half of the frames tracked were measured as negative speed values. Reversal was then counted only in stretches of negative smoothed speed ≥10 frames. Final results were reported for each qualifying worm as a percentage of reversals per frame tracked.

Statistical Analysis

In the final analyses of NGM-agar plates with an *E. coli* lawn, 172 N2 worms on 10 different plates, 189 *npr-1(n1353)* worms on six different plates, 132 *npr-1(ad609)* worms on six different plates and 129 *npr-1(ky13)* worms on six different plates were counted. Analyses of NGM-agar plates with no lawn included 173 N2 worms on 10 different plates, 159 *npr-1(n1353)* worms on six

different plates, 139 *npr-1(ad609)* worms on six different plates, and 167 *npr-1(ky13)* worms on six different plates.

Due to the fact that several worms were analyzed per plate, a nested ANOVA design was used to determine the significance of (i) lawn type (i.e., plates with an *E. coli* lawn vs. plates with no lawn) and (ii) whether the nested nature of this assay contributed to observed differences (c.f. Aarts et al., 2014). In the nested ANOVA, the various investigated parameters were used as the dependent variable, while lawn type was a fixed factor, and plate number was a random factor.

To investigate correlation between analyses, the runs test (c.f. Wald and Wolfowitz, 1940) was used to determine if relationships departed from linearity. If a statistically significant departure was not found, linear regression was used to compare analyses. If departure from linearity was statistically significant, non-parametric correlation (Spearman) was used.

Nested ANOVA was performed in SPSS (Version 23 for Windows; IBM, Armonk, NY, USA), while all other statistical analyses were performed in GraphPad Prism (version 5.04 for Windows; GraphPad Software, San Diego, CA, USA).

A p-value of 0.05 was used as the criterion for statistical significance in all analyses.

RESULTS

Lawn vs. No Lawn

The results of comparisons between worms on NGM-agar plates with an *E. coli* and worms on NGM-agar plates with no lawn are summarized in detail in **Table 2**. Lawn type was found to result

TABLE 2 | Summary of analyses and comparison between *C. elegans* on plates with *E. coli* and no lawn.

Analysis	Strain	Lawn Type				Lawn Type				Plate (Lawn Type)			
		E. coli		No Lawn									
		Mean	*SD*	*Mean*	*SD*	*df1*	*df2*	*F*	*p*	*df1*	*df2*	*F*	*p*
Average speed (μm/s)	N2	128.6	41.6	146.9	55.3	1	19.324	4.4	**0.049**	18	325	2.394	**0.001**
	npr-1(n1353)	110.8	39.6	130.4	49.0	1	10.226	5.2	**0.045**	10	336	3.679	**0.000**
	npr-1(ad609)	119.2	53.5	83.4	46.0	1	10.467	17.5	**0.002**	10	259	1.814	0.058
	npr-1(ky13)	165.9	182.4	182.4	62.7	1	10.551	2.5	0.140	10	298	2.129	**0.022**
Average Angle (°)	N2	34.3	14.2	40.0	17.1	1	19.387	6.3	**0.022**	18	325	2.287	**0.002**
	npr-1(n1353)	25.0	12.7	44.8	20.5	1	10.248	38.0	**0.000**	10	336	3.359	**0.000**
	npr-1(ad609)	28.2	12.1	48.9	24.3	1	11.108	98.6	**0.000**	10	259	0.776	0.652
	npr-1(ky13)	26.7	11.1	36.1	17.7	1	12.138	42.5	**0.000**	10	298	0.568	0.840
St. Dev. Angle (°)	N2	24.3	9.5	29.1	12.1	1	20.047	11.3	**0.003**	18	325	1.562	0.068
	npr-1(n1353)	17.4	8.7	31.1	13.1	1	10.367	59.5	**0.000**	10	336	2.272	**0.014**
	npr-1(ad609)	21.4	10.8	33.0	14.9	1	10.676	47.6	**0.000**	10	259	1.261	0.253
	npr-1(ky13)	18.1	6.6	25.6	12.7	1	11.453	36.9	**0.000**	10	298	0.824	0.606
Average wavelength (μm)	N2	383.0	42.7	347.5	43.9	1	19.931	36.9	**0.000**	18	325	1.653	**0.046**
	npr-1(n1353)	363.2	52.0	330.0	53.3	1	10.398	15.7	**0.002**	10	336	2.097	**0.024**
	npr-1(ad609)	346.1	70.2	318.2	67.3	1	10.580	6.3	**0.030**	10	259	1.465	0.153
	npr-1(ky13)	411.3	45.2	371.8	60.9	1	10.819	29.0	**0.000**	10	298	1.441	0.161
St. Dev. wavelength (μm)	N2	103.3	31.3	91.8	34.3	1	19.533	4.6	**0.045**	18	325	2.073	**0.007**
	npr-1(n1353)	103.4	33.4	90.9	30.8	1	10.419	6.8	**0.025**	10	336	1.996	**0.033**
	npr-1(ad609)	85.0	31.6	99.3	37.8	1	10.451	6.6	**0.027**	10	259	1.880	**0.048**
	npr-1(ky13)	93.1	31.9	86.1	35.4	1	10.803	3.1	0.108	10	298	1.468	0.150
Omega bending percent	N2	2.25	7.69	3.99	8.82	1	20.413	3.7	0.069	18	325	1.331	0.166
	npr-1(n1353)	0.82	4.08	7.31	11.61	1	10.440	27.1	**0.000**	10	336	1.900	**0.044**
	npr-1(ad609)	1.09	3.48	8.89	15.76	1	17.234	172.5	**0.000**	10	259	0.133	0.999
	npr-1(ky13)	0.08	0.75	3.00	9.12	1	11.394	9.0	**0.012**	10	298	0.857	0.574
Reversal percent	N2	2.90	6.59	5.88	10.44	1	21.214	8.7	**0.008**	18	325	1.008	0.449
	npr-1(n1353)	3.19	8.01	14.57	14.77	1	10.259	28.3	**0.000**	10	336	3.215	**0.001**
	npr-1(ad609)	8.22	12.22	21.63	13.23	1	10.566	49.7	**0.000**	10	259	1.501	0.139
	npr-1(ky13)	2.24	6.77	4.68	10.41	1	11.830	8.4	**0.014**	10	298	0.659	0.762

P-values smaller than 0.05 are given boldface.

in a statistically significant difference in 25/28 analyses across the four strains of *C. elegans*.

In all experiments carried out, worms showed substantial interindividual variation in all investigated parameters. For example, speed of locomotion of N2 worms on plates with an *E. coli lawn* varied between 5.5 and 221 μm/s, and on plates with no lawn between 4.0 and 255 μm/s (**Figure 3**). Besides this, mean values of all investigated parameters showed considerable inter-plate variability. For example, mean speed of locomotion of N2 worms on plates with an *E. coli* lawn varied between 106 and 155 μm/s among plates, and on plates with no lawn between 112 and 186 μm/s among plates (**Figure 3**).

Plate Effect

The nested factor—accounting for the fact that multiple specimen can be grouped by plate—accounted for statistically significant difference in 13/28 analyses (all results of statistical analysis are summarized in **Table 2**). Both lawn type and the nested factor were statistically significant in 12 cases. Lawn type, but not the nested factor, was statistically significant in 13 cases, while the nested factor, but not lawn type, was statistically significant in only one case. In only two cases was neither lawn type nor the nested factor statistically significant.

Correlation of Speed with Various Behavioral Analyses

The results of these analyses are summarized in **Table 3** for *C. elegans* on plates with an *E. coli* lawn and in **Table 4** for *C. elegans* on plates with no lawn. When comparing average speed to other analyses in worms on an *E. coli* lawn, statistically significant departure from linearity was found in only five cases out of 24 (six correlations across four strains). Departure from linearity was observed in 8/24 cases for worms on plates with no lawn. Linear regression and Spearman non-linear correlation yielded statistical significance in 12 cases for worms on NGM-agar plates with an *E. coli* lawn and 20 cases for worms on NGM-agar plates with no lawn.

DISCUSSION

Summary of Results

The main results of the present study can be summarized as follows: advanced *C. elegans* behavioral traits, in both wild type and mutant strains, can be used to demonstrate behavioral differences between test groups. Furthermore, such behavioral traits go beyond the standard measure of speed of locomotion and often either do not significantly correlate statistically with speed of locomotion or only correlate with speed of locomotion within certain test groups. Only one analysis, reversal percentage, was found to correlate with average speed of locomotion in all cases. High interindividual variability within analyses was observed, in line with our previously shown data (Angstman et al., 2015), and inter-plate variability was also shown to be a factor in some differences seen in the analyses. This reinforces the need for large sample sizes for behavioral analyses of *C. elegans*, and also shows the importance of using nested analyses when assaying behavior of multiple worms per NGM-agar plate. Using the methods demonstrated in the present study, the ability to accurately measure advanced traits of *C. elegans* behavior offers enhanced functionality in *C. elegans* research.

Relevance

The comparison of *C. elegans* worms moving on NGM-agar plates with an *E. coli* lawn to worms moving on NGM-agar plates with no lawn represents a relevant biological example for behavioral change in *C. elegans*. This methodology has been used previously using behavioral analysis on N2 worms (Schwarz et al., 2015). The *npr-1* strains used in the present study are described in this context as well. This methodology and these strains were, for example, used to identify genes that play a role in feeding in *C. elegans* (de Bono and Bargmann, 1998; de Bono et al., 2002). The behavioral traits used in the present study were also identified as characteristics of *C. elegans* behavior in the literature (e.g., Buckingham and Sattelle, 2008).

At first glance, it seems that the results of the present study are not in line with certain data reported by de Bono and Bargmann (1998) and de Bono et al. (2002). For example, de Bono and Bargmann (1998) found an increase in mean speed of locomotion

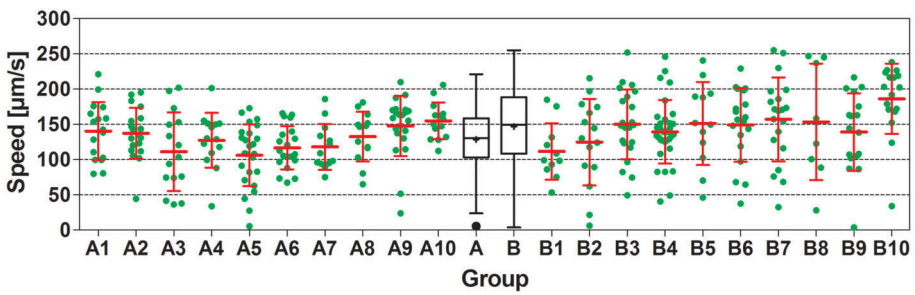

FIGURE 3 | Speed of locomotion of N2 (wild type) *C. elegans* on NGM agar plates with an *E. coli* lawn and on plates with no lawn. Groups A1–A10 and B1–B10 show individual data (green dots) and mean ± standard deviation (red lines) of speed of locomotion of N2 worms on 10 plates with an *E. coli* lawn (Groups A1–A10) and on 10 plates with no lawn (Groups B1–B10). Groups A and B show Tukey boxplots of the speed of locomotion of all worms on plates with an *E. coli* lawn (Group A) and of all worms on plates with no lawn (Group B). Nested ANOVA showed a statistically significant difference between worms on plates with an *E. coli* lawn and worms on plates with no lawn ($p = 0.049$) as well as a statistically significant effect among plates ($p = 0.001$; see also **Table 2**).

TABLE 3 | Summary of correlation between analyses for worms on plates with an *E. coli* lawn.

Calculation	Strain	Runs test			Linear regression			Non-linear correlation	
		Points Above line	Points Below line	*p*	r^2	*F*	*p*	*Spearman*	*p*
Average speed vs. average angle	N2	72	100	0.917	0.030	5.277	**0.023**		
	npr-1(n1353)	74	115	0.242	0.093	19.11	**<0.001**		
	npr-1(ad609)	55	77	0.315	0.01949	2.585	0.110		
	npr-1(ky13)	56	73	0.508	0.232	38.43	**<0.001**		
Average speed vs. St. Dev. angle	N2	76	96	0.810	0.001	0.232	0.631		
	npr-1(n1353)	74	115	0.699	0.014	2.697	0.102		
	npr-1(ad609)	52	80	0.792	0.002	0.310	0.579		
	npr-1(ky13)	62	67	0.766	0.014	1.824	0.179		
Average speed vs. average wavelength	N2	83	89	0.129	0.006	1.042	0.309		
	npr-1(n1353)	98	91	0.962	0.108	22.61	**<0.001**		
	npr-1(ad609)	67	65	0.397	0.403	87.78	**<0.001**		
	npr-1(ky13)	67	62	0.577	0.207	33.06	**<0.001**		
Average speed vs. St. Dev. wavelength	N2	87	85	0.649	0.178	36.93	**<0.001**		
	npr-1(n1353)	87	102	0.214	0.108	22.73	**<0.001**		
	npr-1(ad609)	60	72	0.301	0.017	2.219	0.139		
	npr-1(ky13)	64	65	0.430	0.016	2.048	0.155		
Average speed vs. omega bending Pct	N2	25	147	0.258	0.006	0.989	0.322		
	npr-1(n1353)	45	144	**<0.001**				–0.098	0.178
	npr-1(ad609)	17	115	0.344	0.008	1.084	0.300		
	npr-1(ky13)	22	107	**<0.001**				0.127	0.152
Average speed vs. reversal Pct	N2	54	118	**0.005**				–0.448	**<0.001**
	npr-1(n1353)	60	129	**<0.001**				–0.363	**<0.001**
	npr-1(ad609)	45	87	0.064	0.202	32.82	**<0.001**		
	npr-1(ky13)	32	97	**<0.001**				–0.314	**0.003**

P-values smaller than 0.05 are given boldface.

of wildtype (N2) *C. elegans* of ∼110 μm/s on plates with an *E. coli* lawn to ∼300 μm/s on plates with no lawn (+170%; in de Bono et al.'s (2002) study this difference was +225%). This difference is much greater than what was found in the present study (the mean speed of locomotion of N2 *C. elegans* was 128.6 μm/s on plates with an *E. coli* lawn and 146.9 μm/s (+14%) on plates with no lawn; **Table 2**). However, it is important to note that in the study of de Bono and Bargmann (1998), each average value represented the average speed of locomotion of at least 24 animals investigated on an unknown number of plates during more than 72 min of recording, and in the study of de Bono et al. (2002) each average value represented the average speed of locomotion of at least 25 animals investigated on an unknown number of plates during 4 min of recording. In the present study, the average values of the N2 worms represented the average speed of locomotion during 60 s of recording of 172 worms investigated on 10 plates with an E. coli lawn and 173 worms investigated on 10 plates with no lawn. Unfortunately, de Bono and Bargmann (1998) and de Bono et al. (2002) did not provide essential information about the video recording settings used in their experiments (i.e., the magnification of the objective lens, resolution of the digital camera, scale of the pixels, and size of the field-of-view of the camera). Thus, one cannot determine the relation between the size of the field-of-view of the camera and the size of the circular area in which worms could move during the recording time [this area had a diameter of 2.5 cm in the study of de Bono and Bargmann (1998) and 2.0 cm in the study of de Bono et al. (2002)]. As a result, it remains unknown how worms were handled that moved out of the field-of-view (or moved into the field-of-view, respectively) of the camera particularly during the long recording time of 72 min in the study of de Bono and Bargmann (1998). Because de Bono and Bargmann (1998) and de Bono et al. (2002) did not report standard deviations of speed of movement or potential alterations in speed of movement over

TABLE 4 | Summary of correlation between analyses for worms on plates with no lawn.

Calculation	Strain	Runs test			Linear regression			Non-linear correlation	
		Points above line	Points below line	*p*	r^2	*F*	*p*	Spearman	*p*
Average speed vs. average angle	N2	73	100	**0.032**				–0.2428	**0.001**
	npr-1(n1353)	71	88	0.680	0.316	72.63	**<0.001**		
	npr-1(ad609)	59	80	**0.010**				0.085	0.323
	npr-1(ky13)	69	98	0.088	0.164	32.31	**<0.001**		
Average speed vs. St. Dev. angle	N2	74	99	**0.006**				–0.198	**0.009**
	npr-1(n1353)	70	89	0.172	0.059	9.913	**0.002**		
	npr-1(ad609)	70	69	**<0.001**				0.207	**0.015**
	npr-1(ky13)	67	100	0.177	0.076	13.62	**<0.001**		
Average speed vs. average wavelength	N2	88	85	0.501	0.044	7.806	**0.006**		
	npr-1(n1353)	83	76	0.873	0.193	37.48	**<0.001**		
	npr-1(ad609)	67	72	0.639	0.065	9.456	**0.003**		
	npr-1(ky13)	77	90	0.593	0.170	33.80	**<0.001**		
Average speed vs. St. Dev. wavelength	N2	82	91	0.233	0.220	48.34	**<0.001**		
	npr-1(n1353)	82	77	0.901	0.178	33.94	**<0.001**		
	npr-1(ad609)	67	72	0.887	0.067	9.837	**0.002**		
	npr-1(ky13)	79	88	0.900	0.163	32.20	**<0.001**		
Average speed vs. omega bending Pct	N2	44	129	**0.037**				–0.130	0.089
	npr-1(n1353)	54	105	0.198	0.060	9.997	**0.002**		
	npr-1(ad609)	45	94	0.054	<0.0001	0.070	0.791		
	npr-1(ky13)	30	137	0.153	0.043	7.466	**0.007**		
Average speed vs. reversal Pct	N2	63	110	**0.029**				–0.390	**<0.001**
	npr-1(n1353)	69	90	**<0.001**				–0.624	**<0.001**
	npr-1(ad609)	68	71	0.307	0.252	46.14	**<0.001**		
	npr-1(ky13)	65	102	**<0.001**				–0.436	**<0.001**

P-values smaller than 0.05 are given boldface.

time, the question remains open as to whether worms showed a relatively constant speed of movement during the recording times in these studies or different speed of movement at the beginning, middle, and end of the recording times. In this regard, a study by Swierczek et al. (2011) should be kept in mind in which N2 *C. elegans* showed a drop in average speed of locomotion from ∼230 μm/s immediately after placing worms on agar plates to ∼80 μm/s 10 min later (mean of eight plates). In the present study, videos were taken immediately after worms were placed on agar plates; however, the average speed of locomotion of N2 *C. elegans* on plates with an *E. coli* lawn was only ∼55% of the results reported by Swierczek et al. (2011). In summary, in order to ensure reproducibilty of a study analyzing the behavior of *C. elegans* it is essential to provide information about the video recording settings used in the experiments in sufficient detail to enable comparisons of the outcome of different studies.

Advanced Behavioral Analysis

In order to offer advanced *C. elegans* behavioral analysis, full worm "skeleton and outline" tracing must be present in order to represent full worm behavior and posture rather than only the simple centroid. Some worm trackers described in the literature offer these capabilities, however most trackers that offer skeleton and outline tracking can track only one worm at a time, while most trackers that can track multiple worms offer only centroid tracking (**Table 1**). With these capabilities, the advanced behavioral analyses performed in the present study are either, in the latter case, not possible, or in the former case must be done by tracking only one worm at a time. As demonstrated here, large interindividual variability creates the need for a large sample size to reliably compare test groups, making a low-throughput, one-worm-at-a-time solution ineffective due to the time required to generate an adequate sample size. In two systems, Multi

Worm Tracker (Swierczek et al., 2011) and WormLab (Roussel et al., 2014), both multi-worm tracking and skeleton and outline tracking are provided together.

In the present study, the video recording time was restricted to 60 s in order to limit worms moving out of or moving back into the field-of-view of the camera. However, it was not possible to decrease the magnification at which the videos were recorded. The latter would have resulted in an increased scale of the pixels and, thus, a decreased number of pixels per worm, preventing precise and accurate advanced behavioral analysis as outlined in the present study. In this regard it should be noted that Swierczek et al. (2011) used a camera with a resolution of 2352 $\times$ 1728 pixels and performed video tracking of *C. elegans* at a scale of 24.3 μm/pixel. Accordingly, the field-of-view was 24 cm^2 in their study and, thus, larger than the base area of the 5 cm NGM-agar plates used by Swierczek et al. (2011). This is substantially different from the settings used in the present study. Swierczek et al. (2011) reported a position jitter of only 1 μm and a speed jitter of only 1 μm/s when analyzing moving *C. elegans* using these settings, which is similar to what was reported for the WormLab software (Roussel et al., 2014). On the other hand, Swierczek et al. (2011) reported that identity of worms was lost upon collision with another worm, which is mitigated using the settings used in the present study (c.f. Supplemental Video 2 in Angstman et al., 2015).

Measurement of Subtle Behavioral Change

By measuring behavioral change of worms on plates with and without the presence of *E. coli*, it was demonstrated that certain *C. elegans* strains demonstrate substantially increased grouping behavior in the presence of *E. coli* (de Bono et al., 2002). Furthermore, the same study showed reduction in speed in multiple *C. elegans* strains when exposed to food, while also showing that certain deletion mutations affected this phenomenon. In this case, behavioral change was able to shed light on the roles of individual proteins on *C. elegans* behavioral phenomena.

Further analysis of behavioral change of N2 worms in the presence of an *E. coli* lawn vs. no lawn has been demonstrated using tracking of individual worms (Schwarz et al., 2015). It should be noted that this methodology differs from that of the present study in a number of ways: (i) individual worms are used rather than groups of worms on plates, (ii) worms on plates are allowed to habituate for a 30 min period before assaying, while no habituation time is allowed in the present study (in both studies, worms on plates with no lawn are assayed immediately), and (iii) video recording is performed for 15 min, while in the present study video recording consisted of 1 min. In-depth measurement of individual *C. elegans* posture and its change over time, as demonstrated in Schwarz et al. (2015), could be useful, for example, in the understanding of the neurological functions causing various behaviors, but differences in the methodology used between this and the present study demonstrate two differing scopes.

The present study shows that behavioral change, using the example of *E. coli* lawn presence and four different *C. elegans* strains, can go far beyond simple speed of locomotion measurement to further parameters requiring more in-depth analysis (**Table 2**). The fact that some of the measured behavioral traits were either only weakly or not at all tied to speed of locomotion (**Tables 3, 4**) demonstrates the potential utility of expanded data analyses in advanced analysis of *C. elegans* behavior. In turn, increased behavioral analyses allow for the quantification of behavioral change that may not sufficiently be represented by speed of locomotion. This can be used in combination with knockout *C. elegans* to increase sensitivity in detecting subtle phenotypic changes resulting from genotypic changes. In turn, this could then help in furthering the connection in *C. elegans* between genetics and behavior.

Nested Analysis

Due to the design of the experiment requiring the assaying of multiple worms per NGM-agar plate, nested analysis was used to investigate the potential impact of inter-plate variability on statistical analysis, an issue recently reviewed in the literature (Aarts et al., 2014). As summarized in **Table 2**, the nested factor played a statistically significant role in the observed difference between variables in nearly half (13/28) of the analyses. It has previously been suggested that, due to the high interindividual variability observed in *C. elegans* behavioral assays, a large sample number is required (Angstman et al., 2015). The present study shows that, when using a nested design to accomplish such a sample number, such a design must be accounted for due to inter-plate variability (see also **Figure 2**). Turned around, if this factor is now accounted for, an even greater number of *C. elegans* worms must be assayed to achieve the proper statistical power.

Relevance in Toxicology, Drug Discovery, and RNAi Screening

The methods used in the present study also offer particular relevance in the fields of toxicology, drug discovery, and RNAi screening. Because the effects of various chemical compounds may not be predictable, the ability to screen using multiple parameters offers increased sensitivity in terms of identifying subtle behavioral change. Furthermore, potential changes in behavioral traits in *C. elegans* may be better defined and measured on agar plates rather than on worms swimming in liquid. Although novel worm tracking software for tracking *C. elegans* swimming in liquid have recently been published (Hardaway et al., 2014; Restif et al., 2014), most assays involving chemical exposure and the measurement of behavior were performed via chemicals mixed in with the agar. This is, however, not the ideal delivery method for *C. elegans* as it may require substantially increased concentrations to achieve an effect. This is due to the fact that *C. elegans* have a cuticle barrier that can result in internal concentrations on the order of magnitudes lower than external concentrations (Rand and Johnson, 1995; Davies et al., 2003; Davies and McIntire, 2004). Exposure to chemicals in liquid, however, provides a much more effective delivery method. This may also apply to RNAi screening, as the ability to carry out RNAi in *C. elegans* via soaking is less labor intensive than injection and less variable than via agar plate feeding (for details see, e.g., Ahringer, 2006).

In the present study, worms were maintained solely in a liquid culture until immediately before video capture. Importantly, we have previously demonstrated that *C. elegans* grown in liquid cultures do not demonstrate statistically significant difference in average speed of locomotion compared to those raised on NGM-agar plates (Angstman et al., 2015). Due to our rapid transfer method, previously described in Angstman et al. (2015), both advantageous scenarios can be achieved: chemical exposure in liquid and behavioral analysis on NGM-agar plates. The combination of this and enhanced capability of behavioral analysis provides an ideal model for use in the fields of toxicology, drug discovery, and RNAi screening.

In summary, the advanced analysis model of *C. elegans* behavior presented in the present study demonstrates the potential utility and effectiveness of advanced behavioral analyses. Such analyses go beyond simple speed of locomotion measurements, offering greater sensitivity in measuring *C. elegans* behavioral change. This model potentially offers utility in the connecting of *C. elegans* genetics with behavior as well as in the fields of toxicology, drug discovery, and RNAi screening, to mention only a few.

AUTHOR CONTRIBUTIONS

NA, HF, and CS conceived and designed the experiments, NA performed experiments, and NA, HF, and CS analyzed data and wrote the manuscript.

ACKNOWLEDGMENTS

The authors wish to thank Pia Unterberger (Dept. Neuroanat., Ludwig-Maximilians University of Munich) for expert technical assistance.

SUPPLEMENTARY MATERIAL

The Supplementary Material for this article can be found online at: http://journal.frontiersin.org/article/10.3389/fnbeh.2016.00060

Video S1 | Wild type (N2) *C. elegans* on an NGM-agar plate with an *E. coli* lawn.

Video S2 | Wild type (N2) *C. elegans* on an NGM-agar plate with no lawn.

Table S1 | Tracking settings used in WormLab software.

REFERENCES

Aarts, E., Verhage, M., Veenvliet, J. V., Dolan, C. V., and van der Sluis, S. (2014). A solution to dependency: using multilevel analysis to accommodate nested data. *Nat. Neurosci.* 17, 491–496. doi: 10.1038/nn.3648

Ahringer, J. (2006). "Reverse genetics," in *WormBook*, ed V. Ambros (Cambridge: The *C. elegans* Research Community). doi: 10.1895/wormbook.1.47.1

Albrecht, D. R., and Bargmann, C. I. (2011). High-content behavioral analysis of *Caenorhabditis elegans* in precise spatiotemporal chemical environments. *Nat. Meth.* 8, 599–605. doi: 10.1038/nmeth.1630

Angstman, N. B., Kiessling, M. C., Frank, H. G., and Schmitz, C. (2015). High interindividual variability in dose-dependent reduction in speed of movement after exposing *C. elegans to shock waves. Front. Behav. Neurosci.* 9:12. doi: 10.3389/fnbeh.2015.00012

Buckingham, S. D., and Sattelle, D. B. (2008). Strategies for automated analysis of *C. elegans locomotion. Invert. Neurosci.* 8, 121–131. doi: 10.1007/s10158-008-0077-3

Cleveland, W. S., and Devlin, S. J. (1988). Locally weighted regression: an approach to regression analysis by local fitting. *J. Am. Stat. Assoc.* 83, 596–610. doi: 10.1080/01621459.1988.10478639

Davies, A. G., and McIntire, S. L. (2004). Using C. elegans to screen for targets of ethanol and behavior-altering drugs. *Biol. Proced.* 6, 113–119. doi: 10.1251/bpo79

Davies, A. G., Pierce-Shimomura, J. T., Kim, H., VanHoven, M. K., Thiele, T. R., Bonci, A., et al. (2003). A central role of the BK potassium channel in behavioral responses to ethanol in *C. elegans. Cell* 115, 655–666. doi: 10.1016/S0092-8674(03)00979-6

de Bono, M., and Bargmann, C. I. (1998). Natural variation in a neuropeptide Y receptor homolog modifies social behavior and food response in C. *elegans. Cell* 94, 679–689. doi: 10.1016/S0092-8674(00)81609-8

de Bono, M., Tobin, D. M., Davis, M. W., Avery, L., and Bargmann, C. I. (2002). Social feeding in *Caenorhabditis elegans* is induced by neurons that detect aversive stimuli. *Nature* 419, 899–903. doi: 10.1038/nature01169

Faumont, S., Rondeau, G., Thiele, T. R., Lawton, K. J., McCormick, K. E., Sottile, M., et al. (2011). An image-free opto-mechanical system for creating virtual environments and imaging neuronal activity in freely moving *Caenorhabditis elegans*. *PLoS ONE* 6:e24666. doi: 10.1371/journal.pone.0024666

Geng, W., Cosman, P., Berry, C. C., Feng, Z., and Schafer, W. R. (2004). Automated tracking, feature extraction and classification of *C. elegans* phenotypes. *IEEE Trans. Biomed. Eng.* 15, 1811–1820. doi: 10.1109/TBME.2004.831532

Hardaway, J. A., Wang, J., Fleming, P. A., Fleming, K. A., Whitaker, S. M., Nackenoff, A., et al. (2014). An open-source analytical platform for analysis of *C. elegans* swimming-induced paralysis. *J. Neurosci. Meth.* 232, 58–62. doi: 10.1016/j.jneumeth.2014.04.024

Huang, K. M., Cosman, P., and Schafer, W. R. (2006). Machine vision based detection of omega bends and reversals in *C. elegans. J. Neurosci. Meth.* 158, 323–336. doi: 10.1016/j.jneumeth.2006.06.007

Husson, S. J., Costa, W. S., Schmitt, C., and Gottschalk, A. (2012). "Keeping track of worm trackers," in *WormBook*, ed O. Hobert (Frankfurt: The *C. elegans* Research Community). doi: 10.1895/wormbook.1.156.1

Jorgensen, E. M., and Mango, S. E. (2002). The art and design of genetic screens: *Caenorhabditis elegans*. *Nat. Rev. Genet.* 3, 356–369. doi: 10.1038/nrg794

Leifer, A. M., Fang-Yen, C., Gershow, M., Alkema, M. J., and Samuel, A. D. (2011). Optogenetic manipulation of neural activity in freely moving *Caenorhabditis elegans*. *Nat. Meth.* 8, 147–152. doi: 10.1038/nmeth.1554

Ramot, D., Johnson, B. E., Berry, T. L. Jr., Carnell, L., and Goodman, M. B. (2008). The parallel worm tracker: a platform for measuring average speed and drug-induced paralysis in nematodes. *PLoS ONE* 3:e2208. doi: 10.1371/journal.pone.0002208

Rand, J. B., and Johnson, C. D. (1995). Genetic pharmacology: interactions between drugs and gene products in *Caenorhabditis elegans*. *Meth. Cell Biol.* 48, 187–204. doi: 10.1016/S0091-679X(08)61388-6

Restif, C., Ibáñez-Ventoso, C., Vora, M. M., Guo, S., Metaxas, D., and Driscoll, M. (2014). CeleST: computer vision software for quantitative analysis of *C. elegans* swim behavior reveals novel features of locomotion. *PLoS Comput. Biol.* 10:e1003702. doi: 10.1371/journal.pcbi.1003702

Roussel, N., Sprenger, J., Tappan, S. J., and Glaser, J. R. (2014). Robust tracking and quantification of C. *elegans body shape and locomotion through coiling, entanglement, and omega bends. Worm* 3:e982437. doi: 10.4161/21624054.2014.982437

Schwarz, R. F., Branicky, R., Grundy, L. J., Schafer, W. R., and Brown, A. E. X. (2015). Changes in postural syntax characterize sensory modulation and natural variation of *C. elegans locomotion. PLoS Comput. Biol.* 11:e1004322. doi: 10.1371/journal.pcbi.1004322

Stirman, J. N., Crane, M. M., Husson, S. J., Wabnig, S., Schultheis, C., Gottschalk, A., et al. (2011). Real-time multimodal optical control of neurons and muscles in freely behaving *Caenorhabditis elegans*. *Nat. Meth.* 8, 153–158. doi: 10.1038/nmeth.1555

Sulston, J. E., and Brenner, S. (1974). The DNA of Caenorhabditis elegans. *Genetics* 77, 95–104.

Swierczek, N. A., Giles, A. C., Rankin, C. H., and Kerr, R. A. (2011). High-throughput behavioral analysis in *C. elegans*. *Nat. Meth.* 8, 592–598. doi: 10.1038/nmeth.1625

Tsibidis, G. D., and Tavernarakis, N. (2007). Nemo: a computational tool for analyzing nematode locomotion. *BMC Neurosci.* 8:86. doi: 10.1186/1471-2202-8-86

Wald, A., and Wolfowitz, J. (1940). On a test whether two samples are from the same population. *Ann. Math. Statist.* 11, 147–162. doi: 10.1214/aoms/1177731909

White, J. G., Southgate, E., Thomson, J. N., and Brenner, S. (1986). The structure of the nervous system of the nematode *Caenorhabditis elegans*. *Philos. Trans. R. Soc. Lond. B. Biol. Sci.* 314, 1–340. doi: 10.1098/rstb.1986.0056

Yemini, E., Jucikas, T., Grundy, L. J., Brown, A. E., and Schafer, W. R. (2013). A database of *Caenorhabditis elegans* behavioral phenotypes. *Nat. Methods* 10, 877–879. doi: 10.1038/nmeth.2560

Conflict of Interest Statement: CS serves as paid consultant for MBF Bioscience (Williston, VT, USA), the manufacturer of the WormLab software that was used in the present study to analyze data. However, CS has not received financial support directly or indirectly related to this manuscript. The authors declare that the research was conducted in the absence of any commercial or financial relationships that could be construed as a potential conflict of interest.

References

- Adhikari U, Goliaei A, Berkowitz ML. Nanobubbles, cavitation, shock waves and traumatic brain injury. Phys Chem Chem Phys 2016;18(48):32638–52. doi: 10.1039/c6cp06704b.
- Angstman NB, Kiessling MC, Frank HG, Schmitz C. High interindividual variability in dose-dependent reduction in speed of movement after exposing C. elegans to shock waves. Front Behav Neurosci 2015;9:12. doi: 10.3389/fnbeh.2015.00012.
- Arun P, Spadaro J, John J, Gharavi RB, Bentley TB, Nambiar MP. Studies on blast traumatic brain injury using in-vitro model with shock tube. Neuroreport 2011;22(8):379–84. doi: 10.1097/WNR.0b013e328346b138.
- Bauman RA, Ling G, Tong L, Januszkiewicz A, Agoston D, Delanerolle N, et al. An introductory characterization of a combat-casualty-care relevant swine model of closed head injury resulting from exposure to explosive blast. J Neurotrauma 2009;26(6):841–60. doi: 10.1089/neu.2008.0896.
- Brenner S. The genetics of Caenorhabditis elegans. Genetics 1974;77:71–94.
- Carney N, Totten AM, O'Reilly C, Ullman JS, Hawryluk GW, Bell MJ, et al. Guidelines for the Management of Severe Traumatic Brain Injury, Fourth Edition. Neurosurgery 2017;80(1):6–15. doi: 10.1227/NEU.0000000000001432.
- Centers for Disease Control and Prevention. Traumatic brain injury & concussion: TBI data [Internet]. Atlanta: CDC; 2024 May 15 [cited 2024 Nov 20]. Available from: https://www.cdc.gov/traumatic-brain-injury/data-research/index.html.
- Cernak I. Animal models of head trauma. Neurotherapeutics 2010;7(1):14–26. doi: 10.1016/j.nurt.2009.10.015.
- Cernak I, Noble-Haeusslein LJ. Traumatic brain injury: An overview of pathobiology with emphasis on military populations. J Cereb Blood Flow Metab 2010;30(2):255–66. doi: 10.1038/jcbfm.2009.203.
- Charan S, Chien FC, Singh N, Kuo CW, Chen P. Development of lipid targeting Raman probes for in vivo imaging of Caenorhabditis elegans. Chemistry 2011;17(18):5165–70. doi: 10.1002/chem.201002896.
- Chen N, Harris TW, Antoshechkin I, Bastiani C, Bieri T, Blasiar D, et al. WormBase: A comprehensive data resource for Caenorhabditis biology and genomics. Nucleic Acids Res 2005;33(Database issue)–9. doi: 10.1093/nar/gki066.
- Collin B, Tsyusko OV, Unrine JM. Influence of natural organic matter on dissolution and toxicity of silver nanoparticles in Caenorhabditis elegans. Environ Sci Nano 2014;3:728–36. doi: 10.1039/c4en00015g.
- Contreras EQ, Puppala HL, Escalera G, Zhong W, Colvin VL. Size-dependent impacts of silver nanoparticles on the lifespan, fertility, growth, and locomotion of Caenorhabditis elegans. Environ Toxicol Chem 2014;33(12):2716–25. doi: 10.1002/etc.2705.
- Császár NB, Angstman NB, Milz S, Sprecher CM, Kobel P, Farhat M, et al. Radial shock wave devices generate cavitation. PLoS One 2015;10. doi: 10.1371/journal.pone.0140541.
- Delius M, Gambihler S. Effect of shock waves on gallstones and materials. Lithotripsy and related techniques for gallstone treatment. 1991:27-33.
- Driscoll M, Gerstbrein B. Dying for a cause: Invertebrate genetics takes on human neurodegeneration. Nat Rev Genet 2003;4:181–94. doi: 10.1038/nrg1032.
- Effgen GB, Hue CD, Vogel E, Panzer MB, Meaney DF, Bass CR, et al. A multiscale approach to blast neurotrauma modeling: Part II: Methodology for integrating injury models. Front Neurol 2014;5:47. doi: 10.3389/fneur.2014.00047.

- Effgen GB, Vogel EW, Panzer MB, Meaney DF, Bass CR, Morrison B. A multiscale approach to blast neurotrauma modeling: Part I: Development of novel test devices for in vivo and in vitro blast injury models. Front Neurol 2016;7:89. doi: 10.3389/fneur.2016.00089.
- Elder GA. Blast-induced traumatic brain injury: Experimental models, neuropathology, and implications for injury mechanisms. Exp Neurol. 2015;275:409–20. doi: 10.1016/j.expneurol.2015.06.006.
- Estrada-Rojo F, Martínez-Tapia RJ, Estrada-Bernal F, Martínez-Vargas M, Perez-Arredondo A, Flores-Avalos L, Navarro L. Models used in the study of traumatic brain injury. Rev Neurosci. 2018;29(2):139–49. doi: 10.1515/revneuro-2017-0028.
- Faul M, Xu L, Wald MM, Coronado VG. Traumatic brain injury in the United States: Emergency department visits, hospitalizations, and deaths, 2002–2006. CDC Natl Cent Inj Prev Control. 2010. doi: 10.15620/cdc.5571.
- Galgano M, Toshkezi G, Qiu X, Russell T, Chin L, Zhao LR. Traumatic brain injury: Current treatment strategies and future endeavors. Cell Transplant. 2017;26(7):1118–30. doi: 10.1177/0963689717714102.
- Goeller J, Wardlaw A, Treichler M, O'Bruba J, Weiss G. Investigation of cavitation as a possible damage mechanism in blast-induced traumatic brain injury. J Neurotrauma. 2012;29(10):1970–81. doi: 10.1089/neu.2012.2374.
- Gross AG. A new theory on the dynamics of brain concussion and brain injury. J Neurosurg. 1958;15(5):548–61. doi: 10.3171/jns.1958.15.5.0548.
- Harris JO, Semple BD, Murphy A. Animal models of blast-related brain injury: Challenges and future directions. Neurobiol Dis. 2019;123:20–32. doi: 10.1016/j.nbd.2018.06.015.
- Hayakawa K, Takeda S, Kawabe K, Shimura T. Acoustic characteristics of PVA gel. In: Proceedings, IEEE Ultrasonics Symposium; 1989 Oct 2-5; Montreal, QC, Canada. IEEE; 1989. p. 969-972. doi: 10.1109/ULTSYM.1989.67133.
- Hoge CW, McGurk D, Thomas JL, Cox AL, Engel CC, Castro CA. Mild traumatic brain injury in U.S. soldiers returning from Iraq. N Engl J Med. 2008;358(5):453–63. doi: 10.1056/NEJMoa072972.
- Husson SJ, Costa WS, Schmitt C, Gottschalk A. Keeping track of worm trackers. WormBook: the online review of C. elegans biology. 2013;1-17. doi: 10.1895/wormbook.1.156.1.
- Jokinen LLJ, Wuerfel T, Schmitz C. Opinion: Application of extracorporeal shock wave therapy in nervous system diseases. Front Neurol 2023;14:1281684. doi: 10.3389/fneur.2023.1281684.
- Kang W, Adnan A, O'Shaughnessy T, Bagchi A. Cavitation nucleation in gelatin: Experiment and mechanism. Acta Biomater. 2018;67:295–306. doi: 10.1016/j.actbio.2017.11.030.
- Kong LZ, Zhang RL, Hu SH, Lai JB. Military traumatic brain injury: A challenge straddling neurology and psychiatry. Mil Med Res. 2022;9(1):2. doi: 10.1186/s40779-021-00363-y.
- LaPlaca MC, Simon CM, Prado GR, Cullen DK. CNS injury biomechanics and experimental models. Prog Brain Res. 2007;161:13–26. doi: 10.1016/S0079-6123(06)61002-8.
- Lewis JA, Wu CH, Levine JH, Berg H. Levamisole-resistant mutants of the nematode Caenorhabditis elegans appear to lack pharmacological acetylcholine receptors. Neuroscience. 1980;5:967–89. doi: 10.1016/0306-4522(80)90269-9.
- Ling G, Bandak F, Armonda R, Grant G, Ecklund J. Explosive blast neurotrauma. J Neurotrauma. 2009;26(6):815–25. doi: 10.1089/neu.2007.0484.
- Marklund N, Hillered L. Animal modelling of traumatic brain injury in preclinical drug development: where do we go from here? Br J Pharmacol. 2011;164(4):1207-1229. doi:10.1111/j.1476-5381.2010.01163.x.

- Marsh JL, Bentil SA. Cerebrospinal fluid cavitation as a mechanism of blast-induced traumatic brain injury: A review of current debates, methods, and findings. Front Neurol. 2021;12:626393. doi: 10.3389/fneur.2021.626393.
- Martin E, Laloux H, Couette G, Alvarez T, Bessou C, Hauser O, et al. Identification of 1088 new transposon insertions of Caenorhabditis elegans: A pilot study toward large-scale screens. Genetics. 2002;162(1):521–4. doi: 10.1093/genetics/162.1.521.
- Menon DK, Schwab K, Wright DW, Maas AI. Position statement: Definition of traumatic brain injury. Arch Phys Med Rehabil. 2010;91(11):1637–40. doi: 10.1016/j.apmr.2010.05.017.
- Moore DF, Radovitzky RA, Shupenko L, Klinoff A, Jaffee MS, Rosen JM. Blast physics and central nervous system injury. J Neurotrauma. 2008;25(5):624–36. doi: 10.1089/neu.2007.0483.
- Morrison B, 3rd, Elkin BS, Dollé JP, Yarmush ML. In vitro models of traumatic brain injury. Annu Rev Biomed Eng. 2011;13:91–126. doi: 10.1146/annurev-bioeng-071910-124706
- Nakagawa A, Manley GT, Gean AD, Ohtani K, Armonda R, Tsukamoto A, et al. Mechanisms of primary blast-induced traumatic brain injury: Insights from shock-wave research. J Neurotrauma. 2011;28(6):1101–19. doi: 10.1089/neu.2010.1442
- Panzer MB, Myers BS, Capehart BP, Bass CR. Development of a Finite Element Model for Blast Brain Injury and the Effects of CSF Cavitation. Ann Biomed Eng. 2014;40(7):1530–44. doi: 10.1007/s10439-012-0615-6
- Pierce-Shimomura JT, Morse TM, Lockery SR. The fundamental role of pirouettes in Caenorhabditis elegans chemotaxis. J Neurosci. 1999;19(21):9557–69. doi: 10.1523/JNEUROSCI.19-21-09557.1999
- Pishchalnikov YA, McAteer JA, Williams JC. Cavitation bubble cluster activity in the breakage of kidney stones by lithotripter shockwaves. J Endourol. 2003;17(7):435–46. doi: 10.1089/089277903769013488
- Poulin G, Nandakumar R, Ahringer J. Genome-wide RNAi screens in Caenorhabditis elegans: Impact on cancer research. Oncogene. 2004;23:8340–5. doi: 10.1038/sj.onc.1207944
- Rassweiler JJ, Knoll T, Köhrmann KU, McAteer JA, Lingeman JE, Cleveland RO, Bailey MR, Chaussy C. Shock wave technology and application: an update. Eur Urol. 2011;59(5):784–96. doi: 10.1016/j.eururo.2011.02.033
- Robinson DE, Kossoff G. Pulse echo visualisation. In: Fry FJ, editor. Ultrasound: Its Applications in Medicine and Biology. Amsterdam: Elsevier; 1978. p. 593–596. doi: 10.1016/B978-0-444-41641-4.50008-X
- Rosenfeld JV, McFarlane AC, Bragge P, Armonda RA, Grimes JB, Ling GS. Blast-related traumatic brain injury. Lancet Neurol. 2013;12(9):882–93. doi: 10.1016/S1474-4422(13)70161-3
- Sandestig A, Romner B, Grände PO. Therapeutic hypothermia in children and adults with severe traumatic brain injury. Ther Hypothermia Temp Manag. 2014;4(1):10–20. doi: 10.1089/ther.2013.0024
- Schelling G, Delius M, Gschwender M, Grafe P, Gambihler S. Extracorporeal shock waves stimulate frog sciatic nerves indirectly via a cavitation-mediated mechanism. Biophys J. 1994;66(1):133–40. doi: 10.1016/S0006-3495(94)80758-1
- Schmitz C, Császár NB, Milz S, Schieker M, Maffulli N, Rompe JD, Furia JP. Efficacy and safety of extracorporeal shock wave therapy for orthopedic conditions: a systematic review on studies listed in the PEDro database. Br Med Bull. 2015;116(1):115–138. doi: 10.1093/bmb/ldv047
- Speed CA. Therapeutic ultrasound in soft tissue lesions. Rheumatology. 2014;40(12):1331–6. doi: 10.1093/rheumatology/40.12.1331

- Tümer N, Tachibana R, Roy N, Zhao Z, Hoang T, Smith DH, et al. In vitro models of traumatic brain injury: A commentary on the need for new approaches to meet current and future challenges. Front Neurol. 2018;9:471. doi: 10.3389/fneur.2018.00471
- Wang CJ. Extracorporeal shockwave therapy in musculoskeletal disorders. J Orthop Surg Res. 2012;7(1):11. doi: 10.1186/1749-799X-7-11
- Wu Y, Pang Z, Zhang Z, Wang X, Li Z, Cao B. Effectiveness of radial extracorporeal shock wave therapy for spasticity in children with cerebral palsy: A prospective study. Medicine. 2017;96(27). doi: 10.1097/MD.0000000000008108
- Zimberlin JA, McManus JJ, Crosby AJ. Cavitation rheology for soft materials. Soft Matter. 2007;3(6):763–7. doi: 10.1039/b617050a

Appendix A: Paper III

SCIENTIFIC REPORTS

OPEN

Hypothermia ameliorates blast-related lifespan reduction of *C. elegans*

Received: 19 March 2018
Accepted: 3 July 2018
Published online: 12 July 2018

Nicholas B. Angstman, Hans-Georg Frank & Christoph Schmitz

Blast-related mild traumatic brain injury induces significant long-term health issues, yet treatment procedures remain underdeveloped. Therapeutic hypothermia has been postulated as a potentially effective therapy. In a *Caenorhabditis elegans* model, we demonstrate a dose-dependent reduction in lifespan following exposure to blast-like shock waves. Using polyvinyl alcohol, we show that cavitation is a key injurious factor in the damaging shock wave component. Short and long lifespan *C. elegans* mutants demonstrated the interaction of genetic and environmental longevity-determining factors. Hypothermia reduced the long term effect of shock wave exposure. Thus, we present an effective *C. elegans* model of long term effects of blast-related mild traumatic brain injury, as well as evidence of the merit of therapeutic hypothermia as a therapy option following blast exposure.

Blast-related mild traumatic brain injury (br-mTBI) has been shown to induce long-term effects including, but not limited to, post-traumatic stress disorder and depression[1], and reduced life expectancy[2]. While the effects of br-mTBI have been well described, there lacks a deeper understanding of the connecting steps between a damage causing event and the development of disease. Due to delayed onset of disease, as well as complexity in studying the nervous system of mammals, connection between cause and known damaging effects is not yet completely understood in br-mTBI. While mammalian models are an effective and commonly used tool to investigate br-mTBI, limitations such as low sample size, length of life, and complexity highlight the need for other effective models of br-mTBI[3]. Despite such shortcomings, progress has still been made in the investigation of potentially effective therapies following traumatic brain injury. One example, therapeutic hypothermia, has previously shown promise in recovery following moderate to severe traumatic brain injury (reviewed in[4]), although results appear mixed. A recent randomized controlled trial found that hypothermia treatment did not improve outcomes in patients with intracranial hypertension after traumatic brain injury[5]. Due to the limiting factors in the usage of mammalian models, therapeutic hypothermia has yet to be investigated for br-mTBI, despite suggestion that it may be an attractive therapeutic intervention to prevent reduced lifespan following br-mTBI[6–8].

We have previously shown that *C. elegans* offer a viable alternative to mammalian models, as exposure to shock waves results in behavioral changes that share key features with br-mTBI in humans: initial loss of consciousness followed by recovery[9]. Furthermore, we showed that cavitation was an important factor in causing the observed behavioral change. In the present study, we hypothesized that (i) exposure to shock waves reduces *C. elegans* lifespan in the long term, (ii) this effect is partially dependent on the presence of cavitation, and (iii) therapeutic hypothermia improves the long term outlook of *C. elegans* survival.

Results and Discussion

In order to evaluate *C. elegans* as a potential model for the long term effects of br-mTBI, we exposed wild-type *C. elegans* to shock waves and measured lifespan following exposure. Using a therapeutic shock wave device, shock waves with similar wave properties as primary blast waves were applied as previously described[9]. Exposure to shock waves resulted in a significantly reduced lifespan of both worms raised in liquid cultures (Fig. 1a) and worms raised on NGM-agar plates (Fig. 1b). Furthermore, worms exposed to 500 shock waves exhibited significantly shorter lifespans compared to those exposed to 100 shock waves, particularly in worms raised on NGM-agar plates, indicating a dose-dependent long term effect of shock wave exposure.

It has previously been established that cavitation plays a large role in shock wave effect on nervous tissue[10]. Cavitation has also been hypothesized to be a damaging factor in the induction of br-mTBI[11]. We previously showed that using polyvinyl alcohol (PVA), a medium with low cavitation activity, as a medium for exposing

Chair of Neuroanatomy, Institute of Anatomy, Faculty of Medicine, LMU Munich, Munich, Germany. Correspondence and requests for materials should be addressed to C.S. (email: christoph_schmitz@med.uni-muenchen.de)

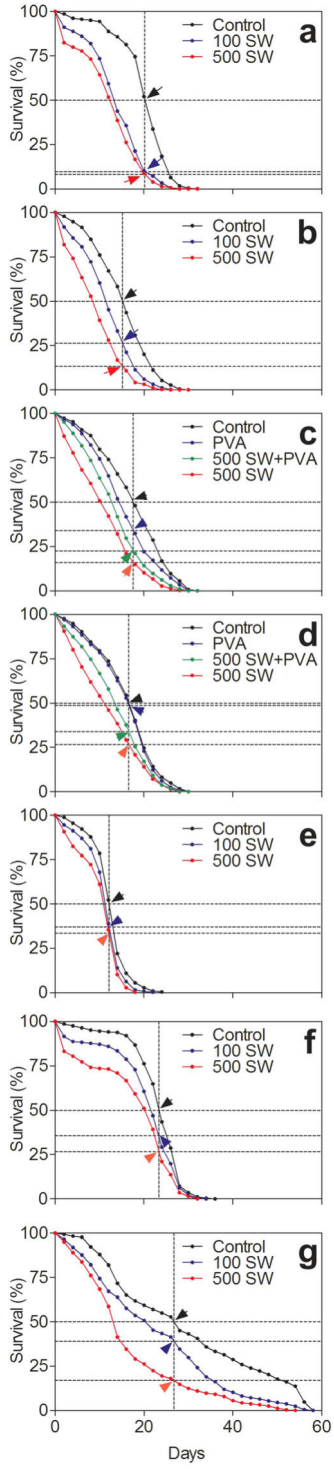

Figure 1. Shock wave exposure decreases lifespan. (**a**) Lifespans of N2 *C. elegans* raised in liquid cultures following shock wave exposure. (**b**) Lifespans of N2 worms raised on NGM agar plates following shock wave exposure. (**c**) Lifespans of N2 worms exposed to shock waves in S-medium or polyvinyl alcohol. (**d**) Lifespans of N2 worms exposed to shock waves in S-medium or polyvinyl alcohol, followed by a short washing step. (**e**) Lifespans of *daf-16(m26)* worms following shock wave exposure. (**f**) Lifespans of N2 worms at 11 °C following shock wave exposure. (**g**) Lifespans of *daf-2(e1370)* worms at 11 °C following exposure to shock waves. In all panels, vertical dotted lines represent 50% lifespan of control. Arrows and horizontal dotted lines represent the percent survival of each test group at time of the corresponding 50% control survival. N > 500 worms in all experiment groups (the exact numbers are provided in the Methods section).

		Remaining Lifespan at 50% Control			
Assay	**50% Lifespan of Control**	**% of 100 SW**	**% of 500 SW**	**% of PVA**	**% of PVA + 500 SW**
Liquid	20.2 days	9.7%	8.2%	—	—
Plates	15.1 days	26.5%	13.4%	—	—
PVA	17.6 days	—	16.0%	34.1%	22.6%
PVA with Wash	16.6 days	—	26.6%	48.7%	33.9%
daf-16(m26)	12.2 days	36.9%	33.5%	—	—
11 °C N2	23.4 days	35.5%	26.5%	—	—
11 °C *daf-2(e1370)*	26.7 days	39.1%	16.9%	—	—

Table 1. Summary of results.

C. elegans to shock waves, resulted in significantly reduced immediate effect[9]. In order to investigate the role of cavitation in long term damage following shock wave exposure, we exposed *C. elegans* to shock waves while in PVA. Attenuating cavitation resulted in significantly longer lifespans, although still significantly lower than control-level, despite a potentially toxic effect observed when using PVA without shock waves (Fig. 1c). Any toxic effect of PVA was effectively mitigated using a short wash step prior to putting worms on NGM-agar plates (Fig. 1d).

Knockout *C. elegans* were previously observed with varied lifespans from wild-type N2 *C. elegans*. While *daf-2(e1370)* mutants can live more than two times longer than N2 *C. elegans*, the gene knockout observed in *daf-16(m26)* mutants also plays a role in the aging pathway[12]. In order to investigate the interaction of shock wave exposure and other lifespan shortening factors, we exposed *daf-16* and *daf-2* worms to shock waves. We found that exposure to shock waves induced a significant further reduction in lifespan of *daf-16* worms (Fig. 1e), although the reduction in lifespan was not as pronounced as in N2 *C. elegans* (Fig. 1a). Following exposure to shock waves and maintenance at 11 °C, N2 (Fig. 1f) and *daf-2* worms (Fig. 1g) exhibited significant reduction of lifespan, although lifespan in *daf-2* worms was still longer than that of N2 counterparts at 11 °C.

Wild-type N2 *C. elegans* maintained at 11 °C following shock wave exposure exhibited significantly shorter lifespan compared to control worms at 11 °C (Fig. 1f). The initial damaging effect of shock wave was evident through the first several days and similar to the N2 worms assayed at 20 °C. In the 20 °C assay (Fig. 1a), at the point when 95% of control worms remained alive (t = 8.0 days), 73.2% of worms exposed to 500 shock waves remained alive. At the 95% living mark of worms at 11 °C (t = 8.6 days) a similar amount of 74.0% of worms remained alive. However, long-term disparity between control worms and those exposed to shock waves was less evident. At the 50% survival point of control worms at 20 °C, only 9.7% and 8.2% of worms survived following exposure to 100 and 500 shock waves, respectively. For the worms assayed at 11 °C, those figures were much higher at 35.5% and 26.5%, respectively (Table 1). At the 5% survival point of worms exposed to 500 shock waves at 20 °C (t = 21.5 days), 38.3% of control worms remained alive. For worms maintained at 11 °C, only 10.4% of control worms remained alive when 5% of worms exposed to 500 shock waves remained alive (t = 27.7 days). These data imply that there is an initial death-causing effect of shock wave exposure observed in the first days, as well as a longer term effect on those worms that survive the initial damaging effect. While the initial effects do not appear to be attenuated by the lower temperature, the long-term prognosis of worms exposed to shock waves is much closer to that of control worms. The lack of improved short-term recovery in hypothermia treated worms seems to agree with previous findings of no improvement in the six month mortality rate of traumatic brain injury patients treated with hypothermia[5]. Of note, the six month recovery endpoint used in the aforementioned study correlates to approximately six hours of *C. elegans* recovery. Thus, the findings in the present study of attenuated long-term effects following hypothermia treatment represent findings of a different scope than in previous studies.

Conclusion

Our results show that *C. elegans* model the long term effects of br-mTBI by showing reduction of lifespan following exposure to shock waves. This effect is reduced in the presence of cavitation, a suspected damage causing component of primary blast waves. Furthermore, there appear to be separate short- and long-term effects of shock wave exposure on *C. elegans*, the latter of which can be attenuated to some extent in reduced temperature settings. This lends credence to usage of therapeutic hypothermia following br-mTBI. Given the utility of *C. elegans*, we believe that the model described in the present study offers a unique opportunity to further understand and investigate long term effects of br-mTBI, especially as they pertain to therapeutic approaches such as therapeutic hypothermia.

Methods

Nematodes. All *C. elegans* strains were obtained from the Caenorhabditis Genetics Center (Minneapolis, MN, USA), which is funded by NIH Office of Research Infrastructure Programs (P40 OD010440). The following *C. elegans* strains were used in the present study: Wild type (N2, Bristol), DR26 *daf-16*(*m26*), and CB1370 *daf-2*(*e1370*). From a stock liquid culture, synchronous young adult worms were produced using sodium hypochlorite treatment and sucrose cleaning as previously described[1]. Worms in liquid cultures were allowed to grow in an incubated shaker (NB 205V, N Biotek, Bucheon, South Korea) at 20 °C, while worms raised on plates were kept in an incubator at 20 °C.

Assays. Seven different assays were performed in the present study. Unless otherwise noted, worms were raised in liquid cultures containing S-medium[13] and allowed to grow to the L4 stage at 20 °C. At this point, worms were cleaned using sucrose cleaning and prepared for use by concentrating via centrifugation to approximately 200 worms/mL. From this dilution, 310 µL were added to a well of a 96-well plate. When called for, shock waves were applied using a therapeutic shock wave device (Swiss DolorClast; Electro Medical Systems, S. A., Nyon, Switzerland) as previously described[9]. Following shock wave application, worms were transferred using a rapid transfer method outlined previously[9] to 10 cm NGM-agar plates containing 400 M 5-Fluoro-2′-deoxyuridine (FUdR) in order to prevent future generations of worms to hinder counting[14]. Each group contained at least 500 worms across 10 FUdR NGM-agar plates. Counting commenced on day zero, corresponding with the young adult stage, and occurred every 2 days until no living worms remained. Death was scored as the absence of any movement and failure to move at all after several light pokes with a platinum wire. The following assays were performed in the present study (the numbers in parentheses represent the numbers of worms per individual assay).

Assay 1. N2 worms were exposed to 0, 100, or 500 shock waves (0 shock waves: 502 worms; 100 shock waves: 508 worms; 500 shock waves: 507 worms).

Assay 2. N2 worms were raised synchronously on 10 cm NGM-agar plates. On day zero (i.e. at the young adult stage), worms were rinsed off of plates with S-medium. Worms were centrifuged to concentrate to 200 worms/mL. Samples were then exposed to 0, 100, or 500 shock waves (0 shock waves: 524 worms, 100 shock waves: 515 worms; 500 shock waves: 518 worms).

Assay 3. N2 worms were exposed to either 0 or 500 shock waves in either S-medium or PVA (0 shock waves, S-medium: 511 worms; 500 shock waves, S-medium: 544 worms; 0 shock waves, PVA: 528 worms; 500 shock waves, PVA: 510 worms).

Assay 4. N2 worms were exposed to either 0 or 500 shock waves in either S-medium or PVA, including an added washing step following shock wave exposure (0 shock waves, S-medium: 502 worms; 500 shock waves, S-medium: 506 worms; 0 shock waves, PVA: 507 worms; 500 shock waves, PVA: 522 worms).

Assay 5. DR26 worms were exposed to 0, 100, or 500 shock waves in S-medium (0 shock waves: 531 worms; 100 shock waves: 583 worms; 500 shock waves: 543 worms).

Assay 6. N2 worms were raised at 11 °C, exposed to 0, 100, or 500 shock waves in S-medium, and assayed at 11 °C (0 shock waves: 568 worms; 100 shock waves: 513 worms; 500 shock waves: 537 worms).

Assay 7. CB1370 worms were raised at 11 °C, exposed to 0, 100, or 500 shock waves in S-medium, and assayed at 11 °C (0 shock waves: 507 worms; 100 shock waves: 503 worms; 500 shock waves: 510 worms).

Data Analysis. Data was analyzed with IBM SPSS Statistics (version 23, IBM Corp., Armonk, NY) using the Kaplan Meier Mantel-Cox log rank test. A p value of 0.05 was used as the criteria for significance. GraphPad Prism (Version 5.04) was used to make Fig. 1.

Data availability. The data that support the findings of this study are available from the corresponding author upon reasonable request.

References

1. Hoge, C. W. *et al*. Mild traumatic brain injury in U.S. Soldiers returning from Iraq. *N. Engl. J. Med.* **358**, 453–463 (2008).
2. Harrison-Felix, C. *et al*. Life expectancy following rehabilitation: a NIDRR Traumatic Brain Injury Model Systems study. *J. Head Trauma Rehabil.* **27**, E69–80 (2012).
3. Morrison, B., Elkin, B. S., Dolle, J.-P. & Yarmush, M. L. Yarmush, *In vitro* models of traumatic brain injury. *Annu. Rev. Biomed. Eng.* **13**, 91–126 (2011).
4. Dunkley, S. & McLeod, A. Therapeutic hypothermia in patients following traumatic brain injury: a systematic review. *Nurs. Crit. Care.* **22**, 150–160 (2017).
5. Andrews, P. J. *et al*. Hypothermia for intracranial hypertension after Traumatic Brain Injury. *N. Engl. J. Med.* **373**, 2403–2412 (2015).
6. Kochanek, P. M. *et al*. Emerging therapies in traumatic brain injury. *Semin. Neurol.* **35**, 83–100 (2015).
7. Kochanek, P. M. & Jackson, T. C. It might be time to let cooler heads prevail after mild traumatic brain injury or concussion. *Exp. Neurol.* **267**, 13–17 (2015).
8. Miyauchi, T., Wei, E. P. & Povlishock, J. T. Evidence for the therapeutic efficacy of either mild hypothermia or oxygen radical scavengers after repetitive mild traumatic brain injury. *J. Neurotrauma.* **31**, 773–781 (2014).
9. Angstman, N. B., Kiessling, M. C., Frank, H. G. & Schmitz, C. High interindividual variability in dose-dependent reduction in speed of movement after exposing *C. elegans* to shock waves. *Front. Behav. Neurosci.* **9**, 12 (2015).
10. Schelling, G., Delius, M., Gschwender, M., Grafe, P. & Gambihler, S. Extracorporeal shock waves stimulate frog sciatic nerves indirectly via a cavitation-mediated mechanism. *Biophys. J.* **66**, 133–140 (1994).
11. Goeller, J., Wardlaw, A., Treichler, D., O'Bruba, J. & Weiss, G. J. Investigation of cavitation as a possible damage mechanism in blast-induced traumatic brain injury. *Neurotrauma.* **29**, 1970–1981 (2012).
12. Kenyon, C., Chang, J., Gensch, E., Rudner, A. & Tabtiang, R. A. *C. elegans* mutant that lives twice as long as wild type. *Nature.* **366**, 461–464 (1993).
13. Sulston, J. E. & Brenner, S. The DNA of *Caenorhabditis elegans*. *Genetics.* **77**, 95–104 (1974).
14. Mitchell, D. H., Stiles, J. W., Santelli, J. & Sanadi, D. R. Synchronous growth and aging of *Caenorhabditis elegans* in the presence of fluorodeoxyuridine. *J. Gerontol.* **34**, 28–36 (1979).

Acknowledgements

The authors wish to thank Pia Unterberger for expert technical assistance.

Author Contributions

N.B.A., H.G.F. and C.S. designed the study. Data collection was performed by N.B.A.; N.B.A., H.G.F. and C.S. analyzed data. The manuscript was drafted by N.B.A., H.G.F. and C.S.

Additional Information

Competing Interests: Nicholas B. Angstman and Hans-Georg Frank declare that no competing interests exist. Christoph Schmitz served (until December 2017) as a paid consultant for and received benefits from Electro Medical Systems (Nyon, Switzerland), the distributor of the Swiss DolorClast extracorporeal shock wave device. However, Electro Medical Systems had no any role in study design, data collection and analysis, decision to publish, or preparation of this manuscript. No other potential conflicts of interest relevant to this article were reported.

Publisher's note: Springer Nature remains neutral with regard to jurisdictional claims in published maps and institutional affiliations.

43. He YL, Liao DL, Kang HY, Ke CF, Chen YL, Liu SF, et al. Comparison of mechanical insufflation-exsufflation and percussors in the treatment of lung infections for children with cerebral palsy. J Pediatr Resp Dis. 2013; 9: 40–47.

44. Smith N, Sankin GN, Simmons WN, Nanke R, Fehre J, Zhong P. A comparison of light spot hydrophone and fiber optic probe hydrophone for lithotripter field characterization. Rev Sci Instrum. 2012; 83: 014301. doi: 10.1063/1.3678638 PMID: 22299970

45. Pishchalnikov YA, Williams JC, McAteer JA. Bubble proliferation in the cavitation field of a shock wave lithotripter. J Acoust Soc Am. 2011; 130: EL87–93. doi: 10.1121/1.3609920 PMID: 21877776

46. Zhou Y, Yang K, Cui J, Ye JY, Deng CX. Controlled permeation of cell membrane by single bubble acoustic cavitation. J Control Release 2012; 157: 103–111. doi: 10.1016/j.jconrel.2011.09.068 PMID: 21945682

47. Angstman NB, Kiessling MC, Frank HG, Schmitz C. High interindividual variability in dose-dependent reduction in speed of movement after exposing C. elegans to shock waves. Front Behav Neurosci. 2015; 9: 12. doi: 10.3389/fnbeh.2015.00012 PMID: 25705183

48. Gonkova MI, Ilieva EM, Ferriero G, Chavdarov I. Effect of radial shock wave therapy on muscle spasticity in children with cerebral palsy. Int J Rehabil Res. 2013; 36: 284–290. doi: 10.1097/MRR.0b013e328360e51d PMID: 23603803

49. Obreschkow D, Tinguley M, Dorsaz N, Kobel Ph, De Bosset A, Farhat M. The quest for the most spherical bubble. Experiments in Fluids 2013; 54: 1503. doi: 10.1007/s00348-013-1503–9

50. Sulston JE, Brenner S. The DNA of *Caenorhabditis elegans*. Genetics. 1974; 77: 95–104. PMID: 4858229

51. Kiessling MC, Milz S, Frank HG, Korbel R, Schmitz C. Radial extracorporeal shock wave treatment harms developing chicken embryos. Sci Rep. 2015; 5: 8281. doi: 10.1038/srep08281 PMID: 25655309

52. Wallis JW, Miller TR, Lerner CA, Kleerup EC. Three-dimensional display in nuclear medicine. IEEE Trans Med Imaging 1989; 8: 297–303. PMID: 18230529

Appendix B: Paper IV

PLOS | ONE

RESEARCH ARTICLE

Radial Shock Wave Devices Generate Cavitation

Nikolaus B. M. Császár[1], Nicholas B. Angstman[1], Stefan Milz[1], Christoph M. Sprecher[2], Philippe Kobel[3], Mohamed Farhat[3], John P. Furia[4], Christoph Schmitz[1]*

1 Extracorporeal Shock Wave Research Unit, Department of Anatomy II, Ludwig-Maximilians-University of Munich, Munich, Germany, **2** AO Research Institute Davos, Davos, Switzerland, **3** Hydraulic Machines Laboratory, École Polytechnique Fédérale de Lausanne, Lausanne, Switzerland, **4** SUN Orthopaedic Group, Lewisburg, Pennsylvania, United States of America

* christoph_schmitz@med.uni-muenchen.de

Citation: Császár NBM, Angstman NB, Milz S, Sprecher CM, Kobel P, Farhat M, et al. (2015) Radial Shock Wave Devices Generate Cavitation. PLoS ONE 10(10): e0140541. doi:10.1371/journal.pone.0140541

Editor: Antal Nógrádi, University of Szeged, HUNGARY

Received: July 1, 2015

Accepted: August 20, 2015

Published: October 28, 2015

Data Availability Statement: All relevant data are within the paper.

Funding: JPF was employed by SUN Orthopaedic Group during this study and received funding in the form of salary. Dr. Furia is paid for clinical work, not for any research activities. Accordingly, neither SUN Orthopaedic Group nor any other organization/ institution have had any role in the study design, data collection and analysis, decision to publish, or preparation of the manuscript.

Competing Interests: CS serves as paid consultant for and receives benefits from Electro Medical

Abstract

Background

Conflicting reports in the literature have raised the question whether radial extracorporeal shock wave therapy (rESWT) devices and vibrating massage devices have similar energy signatures and, hence, cause similar bioeffects in treated tissues.

Methods and Findings

We used laser fiber optic probe hydrophone (FOPH) measurements, high-speed imaging and x-ray film analysis to compare fundamental elements of the energy signatures of two rESWT devices (Swiss DolorClast; Electro Medical Systems, Nyon, Switzerland; D-Actor 200; Storz Medical, Tägerwillen, Switzerland) and a vibrating massage device (Vibracare; G5/General Physiotherapy, Inc., Earth City, MO, USA). To assert potential bioeffects of these treatment modalities we investigated the influence of rESWT and vibrating massage devices on locomotion ability of *Caenorhabditis elegans* (*C*. *elegans*) worms.

Results

FOPH measurements demonstrated that both rESWT devices generated acoustic waves with comparable pressure and energy flux density. Furthermore, both rESWT devices generated cavitation as evidenced by high-speed imaging and caused mechanical damage on the surface of x-ray film. The vibrating massage device did not show any of these characteristics. Moreover, locomotion ability of *C*. *elegans* was statistically significantly impaired after exposure to radial extracorporeal shock waves but was unaffected after exposure of worms to the vibrating massage device.

Conclusions

The results of the present study indicate that both energy signature and bioeffects of rESWT devices are fundamentally different from those of vibrating massage devices.

Systems, the manufacturer and distributor of the radial extracorporeal shock wave device, Swiss DolorClast. JPF is employed by SUN Orthopaedic Group (Lewisburg, PA, USA) and paid for clinical work, not for any research activities. Neither CS nor JPF have received any honoraria or consultancy fee in writing this manuscript. No other potential conflicts of interest relevant to this article were reported. Neither Electro Medical Systems nor SUN Orthopaedic Group or any other institution have had any role in study design, data collection and analysis, decision to publish, or preparation of the manuscript. The conditions of Dr. Schmitz', Dr. Furia's or any other authors' employment do not alter the authors' adherence to PLOS ONE policies on data sharing or materials.

Clinical Relevance

Prior ESWT studies have shown that tissues treated with sufficient quantities of acoustic sound waves undergo cavitation build-up, mechanotransduction, and ultimately, a biological alteration that "kick-starts" the healing response. Due to their different treatment indications and contra-indications rESWT devices cannot be equated to vibrating massage devices and should be used with due caution in clinical practice.

Introduction

Radial extracorporeal shock wave therapy (rESWT) is widely used in the non-invasive treatment of various diseases of the musculoskeletal system and other soft tissue disorders (see, e.g., [1–3]). Several studies addressed the molecular and cellular mechanisms of rESWT on these conditions including the mediation of cell apoptosis, enhanced angiogenesis and wound healing as well as new bone formation (see, e.g., [4,5,6]). The working principle of rESWT devices is illustrated in Fig 1A. Compressed air (or an electromagnetic field) is used to fire a projectile within a guiding tube that strikes a metal applicator placed on the patient's skin. The projectile generates stress waves in the applicator that transmit pressure waves (radial shock waves) non-invasively into tissue.

Because radial shock waves are not real shock waves in the strict physical sense (for details see [2,7,8]) some authors called rESWT "radial pressure wave treatment (RPWT)" [4] or "radial pulse therapy (RPT)" [9]. Furthermore, conflicting reports exist in the literature as to whether at all radial extracorporeal shock waves (rESW) can generate cavitation, which refers to the rapid formation, expansion, and forceful collapse of vapor bubbles in liquids subject to rapid pressure changes [2,10,11]. Cavitation can, next to exerting therapeutic bioeffects, also produce unwanted side effects including hematomas, blood vessel rupture, and permanent injury to organs such as kidneys and lungs [11–17]. In this respect an early review about ESWT published in 2003 [18] concluded that for the only rESWT device available at that time, the Swiss DolorClast (Electro Medical Systems, Nyon, Switzerland) (Fig 1B), it was not possible to detect cavitation at all. Three years later, another group reported that this rESWT device was in fact capable of generating cavitation [7]. Since then the Swiss DolorClast has been used in many prospective, randomized controlled clinical trials that are listed in the open access Physiotherapy Evidence Database, PEDro [19] (i.e. [20–38]).

Recently a novel device, D-Actor 200 (Storz Medical, Tägerwilen, Switzerland) (Fig 1C), was introduced into the treatment for Achilles tendinopathy [39], calf strains [40] and cellulite [41]. Yet whereas one research group called this treatment modality "low-energy radial-pulsed–activated (EPAT) shockwave (sound wave)" and referred to the D-Actor 200 as a radial shock wave device [39] the other research group named treatments performed with the D-Actor 200 "Acoustic Wave Therapy (AWT)" and called the D-Actor 200 a "vibrating massage system (EPAT) that operates via compressed air to perform AWT on targeted tissue" [41]. In fact, the manufacturer of the D-Actor 200 (Storz Medical) listed several vibrating massage devices as predicate device of the D-Actor 200 in Appendix G of the 510[k] summary of the D-Actor 200 with the U.S. Food and Drug Administration (FDA). Among these vibrating massage devices is the Vibracare (G5/General Physiotherapy, Earth City [St. Louis], MO, USA) (Fig 1D). The latter device is electrically powered and causes vibrations by means of a flywheel mass that rotates around a vertical axis within a chamber (Fig 1E). In fact, with regard to design and working principle the D-Actor 200 appears very similar to the Swiss DolorClast but very

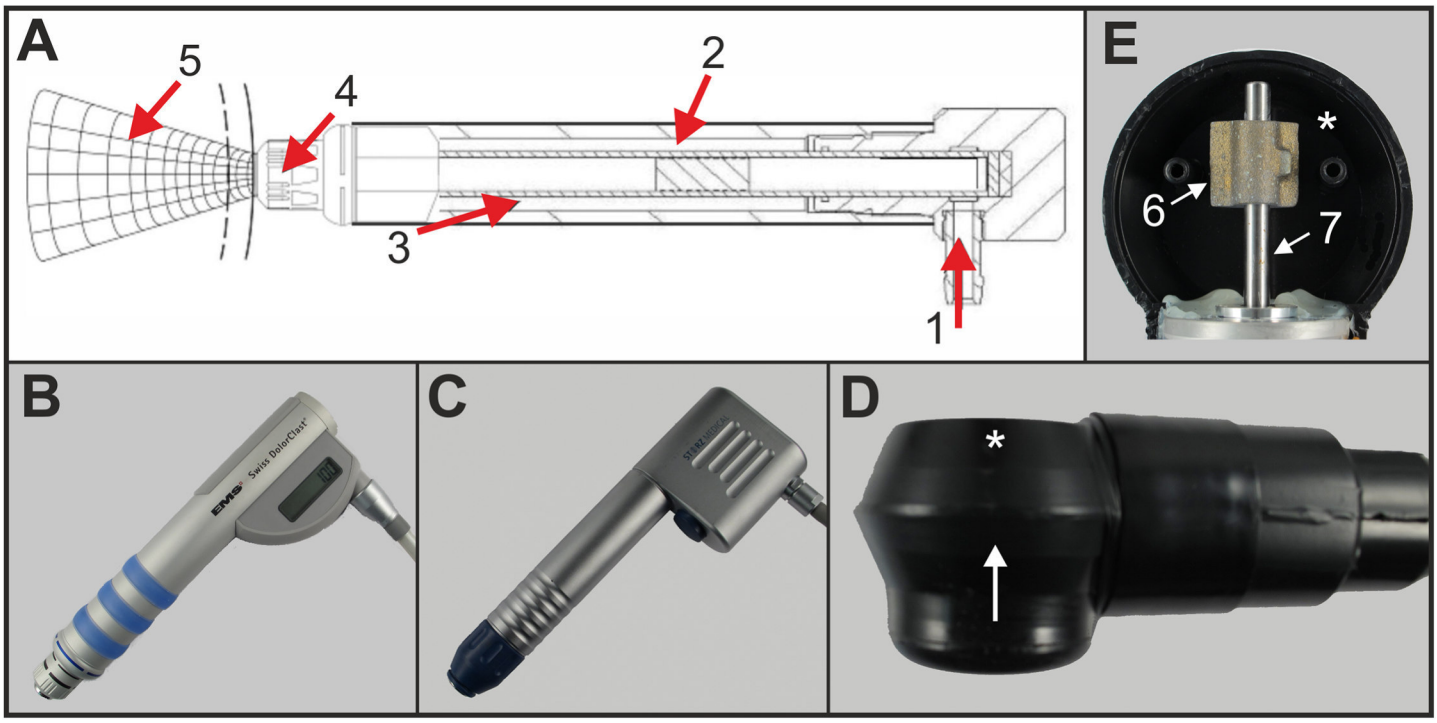

Fig 1. Devices investigated in the present study and their working principles. (A) Working principle of radial extracorporeal shock wave therapy (rESWT) devices. Compressed air (1) is used to fire a projectile (2) within a guiding tube (3) that strikes a metal applicator (4) placed on the patient's skin. The projectile generates stress waves in the applicator that transmit pressure waves (5) non-invasively into tissue. Note that both the Swiss DolorClast (B) and the D-Actor 200 (C) share this construction principle. (B) "Radial" handpiece of the Swiss DolorClast (EMS) with the 15-mm applicator. (C) Handpiece of the D-Actor 200 (Storz Medical) with the 15-mm applicator. (D) Vibracare (G5/General Physiotherapy). The arrow indicates the direction of view into the chamber of the Vibracare head that was opened in (E); the asterisk indicates the backside of the chamber. (E) Working principle of the Vibracare. A flywheel mass (6) rotates around a vertical axis (7) within a chamber (asterisk).

doi:10.1371/journal.pone.0140541.g001

different to that of vibrating massage devices such as the Vibracare. Furthermore, to our knowledge the Vibracare has so far only been studied for percussion treatment of patients with cystic fibrosis [42] and children with cerebral palsy suffering from lung infections [43], but not for treatments of diseases of the musculoskeletal system and cellulite. On the other hand, the D-Actor 200 must not be applied over air-filled tissue such as the lung.

These conflicting descriptions of the D-Actor 200 in the literature have raised the general question whether or not the energy signature of rESWT devices resembles the energy signature of vibrating massage devices. In particular, we compared the energy signature of the D-Actor 200 and the Swiss DolorClast to the energy signature of the Vibracare. This was done by applying techniques that have been established in the literature for the characterization of the energy signature of therapeutic ESW devices: (i) acoustic measurements using a laser fiber optic probe hydrophone (FOPH) [11,44]; (ii) high-speed imaging of cavitation bubbles [45,46]; and (iii) exposure of x-ray films to pressure waves [10]. Furthermore, to investigate cavitation-mediated bioeffects induced by rESWT devices and/or vibrating massage devices we analyzed cultures of the nematode worm *Caenorhabditis elegans* (*C. elegans*) for locomotion ability after their exposure to either treatment modality, a method that has been established recently for radial shock waves generated with the Swiss DolorClast [47].

Methods

Investigated devices

The following devices and applicators were investigated in the present study (see also Fig 1): (i) D-Actor 200 (Model 2007; Storz Medical) operated with the 15-mm applicator as used in [39]; (ii) Swiss DolorClast (EMS) operated with the "Radial" handpiece and the 15-mm applicator as used in many clinical trials (e.g., [21,22,25,27,29,30]); and (iii) Vibracare (Item SKU VC24B; G5/General Physiotherapy, Inc.).

The Supporting Information (S1 File, S1 and S2 Figs) contains additional data from high-speed imaging analysis of cavitation (outlined further down) generated by the D-Actor 200, Swiss DolorClast ("Radial" handpiece) and the following rESWT devices/handpieces: (i) BTL-5000 SWT Power (BTL, Prague, Czech Republic) operated with the 15-mm applicator (used in [48]); (ii) Swiss DolorClast (EMS) operated with the "EvoBlue" and "Power+" handpieces and their 15-mm applicators; and (iii) en Puls V. 2.0 (Zimmer, Neu-Ulm, Germany) with its 15-mm applicator.

Acoustic measurements using a laser fiber optic probe hydrophone

Measurements of the pressure of the acoustic waves generated by the D-Actor 200 and the Swiss DolorClast were carried out according to IEC-61846:1998 (Ultrasonics—Pressure pulse lithotripters—Characteristics of fields) in a tank of 300 liters filled with demineralized water (conductivity approximately 5μS/cm) at the laboratories of Electro Medical Systems (Nyon, Switzerland). The inner dimensions of the tank were 960×560 mm with a height of 660 mm. The water level rose to 470 mm when the applicators were immerged at a height of 330 mm.

Measurements were performed with a laser fiber optic probe hydrophone (FOPH 2000; RP Acoustics, Leutenbach, Germany) coupled to an oscilloscope (LeCroy 9361; LeCroy, Chestnut Ridge, NY, USA) in the x-axis of the applicator. Positioning of the laser hydrophone probe was controlled with step motors, allowing a resolution of the position of 0.1 mm. Measurements were performed at various distances to the applicators (1, 5, 10 and 20 mm) and operating the D-Actor 200 and the Swiss DolorClast at various air pressures (D-Actor 200: 3 bar and [maximum] 5 bar; Swiss DolorClast: 3 bar and [maximum] 4 bar). All measurements were repeated five times and the results were averaged.

The electrical signal recorded by the oscilloscope was linked to the pressure signal (P) according to Eq 1:

$$P = -412MPa \times (1 + \alpha) \times \frac{\Delta U}{U_{Water} - U_B} \quad (1)$$

with α the reflection factor (given at 0.07), ΔU the measured electrical signal, U_{Water} the reference voltage of the noise of the measurement (probe without laser), and U_B the reference voltage of the probe (with laser activated).

The energy flux density (J) is the integral of the pressure as shown in Eq 2:

$$J = \frac{1}{Z} \int_a^b P(t)^2 dt \quad (2)$$

with Z the impedance of sound in water (1.5×10^6 kg×m^{-2}×s^{-1}), $P(t)$ the pressure as a function of time, a the first positive extreme of the first measured pressure peak, and b the second positive extreme of the first measured pressure peak.

Results were graphically represented using GraphPad Prism software (version 5; GraphPad, San Diego, CA, USA).

Because of the oscillating movements of the Vibracare head it was not possible to investigate this device with the laser hydrophone.

High-speed imaging of cavitation bubbles

These investigations were performed at the Hydraulic Machines Laboratory of the École Polytechnique Fédérale de Lausanne (Lausanne, Switzerland). The tips of the 15-mm applicators of the D-Actor 200 and the Swiss DolorClast, mounted on their respective handpieces, as well as the tip of the Vibracare head were submerged one after another in de-ionized water contained within a custom-built transparent cubic vessel made of clear high-density polycarbonate (20 cm side length, 1 cm wall thickness). Measurements of the D-Actor 200 were performed at 3 bar and (maximum) 5 bar air pressure, and measurements of the Swiss DolorClast at 3 bar and (maximum) 4 bar air pressure. Measurements were performed at 1 Hz and 15 Hz. The Vibracare was operated at maximum energy settings (i.e. 50 cycles per second, according to the operation manual). All measurements were run in triplicates. The water was systematically degassed before each test to reduce the nuclei content. To this end, a vacuum pump connected to the vessel was operated for several minutes.

To monitor the cavitation occurrence for each device, a high-speed charge coupled device (CCD) camera (Photron Ultima APX; Photron, Tokyo, Japan) with a framing rate of 300,000 frames per second and exposure time of 1/2,700,000 seconds was used. Each captured frame comprised a total of 8.192 (64 x 128) pixels, encompassing an area of approximately 8.8 x 17.6 mm. A parallel LED background illumination (IMG Stage Line 3W LED-36Spot; Monacor International, Bremen, Germany) provided a white background, against which cavitation bubbles appear as black absorption features. Using the minimal exposure time of 370 ns, this illumination also allows the visualization of shock waves in shadowgraphy [49].

The applicators of the D-Actor 200 and the Swiss DolorClast were lowered from above into the camera frame's top section. Camera recordings were triggered manually prior to the release of a single pulse generated by the D-Actor 200 or the Swiss DolorClast, respectively. Individual film sequences were subsequently visualized using FASTCAM viewer software (Photron, Tokyo, Japan), converted into individual images with 256 greyscales (with zero and 256 representing black and white, respectively), exported as TIF files, and then reduced for data analysis to 1,001 frames each (equivalent to film duration of 3.3 ms) to capture only those frames that showed the cavitation peak caused by a single pulse generated by the D-Actor 200 or the Swiss DolorClast, respectively, plus 500 frames before and after the cavitation peak (i.e., with the peak in between). In case of the Vibracare the head of the device was brought from the side into the camera's field-of-view, the camera was switched on during continuous running of the device, and film sequences were reduced for data analysis to 10,000 frames.

Quantitative evaluation of the individual frames for the presence or absence of labeled pixels caused by cavitation bubbles was performed using a custom macro for Zeiss KS400 software (Carl Zeiss Vision, Eching, Germany). Each greyscale image was binarized with the threshold set to a grey level of 35, and the number of labeled pixels was determined. To account for potential artifacts in the film sequences (caused by, e.g., dirt in the water introduced during the measurements) the numbers of labeled pixels found in the first frame were subtracted from the corresponding numbers of labeled pixels found in all consecutive frames (no. 2–1001) of the corresponding film sequence.

Results were also graphically represented using Prism software (GraphPad).

Exposure of x-ray films to pressure waves

Coleman et al. [10] reported that shock waves can blacken silver grains in x-ray films due to the mechanical impact of collapsing cavitation bubbles on the film sheets' surface. We therefore tested the hypothesis that silver grains in x-ray films can also be blackened by exposing x-ray films to the pressure waves generated by the D-Actor 200, Swiss DolorClast and Vibracare devices. Measurements were performed at the Department of Anatomy II of the Ludwig-Maximilians University of Munich (Munich, Germany) in a dark room that was sparsely illuminated with red light. Individual x-ray films not sensitive to the red light (STRUCTURIX, D4DW, Agfa Gevaert, Mortsel, Belgium) were fixed at their outer edges within a custom-made frame in a horizontal position such that the sheet's main surface was left unrestrained by the frame. The entire construction was then submerged in de-ionized water. The applicators of the D-Actor 200 and the Swiss DolorClast as well as the head of the Vibracare were placed underwater, exactly 3 mm above the center of an individual x-ray sheet. To this end the handpieces of the D-Actor 200 and the Swiss DolorClast were vertically mounted on a drill-stand (Wolfcraft, Kempenich, Germany), with the applicators facing downward into the water. Then a total of 10,000 pulses each were applied to the sheets' center at maximum energy settings (i.e., 5 bar for the D-Actor 200 and 4 bar for the Swiss DolorClast) at a frequency of 1 Hz. The Vibracare was mounted in a custom-made frame with the head facing downward into the water, and was again operated at maximum energy settings (i.e. 50 cycles per second) for one hour.

The exposed films were developed with an x-ray film developing device (Protec C2; Protec, Oberstenfeld, Germany) and examined using a Zeiss Axiophot Microscope (Zeiss, Goettingen, Germany) for evidence of blackened silver grains and potential damage. Photomicrographs were taken using a 2.5x objective (Neofluar, Zeiss) and a camera (AxioCam HRc, Zeiss) attached to the microscope.

Influence of rESWT and vibrating massage devices on *C. elegans* locomotion ability

Maintenance of adult wild type nematodes (N2, Bristol) obtained from the Caenorhabditis Genetics Center (Minneapolis, MN, USA), their exposure to shock waves with subsequent transfer from liquid to agar plates as well as analysis of worm locomotion data after shock wave exposure was performed at the Department of Anatomy II of the Ludwig-Maximilians University of Munich as described in detail previously [47]. Briefly, 20 adult worms were placed together with either 300 μl S-Medium [50] or 31,000 g/mol polyvinyl alcohol (PVA) (i.e. Mowiol 4–88, Karl Roth, Karlsruhe, Germany) into non-adjacent U-bottom wells (n = 5 each for S-medium and PVA) of 96-well plates (VWR, Radnor, PA, USA). With its high viscosity PVA effectively suppresses cavitation generation, thus, by exclusion criterion, enabling to attribute shock wave effects to cavitation [14,47].

In order to assess the effects of rESW on worm locomotion ability, the handpiece of the Swiss DolorClast was set vertically into a drill stand (Wolfcraft, Kempenich, Germany). Here, instead of the 15-mm applicator the handpiece of the Swiss DolorClast was equipped with its 6-mm applicator as it fits into individual wells of 96-well plates (a 6-mm applicator was not available for the D-Actor 200). The handpiece of the Swiss DolorClast was lowered from above into the well and a 5.5 x 2 mm fluorinated rubber O-ring (Vi 670/FKM 80, C. Otto Gehrckens, Pinneberg, Germany) was placed externally around the applicator to provide a tight connection with the well plate and to guard against loss of sample during rESW exposure (Fig 2A). Five hundred impulses of radial shock waves at an intensity of 2 bar (corresponding to an energy flux density of 0.08 mJ/mm^2) and a frequency of 1 Hz were then applied to wells containing

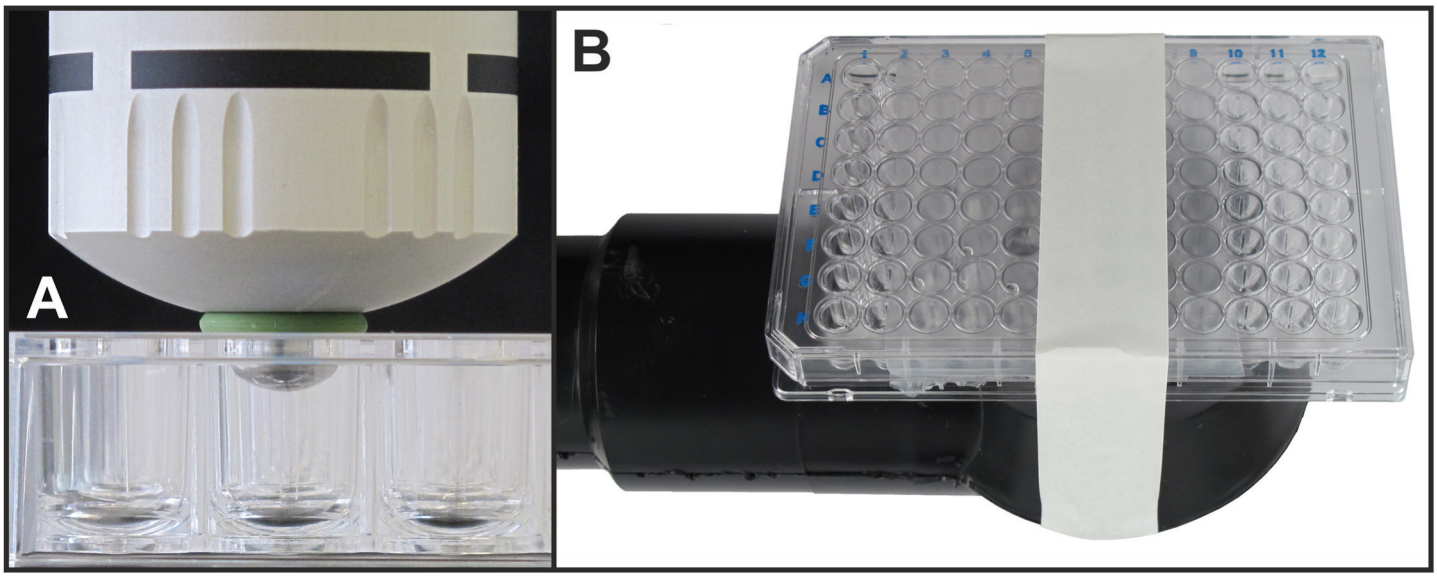

Fig 2. Exposure of *C. elegans* worms to radial shock waves and the movements of the Vibracare head. In (A) the "Radial" handpiece of the Swiss DolorClast (Electro Medical Systems) with the 6-mm applicator was lowered from above into one U-bottom well of a 96-well plate containing *C. elegans* worms either in S-Medium or PVA (see main text). A fluorinated rubber O-ring (green) was used to seal the U-bottom well. In (B) a 96-well plate containing *C. elegans* worms, sealed with parafilm and closed with its lid, was fixed with adhesive tape onto the upwards facing massaging head of the Vibracare (G5/ General Physiotherapy).

doi:10.1371/journal.pone.0140541.g002

worms. To assess the effects of the Vibracare on worm locomotion ability the 96-well plates containing worms with either S-Medium or PVA (n = 5 wells each) as described were sealed with parafilm (M® PM999; Pechiney Plastic Packaging, Chicago, IL, USA) to prevent sample loss. The Vibracare was again placed in the custom-made frame as described above although with the massage head facing upward. Sealed wellplates were then fixed from above on the upward facing massage head using adhesive tape (Fig 2B). The Vibracare was then operated at maximum energy settings (50 cycles per second) for 10 seconds (resulting in 500 vibrations). Control samples (n = 5 wells for each S-Medium and PVA) were treated identically except that the devices (D-Actor 200, Swiss DolorClast, Vibracare) remained switched off.

After exposure to either rESW or the movements of the head of the Vibracare worms were rapidly transferred from their liquid medium to nematode growth media (NGM) agar plates (for details see [47]). After transfer of worms NGM-agar plates were placed under a dissecting microscope (MZ75, Leica, Wetzlar, Germany; equipped with a 1.0x PlanApo objective) with an LCD light illumination set to a color temperature of 2800 K (KL 1500, Schott, Mainz, Germany). Using a 5.0 megapixel, mono digital camera (Grasshopper 2, Point Grey Research, Richmond, BC, Canada) and the video capture function of the software WormLab (Version 2.0.1, MBF Bioscience, Williston, VT) one minute long videos where then captured at 15 frames per second (FPS) with a resolution of 1280 x 960 pixels. Videos were investigated for percent of worms moving (by means of tracking worm mid-point position; i.e. x, y coordinates) and average speed of worm locomotion using Microsoft Excel 2010 (Microsoft, Redmond, WA) transformation of raw data.

Statistical analysis was performed on speed of worm locomotion data. To this end the D'Agostino and Pearson omnibus normality test of the data of all groups (separately for each group) was performed: no group passed the normality test. Kruskal-Wallis test was then performed separately for the worms in S-medium and the worms in PVA, followed each by

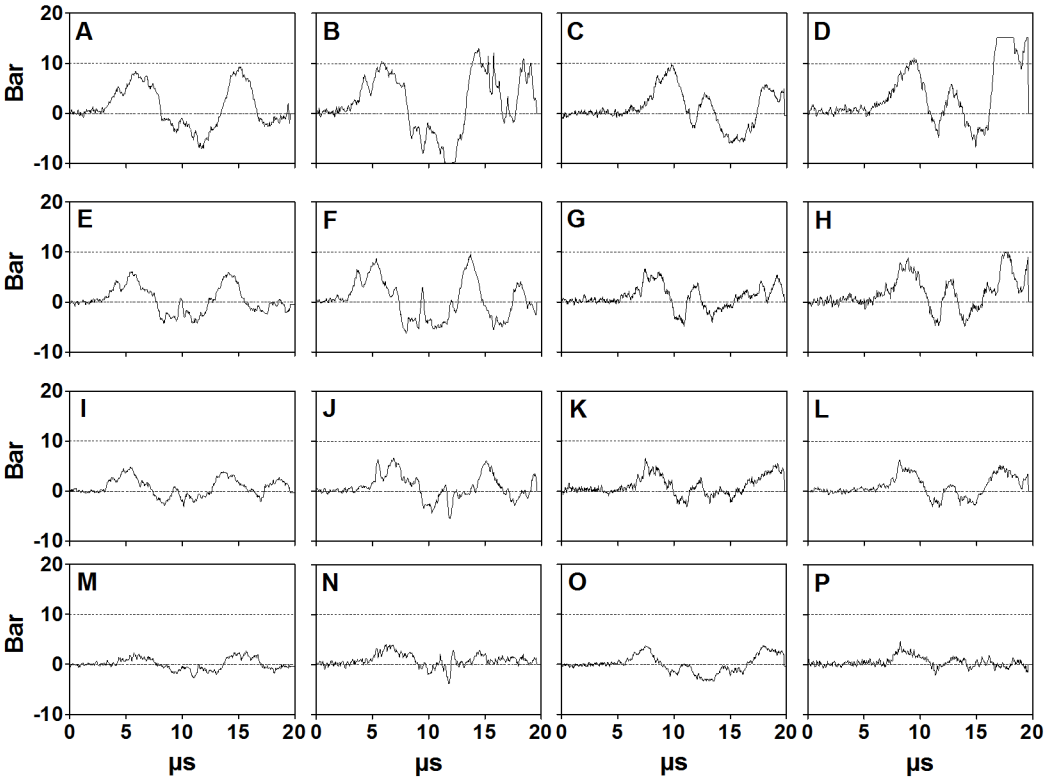

Fig 3. Pressure as a function of time generated by the D-Actor 200 and the Swiss DolorClast devices. The panels show the pressure as a function of time generated by the D-Actor 200 operated at 3 bar (A,E,I,M) and (maximum) 5 bar (B,F,J,N) as well as with the Swiss DolorClast operated at 3 bar (C,G,K, O) and (maximum) 4 bar (D,H,L,P). Measurements were performed five times each; the data shown here represent the measurements (one out of five repetitions) that resulted in the highest positive pressure each. Measurements were performed with a laser hydrophone at a distance of 1 mm (A-D), 5 mm (E-H), 10 mm (I-L) and 20 mm (M-P) to the applicator.

doi:10.1371/journal.pone.0140541.g003

Dunn's multiple comparison test (comparing all groups with each other). Significance was established at $p < 0.05$.

Results

Acoustic measurements using a laser fiber optic probe hydrophone

The pressure waves generated by the D-Actor 200 and the Swiss DolorClast showed very similar waveforms (Fig 3). All pressure waves were characterized by an initial peak of positive pressure (P_+), followed by a peak of negative pressure (P_-), and subsequent waves of positive and negative pressure. The pressure waves lasted approximately 15 µs. Table 1 summarizes P_+, P_- and the energy flux densities of the pressure waves shown in Fig 3. Note that at 3 bar air pressure the pressure waves generated by the two devices had almost the same energy flux density, and operating the D-Actor 200 at (maximum) 5 bar air pressure did not result in a higher energy flux density than operating the Swiss DolorClast at (maximum) 4 bar air pressure (Table 1). For the Vibracare any potential pressure curves could not be measured due to the device's oscillation.

High-speed imaging of cavitation bubbles

High-speed imaging sequences for both the D-Actor 200 and the Swiss DolorClast revealed the build-up of cavitation bubbles as soon as 10 µs following the pressure wave front, and a

Table 1. Peak positive pressure (P_+), peak negative pressure (P_-), rise time (Rt) and positive energy flux density (EFD_+) of pressure waves generated by the D-Actor 200 and Swiss DolorClast devices at different distances to the applicator.

Device	Operating air pressure [bar]	Distance to the applicator [mm]	P_+ [MPa]	P- [MPa]	Rt [μs]	EFD_+ [mJ/mm^2]
D-Actor 200	3	1	8.6	-6.7	2.6	0.10
		5	6.2	-4.5	2.7	0.04
		10	4.9	-4.2	2.1	0.02
		20	2.4	-2.8	1.3	<0.01
	5	1	10.5	-9.0	3.0	0.14
		5	8.2	-6.5	2.7	0.07
		10	6.5	-5.0	1.8	0.04
		20	3.8	-3.6	2.6	0.02
Swiss	3	1	10.1	-5.7	2.9	0.10
DolorClast		5	6.6	-4.8	1.9	0.04
		10	5.9	-3.0	1.9	0.02
		20	4.2	-2.6	2.5	0.02
	4	1	11.3	-6.0	3.4	0.14
		5	8.4	-4.8	2.5	0.06
		10	6.2	-3.2	1.8	0.03
		20	4.5	-2.0	2.5	0.01

All values represent the average of five measurements.

doi:10.1371/journal.pone.0140541.t001

cavitation maximum approximately 120 μs later (Fig 4). Both devices produced larger cavitation bubbles at 1 Hz than at 15 Hz, irrespective of the devices' energy settings (Fig 5). Quantitative analysis of the film sequences also showed that both devices generated more cavitation at 1 Hz than at 15 Hz, with cavitation persisting for approximately 1 ms (Fig 6).

No cavitation bubbles were found in the high-speed imaging film sequences generated for the Vibracare (Fig 7).

Exposure of x-ray films to pressure waves

The pressure waves generated by the D-Actor 200 and the Swiss DolorClast caused clearly discernible damage on the x-ray film's surface (Fig 8). Damage was always characterized by a central impression surrounded by a black ring. The D-Actor 200 caused complete penetration of the x-ray film, leaving a hole within the central impression (Fig 8A). In case of the Swiss DolorClast the central impression on the x-ray film was not entirely penetrated (Fig 8B). In contrast, the Vibracare had no detectable impact on the x-ray film (Fig 8C).

Influence of rESWT and vibrating massage devices on *C. elegans* locomotion ability

When *C. elegans* worms were kept in S-Medium mean speed of locomotion was statistically significantly reduced ($p < 0.001$) following exposure to rESW (8 ± 1 μm/s; Mean ± SEM) relative to controls (88 ± 6 μm/s) (Fig 9, top panel). Accordingly, 77% of worms exposed to rESW were rendered paralyzed compared to 18% in controls (Fig 9, bottom panel). In contrast, mean speed of movement remained virtually unchanged between worms exposed to the movements of the Vibracare head (84 ± 6 μm/s) and controls (Fig 9, top panel). Here, only 8% of worms exposed to the movements of the Vibracare head were rendered paralyzed (Fig 9, bottom panel).

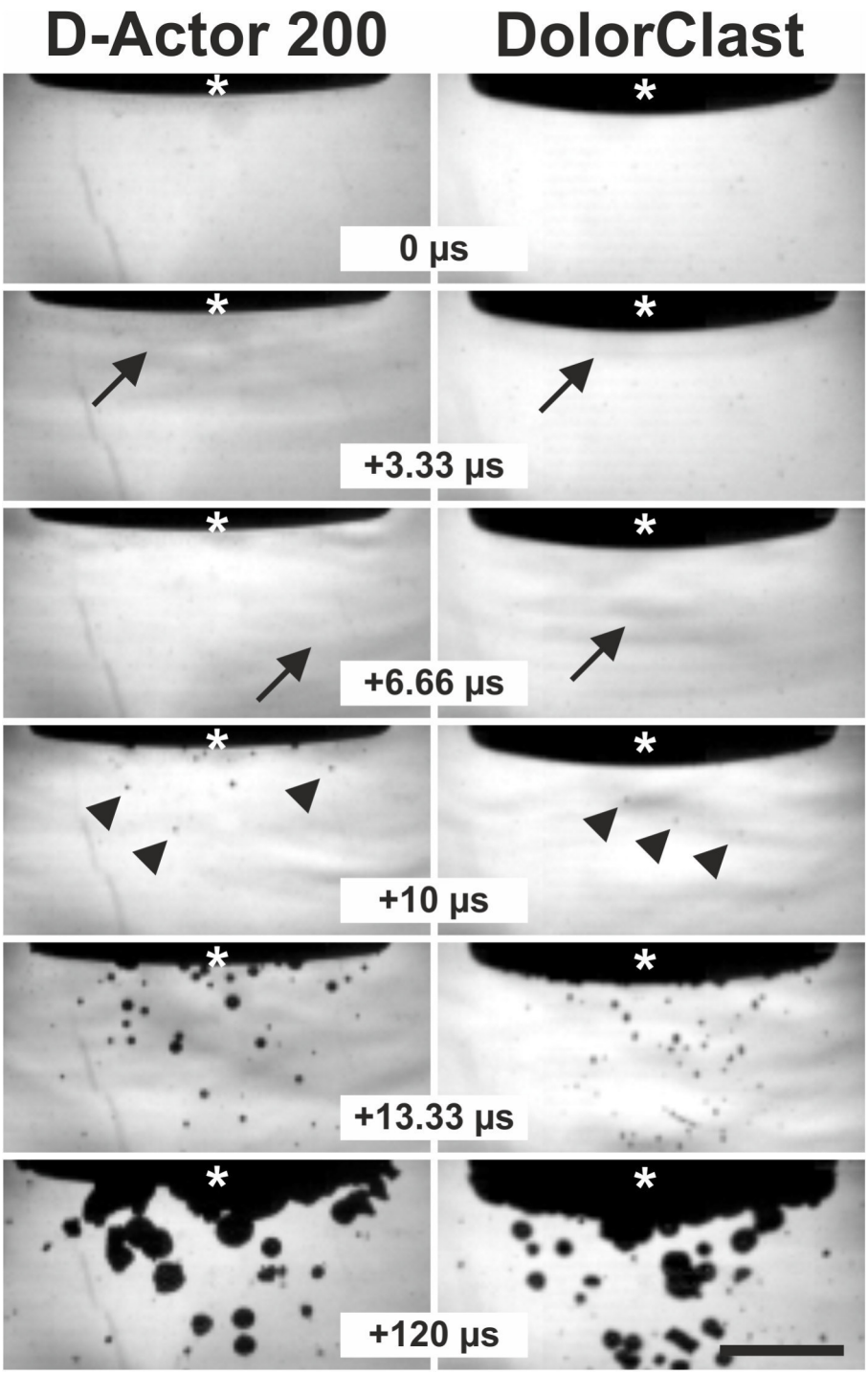

Fig 4. Pressure waves and cavitation bubbles generated by the D-Actor 200 and the Swiss DolorClast devices. Representative frames of the high-speed imaging experiments described in the main text, showing pressure waves (arrows) emitted from the applicators of the D-Actor 200 operated at (maximum) 5 bar air pressure (on the left) and the Swiss DolorClast operated at (maximum) 4 bar air pressure (on the right). The panels show five consecutive frames each 3.33 µs apart, plus a subsequent frame that was captured 120 µs after the first frame. Asterisks indicate the tip of the applicators lowered from above into the top section of the camera's field-of-view. Note that the first cavitation bubbles were already detected at 10 µs after occurrence of the pressure wave (arrowheads in frames "+10 µs"). The scale bar represents 5 mm.

doi:10.1371/journal.pone.0140541.g004

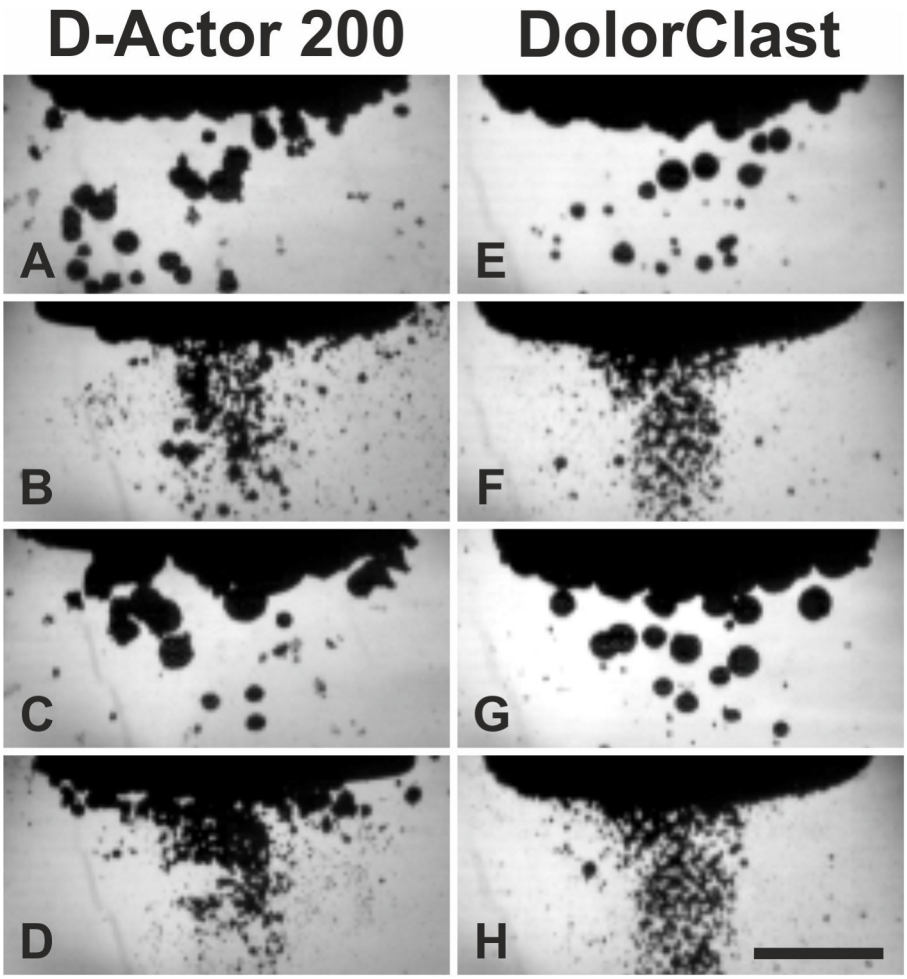

Fig 5. Cavitation bubbles generated by the D-Actor 200 and the Swiss DolorClast devices. The panels show the frames with the highest number of labeled pixels (from the corresponding high-speed imaging film sequences described in the main text) generated by the D-Actor 200 (A-D) operated at 3 bar and 1 Hz (A), 3 bar and 15 Hz (B), (maximum) 5 bar and 1 Hz (C), and 5 bar and 15 Hz (D), as well as with the Swiss DolorClast (E-H) operated at 3 bar and 1 Hz (E), 3 bar and 15 Hz (F), (maximum) 4 bar and 1 Hz (G), and 4 bar and 15 Hz (H). The scale bar represents 5 mm.

doi:10.1371/journal.pone.0140541.g005

When worms were kept in PVA, which effectively diminishes the build-up of cavitation bubbles, no significant differences in mean speed of movement were observed between controls (57 ± 5 μm/s) and worms exposed to either rESW (47 ± 4 μm/s) or the movements of the Vibracare head (59 ± 5 μm/s) (Fig 9, top panel). Consequently, there was no large difference in the percentage of worms paralyzed between controls (17%), and worms exposed to either rESW (29%) or the movements of the Vibracare head (17%) (Fig 9, bottom panel).

Discussion

The main outcome of the present study was that the D-Actor 200 (Storz Medical) more closely resembles the radial extracorporeal shock wave therapy (rESWT) device Swiss DolorClast (Electro Medical Systems) but not the vibrating massage device Vibracare (G5/General Physiotherapy, Inc.), both in terms of working principle and energy signature. Both rESWT devices (D-Actor 200 and Swiss DolorClast) generated characteristic pressure waves and cavitation,

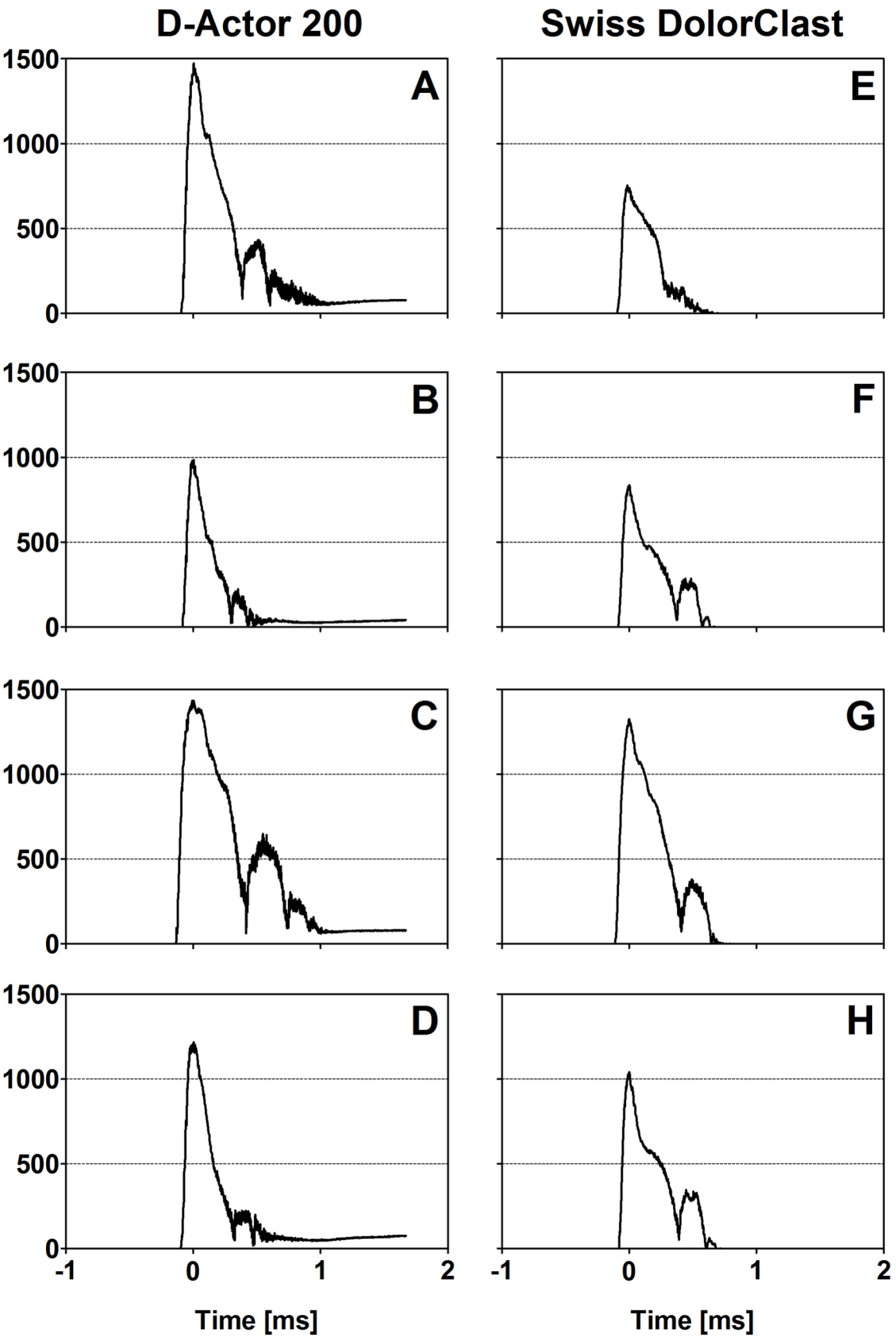
D-Actor 200
Swiss DolorClast
A
B
C
D
E
F
G
H
1500
1000
500
0
-1
0
1
2
Time [ms]
Time [ms]

Fig 6. Results of the quantitative analysis of the high-speed imaging experiments. Number of detected pixels as a function of time in the high-speed imaging experiments described in the main text, obtained for the D-Actor 200 (A-D) operated at 3 bar and 1 Hz (A), 3 bar and 15 Hz (B), (maximum) 5 bar and 1 Hz (C), and 5 bar and 15 Hz (D), as well as with the Swiss DolorClast (E-H) operated at 3 bar and 1 Hz (E), 3 bar and 15 Hz (F), (maximum) 4 bar and 1 Hz (G), and 4 bar and 15 Hz (H).

doi:10.1371/journal.pone.0140541.g006

and caused clearly discernible damage on x-ray films. For the Swiss DolorClast the present study confirms and expands results from earlier studies [2,3,7,8,47,51]. However, this was in sharp contrast to the vibrating massage device, whose energy signature could not be measured due to the device's oscillation, and which neither produced cavitation bubbles nor damage on x-ray films. From its lacking potential to generate cavitation it can be deduced that the Vibracare did not generate a negative (tensile) pressure phase capable of creating cavitation [2,7]. Consequently, the vibrating massage device investigated in the present study per definition "massages" biologic tissues (respectively "move around" water in the present study) whereas rESWT devices generate acoustic pressure waves that propagate in tissues (respectively in water) and, in the process, generate cavitation. The massaging effect could be visualized in high speed imaging by the displacement of the head of the Vibracare (Fig 7) as compared to the rESWT devices' applicator tips, which did not displace (Figs 4 and 5).

The fundamental constructional differences between rESWT devices and the vibrating massage device investigated in the present study (Fig 1) are also reflected in their different bioeffects on locomotion ability in *C. elegans* worms observed in the present study. We found a substantial reduction in the average speed of locomotion and an increase in the percentage of worms rendered paralyzed after their exposure in S-medium to rESW (very similar to our earlier results reported in [47]), but not to the movements of the Vibracare head. However, when worms were exposed to rESW in PVA, which diminishes cavitation due to its high viscosity, these effects were drastically reduced; thus demonstrating that cavitation was one of the biologic working mechanisms primarily responsible.

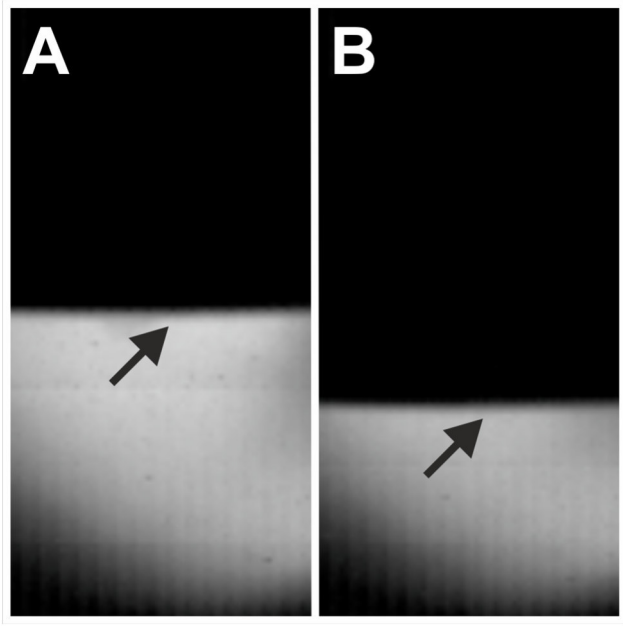

Fig 7. Absence of cavitation bubbles when investigating the Vibracare device with high speed imaging. The arrows point to the surface of the moving head of the device in frames of the high-speed imaging experiments, showing minimum (A) and maximum (B) deflection of the device's head.

doi:10.1371/journal.pone.0140541.g007

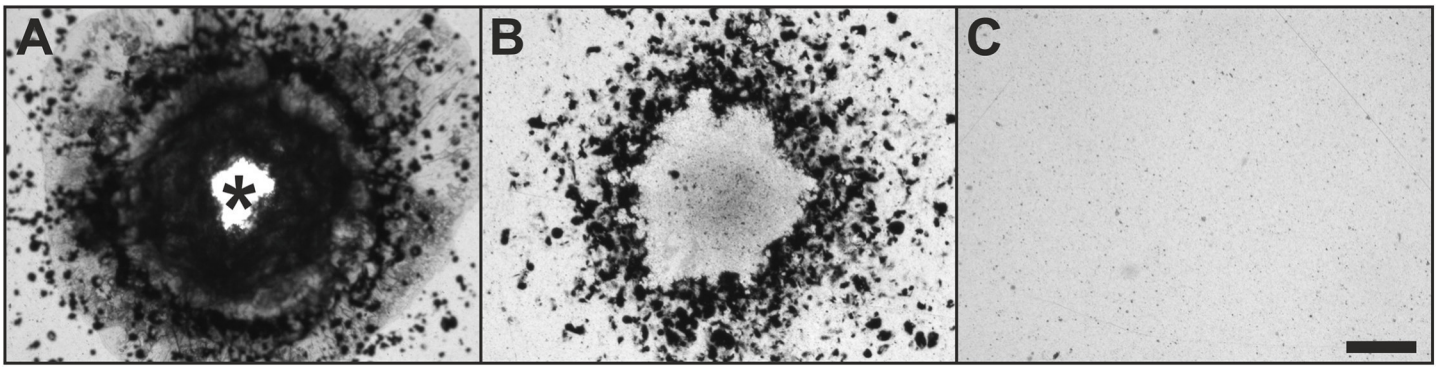

Fig 8. Damage of the surface of x-ray film caused by pressure waves generated by the D-Actor 200 and the Swiss DolorClast devices. The figures show the surface of x-ray film after exposure to 10,000 pressure waves generated by the D-Actor 200 (A) and the Swiss DolorClast (B) at maximum energy settings (i.e., 5 bar for the D-Actor 200 and 4 bar for the Swiss DolorClast). The asterisk in (A) indicates a hole in the x-ray film. The Vibracare device operated at maximum energy settings (50 cycles per second) had no detectable impact on x-ray film (C). The scale bars represent 500 μm.

doi:10.1371/journal.pone.0140541.g008

So far, two models have been established in the literature to observe cavitation-mediated bioeffects of extracorporeal shock waves, both of which utilized PVA to diminish cavitation in comparison to other fluids/media enabling cavitation. The first was an *ex vivo* model established by Schelling et al. [14], who were able to attribute the electrical stimulation of frog sciatic nerves following shock wave administration *ex vivo* unambiguously to cavitation by alternately using in their experiments Ringer's solution and PVA. More recently, Angstman et al. [47] established a *C. elegans* model *in vivo*, in which worms were investigated alternately in S-medium and PVA to demonstrate cavitation-mediated bioeffects of rESW on the musculoskeletal system. Using the latter model, we were able to corroborate the finding that bioeffects of rESWT devices are indeed (at least in part) cavitation-mediated and, to demonstrate that the Vibracare device, due to its lacking cavitation generation potential, does not generate the same bioeffects than rESWT devices.

In more general terms we hypothesize that rESWT devices do not resemble vibrating massage devices, neither in terms of construction principle nor in terms of energy signature nor in terms of bioeffects induced. Hence we propose to sharply separate these two fundamentally different therapeutic systems.

It should be mentioned that for the following reasons an in-depth quantitative comparison of the cavitation output between the two rESWT devices investigated in the present study was not possible: (i) The images obtained with the high-speed camera due to their nature represent maximum intensity projections [52], which project the maximum volume elements of 3D data (i.e., the applicator's head plus cavitation bubbles) onto the camera's two-dimensional field-of-view. Accordingly, from all cavitation bubbles positioned along an axis perpendicular to the CCD chip the camera will only register the cavitation bubble most closely to the CCD chip. (ii) Both rESWT devices generated smaller cavitation bubbles at 15 Hz than at 1Hz. The reason for this phenomenon that has not been addressed in the technical literature, is unknown. Thus, the cavitation fields (i.e. maximum number of labeled pixels) at 15 Hz did not represent the same characteristics of the cavitation fields at 1 Hz. The images shown in Fig 5 demonstrate that it was impossible to separately count small and large cavitation bubbles.

However, the following general conclusions with high clinical relevance can be drawn: (i) Due to their cavitation generating potential, rESWT devices come with clear contraindications such as the proscribed application to target areas located above air filled tissues (e.g. lungs). The Vibracare, on the other hand, is intended for respiratory therapy applications. Thus at least one of the intended uses for the Vibracare represents a clear contraindication for rESWT

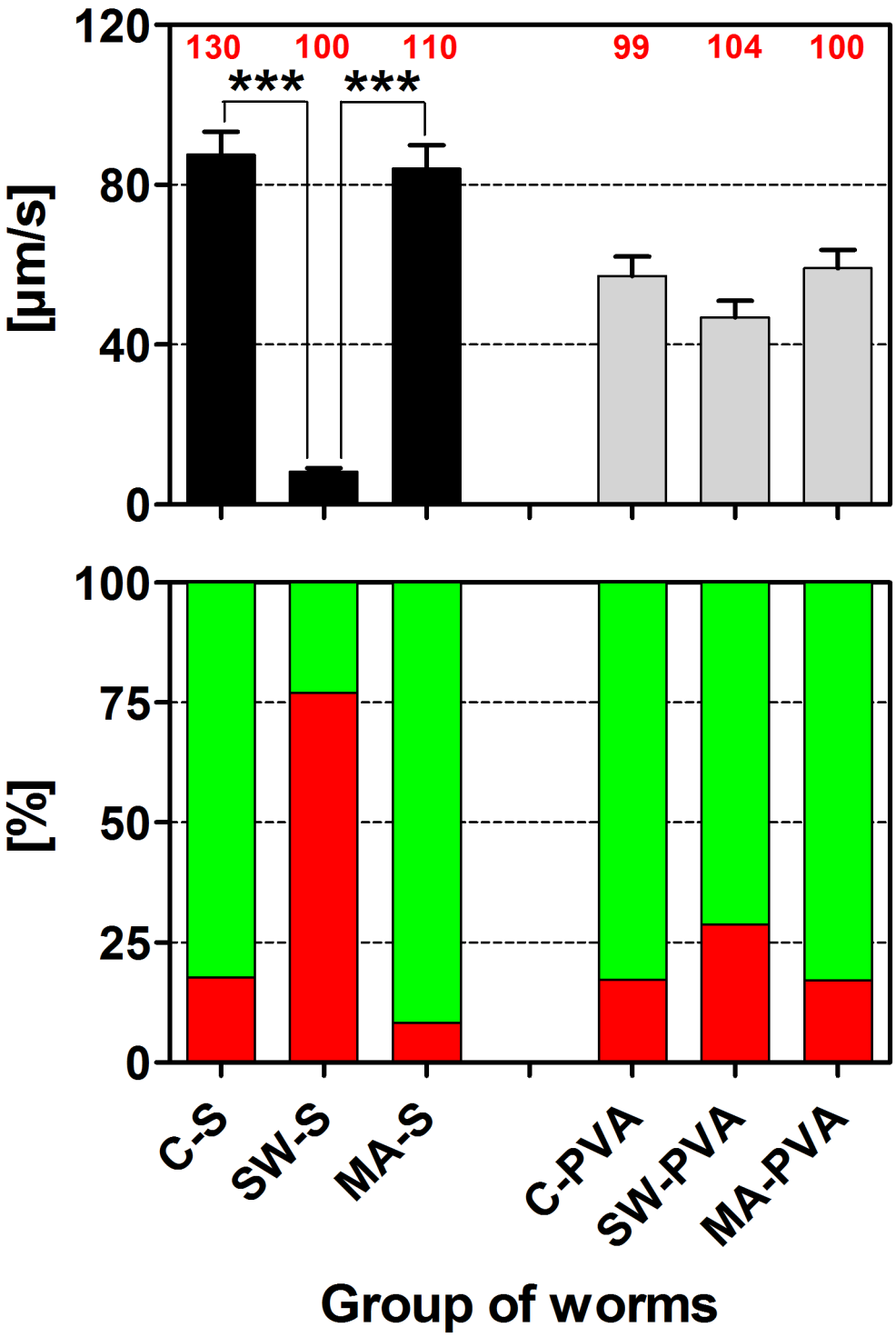

Fig 9. Influence of radial shock waves and the movements of the Vibracare head on *C. elegans* locomotion ability. The upper panel shows mean and standard error of the mean (SEM) of the speed of locomotion of the following groups of *C. elegans*: C-S, control worms in S-medium; SW-S, exposure of worms to 500 impulses of radial shock waves (rESW) in S-medium; MA-S, exposure of worms to the movements of the Vibracare head in S-medium; C-PVA, control worms in polyvinyl alcohol (PVA); SW-PVA, exposure of worms to 500 impulses of rESW in PVA; MA-PVA, exposure of worms to the movements of the Vibracare head in PVA. The lower panel shows the percentages of worms paralyzed (red bars) and not paralyzed (green bars) of the same groups of *C. elegans*. The numbers in red above the bars in the upper panel indicate the numbers of worms per group. ***, $p < 0.001$ (results of Dunn's multiple comparison test).

doi:10.1371/journal.pone.0140541.g009

devices. Characterizing the D-Actor 200 (Storz) as a vibrating massage system (as done in [41]) appears inadequate from a technical and biomedical point of view. (ii) The air pressure of rESWT devices does not predict the energy output of these devices to the patient. This is because for the devices investigated in the present study no linear relationship was found between these two parameters. For example, at 3 bar air pressure both devices generated almost exactly the same amount of energy (i.e. positive energy flux density, EFD_+; Table 1), and yet again when operated at their highest air pressure settings although this was 5 bar in case of the D-Actor 200 and 4 bar in case of the Swiss DolorClast. (iii) Both rESWT devices investigated in the present study generated more cavitation with increasing air pressure settings. Accordingly, the intensity of rESW treatments in the clinic can be adjusted by the device settings. Again, however, no linear relationship exists between cavitation output and air pressure settings: at 3 bar the D-Actor 200 generated substantially more cavitation than the Swiss DolorClast (Fig 6) whereas both devices generated almost the same amount of cavitation when operated at their highest energy settings (i.e. 5 bar for the D-Actor 200 and 4 bar for the Swiss DolorClast). (iv) Both rESWT devices investigated in the present study produced less cavitation at 15 Hz than at 1 Hz, and this was more pronounced for the D-Actor 200 than the Swiss DolorClast. The reason for this phenomenon is unknown. This must be considered in clinical application because rESW treatments performed with these devices at high frequencies may save time but may be less effective than rESW treatments at low frequencies.

Conclusion

This is the first study demonstrating that the potential to generate cavitation is a common feature of rESWT devices which sharply separates them from certain vibrating massage devices, the latter of which do not generate cavitation. Cavitation exerts important therapeutic bioeffects associated with shock waves, but may also cause serious negative effects on the body. Due to the non-linearity between the cavitation output and the devices' energy settings and/or pulse frequencies, future studies should investigate the clinical effects of these observed differences among the various rESWT devices that are available today.

Supporting Information

S1 Fig. High-speed imaging of cavitation bubbles generated with radial extracorporeal shock wave devices.
(TIF)

S2 Fig. Results of the quantitative analysis of additional high-speed imaging experiments.
(TIF)

S1 File. Supporting Information. This file contains methods and results of additional experiments, as well as the corresponding references.
(DOCX)

Author Contributions

Conceived and designed the experiments: NBMC NBA SM CMS PK MF CS. Performed the experiments: NBMC NBA SM CMS PK MF CS. Analyzed the data: NBMC NBA SM CMS PK MF JPF CS. Contributed reagents/materials/analysis tools: NBMC NBA SM CMS PK MF CS. Wrote the paper: NBMC NBA SM CMS PK MF JPF CS.

References

1. Császár NB, Schmitz C. Extracorporeal shock wave therapy in musculoskeletal disorders. J Orthop Surg Res. 2013; 8: 22.
2. Schmitz C, Császár NBM, Rompe JD, Chaves H, Furia JP. Treatment of chronic plantar fasciopathy with extracorporeal shock waves (review). J Orthop Surg Res. 2013; 8: 31. doi: 10.1186/1749-799X-8-31 PMID: 24004715
3. Schlaudraff KU, Kiessling MC, Császár NBM, Schmitz C. Predictability of the individual clinical outcome of extracorporeal shock wave therapy for cellulite. Clin Cosmet Investig Dermatol. 2014; 7: 171–183. doi: 10.2147/CCID.S59851 PMID: 24920933
4. Contaldo C, Högger DC, Khorrami Borozadi M, Stotz M, Platz U, Forster N, et al. Radial pressure waves mediate apoptosis and functional angiogenesis during wound repair in ApoE deficient mice. Microvasc Res. 2012; 84: 24–33. doi: 10.1016/j.mvr.2012.03.006 PMID: 22504489
5. Zhao Z, Ji H, Jing R, Liu C, Wang M, Zhai L, et al. Extracorporeal shock-wave therapy reduces progression of knee osteoarthritis in rabbits by reducing nitric oxide level and chondrocyte apoptosis. Arch Orthop Trauma Surg. 2012; 132: 1547–1553. doi: 10.1007/s00402-012-1586-4 PMID: 22825641
6. Gollwitzer H, Gloeck T, Roessner M, Langer R, Horn C, Gerdesmeyer L, et al. Radial extracorporeal shock wave therapy (rESWT) induces new bone formation in vivo: results of an animal study in rabbits. Ultrasound Med Biol. 2013; 39: 126–133. doi: 10.1016/j.ultrasmedbio.2012.08.026 PMID: 23122639
7. Chitnis PV, Cleveland RO. Acoustic and cavitation fields of shock wave therapy devices. In: Clement GT, McDannold NJ, Hynynen K, editors. Therapeutic ultrasound: 5th international symposium on therapeutic ultrasound (AIP conference proceedings). Boston: AIP Conf Prot.; 2005. pp. 27–29.
8. Cleveland RO, Chitnis PV, McClure SR. Acoustic field of a ballistic shock wave therapy device. Ultrasound Med Biol. 2007; 33: 1327–1335. PMID: 17467154
9. Speed CA. A systematic review of shockwave therapies in soft tissue conditions: focusing on the evidence. Br J Sports Med. 2014; 48: 1538–1542. PMID: 23918444 doi: 10.1136/bjsports-2012-091961
10. Coleman AJ, Saunders JE, Crum LA, Dyson M. Acoustic cavitation generated by an extracorporeal shockwave lithotripter. Ultrasound Med Biol. 1987; 13: 69–76. PMID: 3590362
11. Perez C, Chen H, Matula TJ, Karzova M, Khokhlova VA. Acoustic field characterization of the Duolith: measurements and modeling of a clinical shock wave therapy device. J Acoust Soc Am. 2013; 134: 1663–1674. PMID: 23927207 doi: 10.1121/1.4812885
12. Gerdesmeyer L, Maier M, Haake M, Schmitz C. Physical and technical principles of shock wave therapy. Orthopaede 2002; 31: 610–617.
13. Ogden JA, Tóth-Kischkat A, Schultheiss R. Principles of shock wave therapy. Curr Orthop Rel Res. 2001; 387: 8–17. PMID: 11400898
14. Schelling G, Delius M, Gschwender M, Grafe P, Gambihler S. Extracorporeal shock waves stimulate frog sciatic nerves indirectly via a cavitation-mediated mechanism. Biophysical J. 1994; 66: 133–140. PMID: 8130332
15. Evan AP, Willis LR, McAteer JA, Bailey MR, Connors BA, Shao Y, et al. Kidney damage and renal functional changes are minimized by waveform control that suppresses cavitation in shock wave lithotripsy. J Urol. 2002; 168: 1556–1562. PMID: 12352457
16. Miller DL. Overview of experimental studies of biological effects of medical ultrasound caused by gas body activation and inertial cavitation. Prog Biophys Mol Bio. 2007; 93: 314–330. PMID: 16989895
17. Chen H, Brayman AA, Bailey MR, Matula TJ. Blood vessel rupture by cavitation. Urol Res. 2010; 38: 321–326. doi: 10.1007/s00240-010-0302-5 PMID: 20680255
18. McClure S, Dorfmüller C. Extracorporeal shock wave therapy: theory and equipment. Clin Tech Equine Pract. 2003; 2: 348–357.
19. Blobaum P. Physiotherapy Evidence Database (PEDro). J Med Libr Assoc. 2006, 94: 477–478.
20. Mehra A, Zaman T, Jenkin AI. The use of a mobile lithotripter in the treatment of tennis elbow and plantar fasciitis. Surgeon. 2003; 1: 290–292. PMID: 15570782
21. Rompe JD, Nafe B, Furia JP, Maffulli N. Eccentric loading, shock-wave treatment, or a wait-and-see policy for tendinopathy of the main body of tendo Achillis: a randomized controlled trial. Am J Sports Med. 2007; 35: 374–383. PMID: 17244902
22. Rompe JD, Furia JP, Maffulli N. Eccentric loading compared with shock wave treatment for chronic insertional Achilles tendinopathy. A randomized, controlled trial. J Bone Joint Surg Am. 2008; 90: 52–61.
23. Marks W, Jackiewicz A, Witkowski Z, Kot J, Deja W, Lasek J. Extracorporeal shock-wave therapy (ESWT) with a new-generation pneumatic device in the treatment of heel pain. A double blind randomised controlled trial. Acta Orthop Belg. 2008; 74: 98–101. PMID: 18411608

24. Greve JM, Grecco MV, Santos-Silva PR. Comparison of radial shockwaves and conventional physiotherapy for treating plantar fasciitis. Clinics. 2009; 64: 97–103. PMID: 19219314

25. Rompe JD, Furia JP, Maffulli N. Eccentric loading versus eccentric loading plus shock-wave treatment for midportion Achilles tendinopathy: a randomized controlled trial. Am J Sports Med. 2009a; 37: 463–470.

26. Rompe JD, Segal NA, Cacchio A, Furia JP, Morral A, Maffulli N. Home training, local corticosteroid injection, or radial shock wave therapy for greater trochanter pain syndrome. Am J Sports Med. 2009b; 37: 1981–1990.

27. Rompe JD, Cacchio A, Weil L Jr, Furia JP, Haist J, Reiners V, et al. Plantar fascia-specific stretching versus radial shock-wave therapy as initial treatment of plantar fasciopathy. J Bone Joint Surg Am. 2010; 92: 2514–2522. doi: 10.2106/JBJS.I.01651 PMID: 21048171

28. Chow IHW, Cheing GLY. Comparison of different energy densities of extracorporeal shock wave therapy (ESWT) for the management of chronic heel pain. Clin Rehabil. 2007; 21: 131–141. PMID: 17264107

29. Gerdesmeyer L, Frey C, Vester J, Maier M, Weil L Jr, Weil L Sr, et al. Radial extracorporeal shock wave therapy is safe and effective in the treatment of chronic recalcitrant plantar fasciitis: results of a confirmatory randomized placebo-controlled multicenter study. Am J Sports Med. 2008; 36: 2100–2109. PMID: 18832341 doi: 10.1177/0363546508324176

30. Ibrahim MI, Donatelli RA, Schmitz C, Hellman MA, Buxbaum F. Chronic plantar fasciitis treated with two sessions of radial extracorporeal shock wave therapy. Foot Ankle Int. 2010; 31: 391–397. doi: 10.3113/FAI.2010.0391 PMID: 20460065

31. Shaheen AAM. Comparison of three different treatment protocols of low-energy radial extracorporeal shock wave therapy for management of chronic plantar fasciitis. Ind J Physiother Occup Ther. 2010; 4: 8–12.

32. Cacchio A, Rompe JD, Furia JP, Susi P, Santilli V, De Paulis F. Shockwave therapy for the treatment of chronic proximal hamstring tendinopathy in professional athletes. Am J Sports Med. 2011; 39: 146–153. doi: 10.1177/0363546510379324 PMID: 20855554

33. Engebretsen K, Grotle M, Bautz-Holter E, Ekeberg OM, Juel NG, Brox JI. Supervised exercises compared with radial extracorporeal shock-wave therapy for subacromial shoulder pain: 1-year results of a single-blind randomized controlled trial. Phys Ther. 2011; 91: 37–47. doi: 10.2522/ptj.20090338 PMID: 21088117

34. Grecco MV, Brech GC, Greve JM. One-year treatment follow-up of plantar fasciitis: radial shockwaves vs. conventional physiotherapy. Clinics. 2013; 68: 1089–1095. doi: 10.6061/clinics/2013(08)05 PMID: 24037003

35. Vidal X, Morral A, Costa L, Tura M. Radial extracorporeal shock wave therapy (rESWT) in the treatment of spasticity in cerebral palsy: A randomized, placebo-controlled clinical trial. NeuroRehabilitation. 2011; 29: 413–419. doi: 10.3233/NRE-2011-0720 PMID: 22207070

36. Liu S, Zhai L, Shi Z, Jing R, Zhao B, Xing G. Radial extracorporeal pressure pulse therapy for the primary long bicipital tenosynovitis a prospective randomized controlled study. Ultrasound Med Biol. 2012; 38: 727–735. doi: 10.1016/j.ultrasmedbio.2012.01.024 PMID: 22425375

37. Lee SS, Kang S, Park NK, Lee CW, Song HS, Sohn MK, et al. Effectiveness of initial extracorporeal shock wave therapy on the newly diagnosed lateral or medial epicondylitis. Ann Rehabil Med. 2012; 36: 681–687. doi: 10.5535/arm.2012.36.5.681 PMID: 23185733

38. Kolk A, Yang KG, Tamminga R, van der Hoeven H. Radial extracorporeal shock-wave therapy in patients with chronic rotator cuff tendinitis: a prospective randomised double-blind placebo-controlled multicentre trial. Bone Joint J. 2013; 95: 1521–1526. doi: 10.1302/0301-620X.95B11.31879 PMID: 24151273

39. Saxena A, Ramdath S Jr, O'Halloran P, Gerdesmeyer L, Gollwitzer H. Extra-corporeal pulsed-activated Therapy ("EPAT" Sound Wave) for Achilles tendinopathy: a prospective study. J Foot Ankle Surg. 2011; 50: 315–319. PMID: 21406328 doi: 10.1053/j.jfas.2011.01.003

40. Saxena A, St. Lois M, Fournier M. Vibration and pressure wave therapy for calf strains: a proposed treatment. Muscles, Ligaments and Tendons Journal 2013; 3: 60–62. doi: 10.11138/mltj/2013.3.2.060 PMID: 23888287

41. Russe-Wilflingseder K, Russe E, Vester JC, Haller G, Novak P, Krotz A. Placebo controlled, prospectively randomized, double-blinded study for the investigation of the effectiveness and safety of the acoustic wave therapy (AWT(®)) for cellulite treatment. J Cosmet Laser Ther. 2013; 15: 155–162. doi: 10.3109/14764172.2012.759235 PMID: 23688206

42. Bauer ML, McDougal J, Schoumacher RA. Comparison of manual and mechanical chest percussion in hospitalized patients with cystic fibrosis. J Pediatr. 1994; 124: 250–254. PMID: 8301432

Acknowledgements

I would like to thank Pia Unterberger (Chair of Neuroanatomy, Institute of Anatomy, Faculty of Medicine, LMU Munich) for expert technical assistance, Prof. Dr. Christoph Schmitz (same affiliation) for the wonderful opportunity to do research at his lab, as well as all my former colleagues for the wonderful time together.